Optimal Location of Charging Stationfor Electric Vehicles in Radial Distribution System with Distributed Generation

Submitted in partial fulfilment of the requirements
for the award of the degree of

Doctor of Philosophy

in

Electrical Engineering

By

Ajit Kumar Mohanty

(Roll no: 718014)

Supervisor

Dr. Suresh Babu Perli

Associate Professor

Department of Electrical Engineering

National Institute of Technology Warangal

January 2023

©National Institute of Technology Warangal- 2022.
ALL RIGHTS RESERVED.

APPROVAL SHEET

This Thesis entitled **"Optimal Location of Charging Station for Electric Vehicles in Radial Distribution System with Distributed Generation"** by **Mr. Ajit Kumar Mohanty**, having **Roll no: 71804** is approved for the degree of **Doctor of Philosophy**

Examiners

_____

_____

_____

Supervisor

Dr. Suresh Babu Perli

Associate Professor

EED, NIT Warangal

Chairman

Prof. Srikanth N V

Professor

EED, NIT Warangal

Date:_____

Department of Electrical Engineering
National Institute of Technology Warangal
Warangal- 506004, Telangana, India

Department of Electrical Engineering
National Institute of Technology Warangal
National Institute of Technology Warangal - 506004

CERTIFICATE

This is to certify that the thesis entitled "**Optimal Location of Charging Station for Electric Vehicles in Radial Distribution System with Distributed Generation**" being submitted by **Ajit Kumar Mohanty (718014)** is a bonafide research work carried out under my supervision and guidance in fulfillment of the requirement for the award of the degree of **Doctor of Philosophy** in the Department of Electrical Engineering, National Institute of Technology Warangal-506004, Telangana, India. The matter embodied in this thesis is original and has not been submitted to any other University or Institute for the award of any other degree.

Place: Warangal
Date: 20/01/2023

Dr. Suresh Babu Perli
Associate Professor
Department of Electrical Engineering
NIT Warangal

DECLARATION

This is to certify that the work presented in the thesis entitled "**Optimal Location of Charging Station for Electric Vehicles in Radial Distribution System with Distributed Generation**" is a bonafide work done by me under the supervision of **Dr. Suresh Babu Perli**, Associate Professor, Department of Electrical Engineering, National Institute of Technology Warangal, and was not submitted elsewhere for the award of any degree.

I declare that this written submission represents my ideas in my own words and where others ideas or words have been included, I have adequately cited and referenced the original sources. I also declare that I have adhered to all principles of academic honesty and integrity and have not misrepresented or fabricated or falsified any idea / data / fact / source in my submission. I understand that any violation of the above will be a cause for disciplinary action by the Institute and can also evoke penal action from the sources which have thus not been properly cited or from whom proper permission has not been taken when needed.

Ajit Kumar Mohanty

(**718014**)

Date: 20/01/2023

ACKNOWLEDGEMENTS

The research work and the current thesis are outcomes of constant inspiration and support of the kind people around me. I would like to convey my most sincere recognition to each and every one for their respective assists.

Foremost, I would like to express my deepest gratitude to my respected research supervisor, **Dr. Suresh Babu Perli**, Associate Professor, Department of Electrical Engineering, National Institute of Technology Warangal, for his guidance, scholarly input and consistent encouragement. This work is possible only because of the unconditional moral support provided by him. I had great freedom to plan and execute my ideas in research without any pressure. This made me identify my strengths and drawbacks and boosted my self-confidence.

I am very much thankful to **Prof. Srikanth N V**, Chairman of DSC, Department of Electrical Engineering for his constant technical suggestions, encouragement, support and cooperation.

I take this privilege to thank all my DSC Committee members, **Dr. A. Kirubakaran**, Associate Professor, Department of Electrical Engineering, **Dr. A. V. Giridhar**, Associate Professor, Department of Electrical Engineering and **Prof. Srinadh K V S**, Department of Mechanical Engineering, for their detailed technical review, constructive suggestions and excellent advice during the progress of this research work.

I am very much thankful to **Prof. Narasimharaju B. L**, Head, Department of Electrical Engineering for her constant encouragement, support and cooperation.

I wish to express my sincere thanks to **Prof. N.V. Ramana Rao**, Director, NIT Warangal for his official support and encouragement.

I also appreciate the encouragement from teaching, non-teaching members, and the Department of Electrical Engineering fraternity of NIT Warangal. They have always been encouraging and supportive.

Finally, I would like to express profound gratitude to my family members for all they have undergone to bring me up to this stage. I wish to express gratitude to my parents, **Sh. Dhirendra Kumar Mohanty** and **Smt. Rashmi Mohanty**, for their kind support, the confidence and the love they have shown to me. You are my greatest strength, and

I am blessed to be your son. I want to thank my wife, **Mrs. Abhinita Mohanty** for her continuous support and belief in me. You always supported and motivated me and believed in me for who I am. I also would like to thank my sister, **Ms. Archana Mohanty** for being a good friend and understanding me well during this challenging situation.

Ajit Kumar Mohanty

ABSTRACT

The transportation sector's increased use of conventional gasoline led to fossil fuel's quick exhaustion. Consequently, the electrification of the transportation sector served as the primary study focus throughout the decade. Electric vehicles (EVs) have supplanted fossil-fueled vehicles due to the rising cost of fossil fuels and related environmental problems. It is anticipated that their utilisation will increase considerably within a short time. However, several technological and operational difficulties will be brought on by the widespread usage of EVs and their deep integration with the power system.

Interestingly, current academics have been looking at the optimal places to deploy Electric Vehicle Charging Stations (EVCS) due to the electrification of the transportation system and the rising demand for EVs. Inadequate EVCS infrastructure, optimum EVCS sites, and charge scheduling in EVCS are a few examples. Furthermore, a vital EVCS infrastructure would be necessary to partially address a most basic EVs question, namely EVs pricing and range.

In order to increase charging efficiency and reduce owner energy costs, Fast Charging Stations (FCE) must also be used in addition to domestic chargers. That will lessen the impact of domestic chargers on the electrical grid's power quality. The primary elements that significantly impact the development and progress of electricity are the cost of electric vehicles, their autonomy, the charging procedure, and the infrastructure for charging.

The placement of charging stations is a challenging issue involving the transport network and the electrical distribution system. The installation of charging stations within the distribution system must be done to minimise their detrimental effects on the distribution system's operational characteristics. All the considerations mentioned earlier inspire this thesis, which explores the planning of charging stations. Investigating and addressing the planning issue for charging infrastructure may be broadly divided into two groups in this research endeavour.

First the optimal location for Charging Station (CS) is solely taking the distribution system into account. This work proposes an optimal simultaneous method for improving power system performance in a sustainable distribution system that considers EVCS, Distributed Generators (DGs), Shunted Capacitors (SCs) or Distribution Static Compensator (DSTATCOM) and high integration of EVs using fuzzy multi-objective stochastic

optimisation. The main goal of the suggested approach is to 1) minimise active power loss, 2) improve voltage profile, 3) improve substation power factor and 4) deploy the maximum number of EVs to charging stations. In order to develop models for EV battery charging loads, load flow analysis makes use of the Li-ion battery's characteristic curves. The proposed simultaneous fuzzy multi-objective is conducted with and without system reconfiguration. The numerical results indicate that the simultaneous technique with system reconfiguration is computationally efficient and scalable, outperforming the two-stage methodology and the method without system reconfiguration. Simulation results obtained with the Rao-3 algorithm are compared with other conventional algorithms.

Second the optimal location for the CS considers the network's superimposition for distribution and transportation. The multi-objective optimization proposed in this study aims to simultaneously allocate CS, DGs, and SCs at their best possible efficiency. In terms of reducing (a) active power loss costs, (b) voltage deviations, (c) CS capital costs, (d) EV energy usage costs, and (e) DG costs, in addition to fulfilling the number of CS and EVs throughout all zones based on road transport and the electrical network with the help of hybrid Grey Wolf Optimiser (GWO) and Particle Swarm Optimisation (PSO) algorithm.

The suggested solutions to the location problem of charging stations are tested on radial distribution systems for 69 and 118 buses.

Contents

Certificate ii

Declaration iii

Acknowledgements iv

Abstract vi

Contents viii

List of Symbols xii

List of Abbreviations xiv

List of Figures xv

List of Tables xvii

1 Introduction 1
- 1.1 Background . . . 1
- 1.2 Different types of EVs . . . 2
- 1.3 Infrastructure and charging options for EVs . . . 3
- 1.4 EVs' effects . . . 5
  - 1.4.1 EVs' effect on the power grid . . . 5
  - 1.4.2 Effects on the environment . . . 5
  - 1.4.3 Impact on the economy . . . 6
- 1.5 Outline of the planning process for charging stations . . . 6
- 1.6 The proposed work's objectives . . . 6
  - 1.6.1 The optimal location for charging station is solely taking the distribution system into account . . . 7
    - 1.6.1.1 Two-stage placement . . . 7
    - 1.6.1.2 Simultaneous stage placement . . . 7
    - 1.6.1.3 Network reconfiguration placement . . . 8
  - 1.6.2 The optimal location for the charging station considers the network's superimposed for distribution and transportation . . . 8
- 1.7 Organisation of the thesis . . . 8

2 Literature Review 10
- 2.1 Introduction . . . 10
- 2.2 Optimal Placement of EVCS . . . 10
- 2.3 The optimal location for CS is solely taking the distribution system into account . . . 11

2.4 The optimal location for the CS considers the network's superimposed for distribution and transportation. 14
2.5 Optimisation methods to address the charging station placement problem 15
2.5.1 Selection of the optimisation technique 15
2.5.2 Mechanisms for addressing constraints 15
2.5.3 EV optimisation is considered necessary 15
2.6 Summary 18
2.6.1 Limitation 18

3 Two-Stage Optimal Placement of Electric Vehicle Charging Stations in a Distribution System 22
3.1 Introduction 22
3.2 Problem Formulation 23
3.2.1 Fuzzification of Real Power Loss of the DST 23
3.2.2 Fuzzification of Voltage Nodes of the Distribution Network . . 24
3.2.3 Fuzzification of DG Penetration 26
3.2.4 Fuzzification of the EV Power Loss Index 27
3.2.5 Multi-Objective Fuzzy Function for Optimal Sizing and Location of EVCS, DG, and DSTATCOM 28
3.3 Summary of RAO-3 29
3.4 Results and Discussion 32
3.4.1 Cases 32
3.4.1.1 Stage 1 32
3.4.1.2 Stage 2 33
3.5 Summary 34

4 Simultaneous Optimal Placement of Electric Vehicle Charging Stations in a Distribution System 41
4.1 Introduction 41
4.2 Problem Formulation 41
4.2.1 Fuzzification of Real Power Loss of the DST 42
4.2.2 Fuzzification of Voltage Nodes of the Distribution Network . . 43
4.2.3 Fuzzification of DG Penetration 45
4.2.4 Fuzzification of the EV Power Loss Index 46
4.2.5 Multi-Objective Fuzzy Function for Optimal Sizing and Location of EVCS, DG, and DSTATCOM 47
4.3 Modeling Battery Charging Load for EV 47
4.4 Summary of RAO-3 49
4.5 Results and Discussion 50
4.5.1 Analysis of the Enhancement of Distribution Load Growth . . . 54
4.5.2 Analysis of Enhancement of EV Load 54
4.5.3 Analysis of Transient Responses 55

4.6 Summary 55

5 Optimal Network Reconfiguration of Distribution System with Electric Vehicle Charging Stations, Distributed Generation, and Shunt Capacitors 67
5.1 Introduction 67
5.2 Problem Formulation 67
5.2.1 Substation Power Factor Membership Function: 68
5.2.2 DGs penetration membership function: 68
5.2.3 Active power loss membership function: 69
5.2.4 Distribution system voltage membership function: 70
5.2.5 Distribution Network Reconfiguration methodology 71
5.2.6 Optimal allocations of EVs, DGs, and SCs using a multi-objective fuzzy function: 71
5.2.7 Battery charging load modelling for EVs: 72
5.3 RAO-3 algorithm 73
5.4 Result and discussions 76
5.4.1 Scenario 1 76
5.4.2 Scenario 2 77
5.5 Summary 80

6 Optimal Placement of Fast Charging Station for Integrated Electric-Transportation System using Multi-Objective Approach 93
6.1 Introduction 93
6.2 Problem Formulation 93
6.2.1 Development Cost of FCEs (DFC) 94
6.2.2 Energy Consumption of EVs User Cost (EUC) 95
6.2.3 Active Power loss of Distribution Network Cost (CPDN) 95
6.2.4 Cost of DGs (DGC) 96
6.2.5 DVT 96
6.2.6 Multi-Objective Function 97
6.2.6.1 Constraints 97
6.3 Overview of Hybrid GWO-PSO Algorithm 97
6.3.1 Encircling the Victim 98
6.3.2 Hunting Procedure 99
6.3.3 Exploring and Attacking a Victim 99
6.3.4 Hybrid GWO-PSO 99
6.4 Results and Discussion 102
6.4.1 Proposed Methodology 102
6.4.2 Scenario 1: Optimum Placement of FCE in DST Conjunction with Transportation Network 106
6.4.3 Scenario 2: Optimal Positioning of DGs in DST with Previous Optimum FCE Load 108

6.4.4 Scenario 3: Allocation of DGs and SCs in DST Optimally Using the Previous Optimal FCE Load . . . 108
6.4.5 Scenario 4: Simultaneous Optimum Location and Sizing of FCE, DGs, and SCs in DST . . . 109
6.5 Summary . . . 109

7 Conclusion **122**
7.1 Summary and Important Finding . . . 122
7.2 Future Scope . . . 123

Bibliography **125**

Author's Publications **138**

List of Symbols

$RPLX$	Real power loss index
RPL_{DGSC}	Active power loss with DG and DSTATCOM
RPL_{Base}	Real power loss with base case
P^{DG}	Capacity of DG
ndg	Number of DG
P_j^{load}	Active power load connected at j^{th} bus
nb	Total number of buses in the distribution network
Pl	Active power loss of the distribution network when DG or DSTATCOM or EV charging stations are installed
Ql	Reactive power loss of the distribution network when DG or DSTATCOM are installed
$EVPI^{EVLD}$	Active power loss with EV and other load losses
$EVPI^{LD}$	Load losses
F_{zdc}	Multi-objective fuzzy functions for optimum location and sizing of DG and DSTATCOM
F_{ze}	Fuzzy objective functions for optimum location and sizing of EVCS
F_{zs}	Multi-objective fuzzy functions for simultaneous optimum location and sizing of EV, DG and DSTATCOM
P_k^{DG}	DG power injection at the nodes in the distribution network
Q_m^{sc}	DSTATCOM reactive power injection at the nodes in the distribution network
$itrmax$	Maximum iteration
itr	Present iteration
$EV_{n,z}$	Total no-of committed EVs in zone
zn	No-of zones in the assumed study area
C_{fixed}	The fixed cost of charging stations
C_{land}	Land rental cost yearly
C_{cond}	Development cost of chargers
n_y	Number of years in the study period
$NC(i)$	Number of connectors in charging stations in i^{th}FCE period

PR_{EV}	Probability of charging of EVs in hour (h) in a day
P_{cg}	Charging connector rated power
$L(zn,i)$	Trajectory length between zone zn and i^{th} FCE
CSE	Specific energy consumption of EVs
EP_h	Electricity price in dollars
n_s	No-of seasons
N_{hr}	Total no-of hours of all seasons in a year
d	Index of DG
$P_{dg,d}$	Active power generated by d^{th} unit
$Cost_{INV,d}$	Cost of investment of each d^{th} unit
C_{INV}	Cost of Investment
C_{OPR}	Cost of operation
C_{MAT}	Cost of Maintenance
TL_h	No-of hours in a year
n_{yr}	Total no-of years for planning of DGs
n_{dg}	Number of DGs
nb	Bus number of the distribution system
$V(j)$	Voltage of j^{th} bus
N_{FCE}	No-of FCE
NP_{FCE}	No-of possible FCE

List of Abbreviations

ABC	Artificial Bee colony
CPDN	Active power loss of distribution network cost
CS	Charging Stations
DFC	Development Cost of FCE
DG	Distributed Generators
DGC	Cost of DGs
DST	Distribution System
DSTATCOM	Distribution Static Compensator
DVTs	Voltage Deviations
EUC	Energy Consumption of EV user cost
EVs	Electrical Vehicles
GWO	Grey Wolf Optimizer
NTEV	Total number of EVs
pf	power factor
PSO	Particle Swarm Optimization
SCs	Shunt Capacitors
SS	Substation
SN	Substation
TGL	Gross power loss of the distribution network without EV load
TPL	Total power loss of the distribution network including EV load
TNL	Transportation network without EV load
TLBO	Teaching-Learning-Based Optimization

List of Figures

1.1 List of nations where the sale of new consumer vehicles will consist primarily of EVs in 2020 . . . 2

2.1 The charging station framework only considers the distribution system . 20
2.2 The charging station framework considering both distribution system and transportation network . . . 21

3.1 Reduction of real power loss. . . . 24
3.2 Bus voltage. . . . 25
3.3 SS power factor. . . . 26
3.4 DG penetration. . . . 27
3.5 EV real power index. . . . 28
3.6 RAO-3 algorithm implementation flow chart. . . . 31
3.7 Voltage Curve. . . . 33
3.8 Fitness Curve of DG and DSTATCOM. . . . 33
3.9 The single-line diagram of the 69-bus radial distribution system of two-stage methodology. . . . 34

4.1 Reduction of real power loss. . . . 43
4.2 Bus voltage. . . . 44
4.3 SS power factor. . . . 45
4.4 DG penetration. . . . 46
4.5 EV real power index. . . . 47
4.6 Li-ion battery charging characteristics. . . . 48
4.7 RAO-3 algorithm implementation flow chart. . . . 51
4.8 Voltage curve. . . . 52
4.9 Fitness curve. . . . 52
4.10 The single-line diagram of the 69-bus radial distribution system of Simultaneous methodology. . . . 53
4.11 The impact of the rising DST system load on the performance of the 69-bus radial distribution system. . . . 54
4.12 EVCS voltage transients. . . . 55

5.1 Fuzzy Membership function . . . 70
5.2 Li-ion Battery Charging Characteristics . . . 72
5.3 Rao-3 flow chart for the placment of EVCS, DGs, and SCs . . . 75
5.4 fitness curve . . . 77
5.5 Voltage profile curve . . . 77
5.6 Single line Diagram of 69 bus with EVCS, DGs and SCs . . . 78
5.7 Voltage curve before and after reconfiguration . . . 79
5.8 fitness curve . . . 79

5.9 Voltage profile curve 80
5.10 Single line Diagram of 69 bus with EVCS, DGs and SCs 81
5.11 EVCS Voltage transients. 91

6.1 Illustrative zones with area. 94
6.2 Hybrid GWO-PSO flowchart. 101
6.3 Zone EV population. 103
6.4 118 bus distribution system in the proposed testing area. 104
6.5 Load curve on an hourly basis for various seasons. 105
6.6 EVs' probability of being charged. 105
6.7 Optimal Pareto-front 107

List of Tables

3.1 DG optimum location and sizing 36
3.2 DSTATCOM optimum location and sizing 37
3.3 Performance comparison of 69 bus system 38
3.4 Optimum number of EV and optimum location of EVCS 39
3.5 Performance of 69 bus radial distribution system after installation of EVCS 40

4.1 DG optimum location and sizing 57
4.2 DSTATCOM optimum location and sizing 58
4.3 Optimum number of EV and optimum location of EVCS 59
4.4 Performance comparison of 69 bus system 60
4.5 The impact of increased Distribution load on the 69 bus 61
4.6 Impact on Active power loss (kW) in 69 bus radial DST 62
4.7 Impact on Active power (kW) consumed from SS in 69 bus radial DST . 63
4.8 Impact on Reactive power (kVAr) consumed from SS in 69 bus radial DST 64
4.9 Impact on minimum distribution bus node 69 bus radial DST 65
4.10 Comparison results 66

5.1 DG optimum location and sizing 82
5.2 SCs optimum location and sizing 83
5.3 Optimum number of EV and optimum location of EVCS 84
5.4 Performance comparison of 69 radial bus system 85
5.5 Performances of distribution system after network reconfiguration . . . 86
5.6 DGs optimum location and sizing 87
5.7 SCs optimum location and sizing 88
5.8 Optimum number of EV and optimum location of EVCS 89
5.9 Performance comparison of 69 bus system 90
5.10 Comparison results 92

6.1 Study parameters. 104
6.2 The optimum FCE location and the optimum number of EVs 110
6.3 Objectives of scenario 1 that are optimal 111
6.4 Scenario 2: Optimal location and sizing of DGs 112
6.5 Objectives of scenario 2 that are optimal 113
6.6 DGs' optimal location and sizing for scenario 3 114
6.7 Optimal location and sizing of SCs for scenario 3 115
6.8 Scenario 3's Optimal objective parameters 116
6.9 Optimal FCE location and EVs optimal numbers in scenario 4 117
6.10 Optimal positioning and sizing DGs for scenario 4 118
6.11 Optimal positioning and sizing of SCs for scenario 4 119

6.12 Scenario 4's optimal objective parameters 120
6.13 Four scenarios' comparison results 121

Chapter 1
Introduction

1.1 Background

The increased demand for traditional fossil fuels caused several consequences that hurt the environment. Global climate change, resource depletion, and excessive CO_2 emissions that cause the greenhouse effect are a few of their unfavorable effects [1]. In order to minimise CO_2 emissions and contain the earth's temperature increase, the Paris Agreement was signed. The emphasis was switched to the generation and utilisation of renewable energy sources and the ensuing technologies to counteract such impacts. Despite all technological innovations, the transportation industry still accounts for around 25 % of greenhouse gas emissions [2]. Utilising renewable energies has emerged as a more reliable supply option to provide social and economic advantages induced by energy use while minimising the environmental effects of the emissions of the broadest range of pollutants.

In order to prevent a significant decline in the global economy, it is intended to keep the pace of emissions nearer to the predicted value as renewable and cleaner transportation technologies develop. Due to the factors above, there should be a significant change in focus toward studying and implementing Electric Vehicles (EVs). Propelled by sustainable, renewable energy sources, EVs are crucial to a working transportation system.

Additionally, EVs may be a lifesaver in declining natural gas and oil resources. These points demonstrate the need for EVs, but significant optimisation and hybridisation are also necessary for a seamless transition from conventional transportation to electricity [3]. Studies suggest that by 2030, EVs might cut Carbon footprints by 28 % [4]. Unfortunately, the two main obstacles that could impact the general public when switching to EVs are the high price and the inadequacy of charging infrastructure. Over 2020 to 2027, various industries and governments are anticipated to expand the global EV industry to USD 974,102.5 million [5].

EVs advanced significantly in several nations in 2020 despite challenging conditions and the Covid-19 pandemic's detrimental effects on the automobile industry. As seen in Fig. 1.1, as many as 13 nations were able to increase sales of new light automobiles from EVs to surpass 10 % in 2020 [6]. According to the International Energy Agency's (IEA)

framework, EVs and plug-in hybrids will account for 50 % of lightweight automobile purchases by 2050 [7].

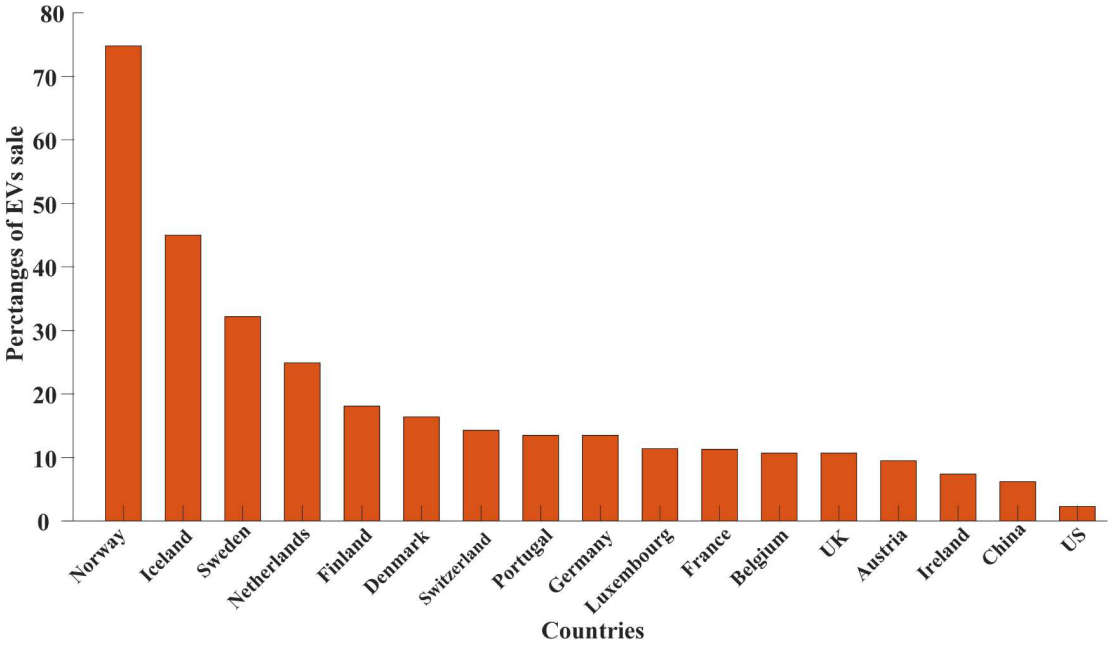

Figure 1.1: List of nations where the sale of new consumer vehicles will consist primarily of EVs in 2020

1.2 Different types of EVs

EVs are the answer to a thriving global fight against climate change strategy. In addition, EVs may save lives when depleting natural gas and oil supplies. The batteries provide the necessary energy in automobiles and lorries, which must be recharged by plugging them in. Plug-in Electric Vehicles (PEVs) come in various styles, each with unique attributes. Battery Electric Vehicles (BEV) and Hybrid Electric Vehicles (HEV) are two forms of PEVs. Photovoltaic and fuel cell electric vehicles are two other electric drive vehicles [8, 9].

1. A BEV is entirely electric. The internal battery provides all of the vehicle's electricity. BEVs are anticipated to go over 100 miles with a single charge in their early variants. After then, a power supply will be plugged into the battery to charge them.

2. In an HEV, the vehicle is propelled by an electric motor and regular internal combustion. The internal computer manages the car's gasoline and electric engines to provide power and achieve excellent overall fuel economy. The electric motor in these vehicles is supported by an onboard battery, which will be fully recharged when the car is plugged in. Additionally, the batteries recycle the energy recovered during braking and retardation to power the automobile. The automobile switches back to regular hybrid operation whenever the plug-in battery is exhausted. Parallel-hybrid, series-hybrid, and combination series-parallel hybrid topologies are among the types of HEVs that can be built.

1.3 Infrastructure and charging options for EVs

Infrastructure for adequate charging is urgently needed to ensure the seamless operation of EVs. A battery charger is a component that processes and controls the electrical current that flows through it to transmit energy to an EV battery. EV chargers include a rectifier that converts AC to DC to charge an EV battery. EVs charging techniques are categorised as follows:

1. Direct contact is used in the conductive charging technique to transmit power. For energy transfer, this method connects the electronic equipment with a conductor. It is easy to use and very effective. On-board or off-board techniques are both acceptable. An off-board charging is placed at fixed places to provide fast charging service, whereas onboard charging is typically used for slow recharging, and the recharging process is completed inside the EV [10].

2. An EV battery receives electricity using inductive charging, commonly referred to as contactless charging, using an electromagnetic field. Because it offers electrical safety in all weather conditions, inductive chargers have this advantage. Poor performance and significant power loss are inductive chargers' flaws [11].

3. With a battery switching station, consumers can exchange their dead battery for one wholly charged. Since batteries are gathered and controlled in centralised places, it provides many advantages, including extended battery lifespan, low time requirements, and relatively low management costs [12].

The primary location for recharging electric vehicles is at charging stations. Amongst the most critical elements in the introduction of EVs is efficient charging infrastructure. The charging levels are described as follows by the Electric Power Research Institute.

1. Level 1 uses 120 V AC home plugs with a current 15 A (12 A useable) or 20 A (16 A useable) processing capacity, where a 16 A plug charged in half the time of a 12 A plug. Level 1 can consume between 1.4 and 1.9 kW of power [12, 13]. Accordingly, depending on the size and type of the battery, this level of charging takes 8 to 16 hours to charge EVs battery fully. The most affordable and practical method of recharging at home is at this level. The slowest and cheapest typical level is present in both commercial and residential buildings. Infrastructure expenses for residential Level 1 chargers are projected to be between $500 and $880 [14].

2. The standard definition of Level 2 is that it is the most common and popular approach for both residential and commercial facilities; For residential installations, this level allocates a single-phase 240 V AC with a 40 A current capacity, and for commercial installations, a three-phase 400 V AC with an 80 A current capacity [15]. EVs battery may be charged in 4 to 8 hours with this level of charging, which has a power range of 7.7 to 25.6 kW [12, 13]. Due to the accessibility of 240V AC connection, EV customers may typically recharge EV batteries overnight without impacting their household electronics. Installation expenses for residential Level 2 infrastructures are projected to be between $2150 and $2300 [14], whereas those for commercial stations are higher at around $ 15000 [16]. Customers strongly identify with Level 2 techniques to their quick recharging times and standardised vehicle-to-charger connections. The connections used to power common domestic appliances like electric ovens and laundry dryers/washers are also used by Level 2 EV supply devices [17]. On the other hand, a household's current demand could rise by up to 25 % [18].

3. With a DC quick charging, level 3 charging, which is appropriate for private and public use, aims to give customers an experience resembling a conventional petrol pump. 80 % of a battery's capacity may typically be reached via rapid charging in 10 to 15 minutes, according to the size and kind of battery. Since the final 20 % of a battery charge for an EV takes a long time to complete, DC charging is often measured up to 80 % [19]. In Level 3, an off-board charger typically converts AC to DC; as a result, DC power is supplied to the EVs [13]. In order to allow quick EV charging, a 3-phase connection with 208–600 V AC and a maximum capacity of 200 A is used to power the off-board charger. Level 3 charging infrastructure expenses range from $50,000 to $160,000, based on the component's grade and type.

1.4 EVs' effects

Future electric power grid penetration is expected to be significantly influenced by the present expansion of EVs. EVs may burden power infrastructures heavily due to their additional power consumption. On the current distribution systems, these extra loads have many negative repercussions. Contrarily, the widespread use of EVs equipped with intelligent technology has beneficial effects on the environment and economics. An EV increases the usage of renewable energy sources and reduces the emission of greenhouse gases into the atmosphere [20]. Information on these different implications is provided in the following subsections.

1.4.1 EVs' effect on the power grid

Considering that the transport industry is regarded as the second most significant source of carbon emissions, EVs are the focus of substantial interest in addressing the problems caused by global climate change [21]. Even a conventional distribution system will need more power if EVs are deployed widely. This case indicates a wide range of significant negative effects on this distribution system. Additionally, the distribution system benefits noticeably from EVs. Following are some categories for how EVs affect distribution networks:

1. **Negative effect**: Voltage instability, a rise in peak load, power quality issues, power loss, transformer overheating, and overload are some of the negative effects of EVs on the current distribution system [22–28].

2. **V2G technology's beneficial effects**: Due to its unique capabilities of discharging energy stored back into the distribution system, V2G technology is the most valuable opportunity to adopt an EV in an electrical network. Due to this technique, the power system's reliability is improved, and system expenses are decreased [29, 30].

1.4.2 Effects on the environment

Instead of using fuel-based conventional techniques, EVs get their energy needs from the power grid, which lowers carbon emissions. Additionally, the increased use of renewable and sustainable energy sources to recharge EV batteries can help reduce pollution emissions even more [31]. Using fossil fuel or other polluting-fuel-based electric power

systems to charge EVs could increase greenhouse gas emissions. However, the correct inclusion of renewable power has the potential to lower Greenhouse gas and other pollutant emissions both from generating electricity and transportation [32]. Since only a few businesses can recycle lithium-ion batteries, dead lithium-ion batteries might contaminate groundwater when disposed of in landfills [33].

1.4.3 Impact on the economy

From the viewpoints of EV owners and utility companies, the economic effects of EVs can be seen [34]. While EVs are more efficient than internal combustion engines, owners believe that their vehicles' operational and fuel expenses are lower than those of conventional vehicles [35]. From the viewpoint of the power grid, the addition of EVs to a distribution system raises the system's cost and other losses; nevertheless, a suitable charging plan can significantly reduce those negative effects [36].

1.5 Outline of the planning process for charging stations

The location of CS is an essential planning issue that involves the best placement and sizing of CS while considering financial factors, distribution system operational characteristics, and the comfort of EV users. The qualities of an effective CS placement model include the following:

1. Both parameters for the distribution and transportation systems must be considered in the model.
2. The model needs to consider the economic aspects of the installation of CS.
3. The model should incorporate the comfort of EV users.
4. The distribution system's stability must be considered in the model.
5. The model must use lower computational expenses to achieve the output planning outcomes.

1.6 The proposed work's objectives

The objective of this thesis is to analyse many aspects of the issue of planning for charging stations. Using meta-heuristic algorithms to solve the location problem, formulating the charging station location, and sizing are the main tasks in this research study. The following list highlights the significant outcomes of the research presented in this thesis.

1. To lessen the effect of the EVCS, the two-stage integration of the distribution system, charging station, DSTATCOM, and DGs.
2. To improve the substation power factor, simultaneous integration of the distribution system, charging station, DSTATCOM, and DGs.
3. Further, improving the distribution system's performance distribution system reconfiguration is utilised for simultaneous integration of the distribution system, charging station, Shunt Capacitors (SCs), and DGs.
4. The distribution system's stability must be considered in the model.
5. Simultaneous optimal positioning of fast charging stations (FCE), DGs, and SCs in the radial distribution system coupled via a transportation network

Investigating and addressing the planning issue for charging infrastructure may be broadly divided into two groups in this research endeavour. Following are the two subdivisions:

1.6.1 The optimal location for charging station is solely taking the distribution system into account

1.6.1.1 Two-stage placement

The optimal size and positioning of DGs, DSTATCOM, and EVCS for distribution systems are addressed in this section using a two-stage fuzzy multi-objective method. In the first stage, a fuzzy technique is utilised to size and allocate DGs and DSTATCOM optimally to increase the substation power factor, reduce real power loss, and enhance the distribution system's voltage level. The optimal sites for EVCS and the number of EVs at the EVCS are determined using a fuzzy method in the second stage distribution system integrated with DGs and DSTATCOM.

1.6.1.2 Simultaneous stage placement

Traditional multi approaches do not consider the substation pf for EVCS, DGs, and DSTATCOM optimal allocation. A fuzzy multi-objective strategy was used in this work to assign EVCS, DGs, and DSTATCOM simultaneously in the electrical distribution network. As a result, in this work, simultaneous EVCS, DGs, and DSTATCOM allocation in the electrical distribution system was done with a fuzzy multi-objective strategy

for improved distribution system performance, including reducing active power loss, enhancing the voltage level, and keeping SS pf at the preferred level. Furthermore, models for EV charging loads were created using the load flow analysis and the characteristic curves of Li-ion batteries. The current system's performance under enhanced EV and distribution network loads is also demonstrated.

1.6.1.3 Network reconfiguration placement

The electrical distribution system is reconfigured in this analysis, and the optimum simultaneous EVCS, DGs, and SCs are deployed. The proposed technique achieves its primary goal of (a) reducing active power loss, (b) enhancing the substation power factor, (c) boosting the distribution system's voltage profile, and (d) deploying the optimum number of EVs to EVCS. The influence of transient battery charging load impacts node voltages at the EVCS, and with the help of DGs and SCs, node voltages are kept at acceptable levels during steady-state charging.

1.6.2 The optimal location for the charging station considers the network's superimposed for distribution and transportation

A multi-objective optimisation for the simultaneous optimal allocation of Fast Charging Stations (FCEs), DGs, and Shunted Capacitors (SCs) is used. The proposed Pareto dominance-based hybrid methodology incorporates the advantages of the Grey Wolf Optimiser and Particle Swarm Optimisation algorithm to minimise the objectives of 118 bus radial distribution systems. The proposed method outperforms some other existing algorithms in terms of minimising (a) active power loss costs of the distribution system (CPDN), (b) Voltage Deviations (DVT), (c) FCE development costs (DFC), (d) EV energy consumption costs (EUC) and (e) DG costs (DGC) as well as satisfying the number of FCEs and EVs in all zones based on transportation and the electrical network.

1.7 Organisation of the thesis

This thesis is organised into six chapters. The work presented in each chapter is outlined as follows:

Chapter 1 provides a history of the planning challenge for the charging facilities for electrical Vehicles.

Chapter 2, provides a description of the research that has already been conducted on the subject of planning charging infrastructure.

Chapter 3 suggests a fuzzy categorised two- stage method for EVCS, DGs, and DSTATCOM optimal sizing and positioning using the RAO-3 algorithm for 69 bus radial distribution systems.

Chapter 4 suggests a fuzzy categorised simultaneous method for EVCS, DGs, and DSTATCOM optimal sizing and positioning using the RAO-3 algorithm for 69 bus radial distribution systems. Li-ion characteristic curves are used to develop P and Q load models for EV battery charging. The node voltages at the EVCS are impacted by the transient battery charging load, and at steady state charging, the node voltage is maintained fair values with the help of DGs and DSTATCOM. Additionally, the current system's performance under enhanced EV and distribution network load is illustrated.

Chapter 5 suggests a fuzzy categorised simultaneous distribution network reconfiguration method for EVCS, DGs, and DSTATCOM optimal sizing and positioning using the RAO-3 algorithm for 69 bus radial distribution systems.

In **Chapter 6**, a multi-objective hybrid GWO-PSO algorithm is shown for the simultaneous optimal placement of fast charging stations, distributed generators, and shunt capacitors in an interconnected electric transportation system.

Chapter 7 summarises the research's significant findings and outlines the potential future study in this paradigm.

Chapter 2
Literature Review

2.1 Introduction

This chapter discusses the body of research on several facets of formulating the optimal placement for charging stations and using optimisation techniques to address the challenge. This chapter concludes with a summary of the literature review, the shortcomings of the available literature, and the scope of the current research.

2.2 Optimal Placement of EVCS

Astonishingly, the innovation and spread of new energies have garnered much attention in today's society. Most buyers, therefore, embrace and perceive innovative energy electric vehicles as a representation of the development and application of new energy. The adoption of electric and hybrid automobiles is anticipated to offer the best chances for lowering the use of fossil fuels in transportation. The need for EVCS is growing in tandem with the growth in EV sales. In order to properly handle the charging requirements of EVs, the distribution of EVCS must be as reasonable as possible.

The exponential growth of EVs presents a new challenge for the infrastructure of the distribution system and utility operators. The distribution system may be significantly impacted by high electrical power demand brought on by the integration of EVs, bus voltages, power loss, voltage imbalance, and power efficiency. Additionally, as more EVs are on the road, more effective EVCS systems and shorter EVs charging times are needed. Therefore, rapid charging in EVCS is practical for recharging an EV's battery in 20 to 30 minutes [37]. Besides its disadvantages, fast charging negatively affects the distribution network, which might be avoided with careful EVCS planning [38].

Meanwhile, in the past ten years, research subjects on the optimal placement for Charging Stations (CS) and the effect of EV load on the distribution network have grown in importance [39]. Investigating and addressing the planning issue for charging infrastructure may be broadly divided into two groups in this research endeavour. Following are the two subdivisions:

1. The optimal location for CS is solely taking the distribution system into account.

2. The optimal location for the CS considers the network's superimposition for distribution and transportation.

2.3 The optimal location for CS is solely taking the distribution system into account

The utility operator strategy is used to position CS in the optimum possible way, taking the distribution system solely into account. The utility operator's placing of EVCS considers factors, including reducing bus voltage and the distribution system's overall power loss. Poorly coordinated EVCS inclusion into the distribution system may result in problems with the control, management, and operation of the electrical system and risk its stability by creating a new surge load for the power grid [40, 41]. Chen et al. [42] could determine the charging station's optimum placement by considering the operating, power loss, and voltage deviation cost as indicators with the help of the balanced mayfly algorithm. Moradi et al. [43] suggest power loss, voltage profile, and EV charging costs as goal functions for the research framework of where to locate charging stations and renewable technologies most effectively using a differential evolution algorithm. Gomez et al. [44] have built a straightforward method to determine the effect of charging devices on a transformer, cable, circuit breakers, and switches in distribution systems. Hadley et al. [45] investigated the need for hydrocarbon resources due to the possible usage of EVs in distribution networks. Sharma et al. [46] proposed a system for smart distribution to evaluate the problems connected with EVs' uncontrolled charging. The effect of charging EVs on British distribution systems was examined by Papadopoulos et al. [47] while taking into account the unknowns surrounding residential loads. Dubey et al. [48] studied the effect of EV charging on home distribution networks and discovered that secondary circuit voltage profiles were more significantly impacted than primary line voltage profiles. To maximise the power given to EVs, Richardson et al. [49] have suggested a linear programming-based method for identifying the optimum charging rate for a vehicle. According to Salihi et al. [50], a solution based on a two-step process is suggested to best schedule EVs' reactive and active power. The method's initial stage includes real power scheduling, which aims to reduce the total costs aggregators must bear for charging. The second aspect of the strategy is reactive power scheduling, which aims to reduce the bus voltages' deviation from the desired levels. Zhang et al. [51] provide a probabilistic approach for aggregated EVs and their effect on the ideal load profile of the power network. A new electrical corridor will be needed, which is costly,

to handle a rise in the development and redevelopment by EVs in the future. DGs and EVCS are installed simultaneously in the distribution systems to find a solution to this issue.

The sizing and positioning of EVCS without the usage of DGs were the main focuses of the abovementioned strategies. The changing distribution system landscape has increased interest in how EVs, battery banks, and DGs interact in a microgrid setting. Chen et al. [52] developed a novel GA-based technique for the optimum integration of EVs in microgrids taking into account the unpredictability in photovoltaics, energy market price, and load demand. Longo et al. [53] devised a MILP-based method for the best plan for a rapid charging station taking into account financial indicators. Kumar et al. [54] created a bi-level optimisation model for allocating battery energy storage systems and wind production entities with supplementary provisions in a distribution system. Ahmad et al. [55] presented an ideal energy-management system to reduce the cost of energy used to charge the EV. Sabillion et al. [56] suggested a dynamical schedule strategy based on the MILP framework to maximise the cooperative functioning of PVs and EVs in a home distribution system employing energy storage devices.

DGs are electrical energy sources that provide electricity at the unity power factor, and they include solar panels, fuel cells, and microturbines (as discussed in the literature previously mentioned). DSTATCOM or shunt capacitors (SCs). Sirjani et al. [57] thoroughly analysed numerous research studies on the optimum sizes and locations of DSTATCOM in the distribution network. The DSTATCOM allocations issue was proven to have aims such as minimal power losses, limiting voltage fluctuations, enhancing voltage stabilities, and increasing reliability measures. By using the differential evaluation approach for DSTATCOM best allocation in the distribution system, Jazebi et al. [58] minimised power losses and bus voltage variations. Taher et al. optimised DSTATCOM placements and size in the 33 and 69 radial distribution networks using an immune method to reduce power loss. In order to further minimise real power loss, DGs are integrated with DSTATCOM in the distribution system [59–62]. The concurrent incorporation of DSTATCOM and DGs while EVCS-loading reduced the power loss and voltage fluctuation described by Pratap et al. [63].

Mohammadi et al. [64] developed and implemented an optimisation method to address the issue of SCs location and active power conditioner sizing in distribution networks for power quality enhancement. In order to minimise system power losses, optimum simultaneous deployment of DGs and SCs in the distribution network was proposed

in [65–68]. A two-stage system was put forth by Gampa et al. [69] for the best placement of EVCS, DGs and SCs.

In order to promote the use of EVs in mobility in the future, network reconfiguration is a valuable strategy. The distribution system's voltage stability and network losses are both impacted by the introduction of electric vehicles. Reconfiguring the distribution network helps to lessen the effects of this.

Utility companies now have a tremendous operational option to use the available tie lines. Network reconfiguration involves rearranging a system's topological structure by controlling distant sectionalising switch and tie switches to achieve specific goals while satiating all operational requirements without islanding any nodes [70]. The radial topology of the system should be retained, which is the most fundamental restriction. By reducing losses and voltage variation, balancing load, and improving dependability, network reconfiguration seeks to optimise the grid's performance.

The subject of network reconfiguration in the presence of EVs has recently received much attention due to the potential repercussions. For managing congestion and reducing line loss in distribution networks with high EV penetration, Huang et al. [71] suggest combining dynamic tariff and network reconfiguration. Cui et al. [72] investigate network reconfiguration with random, uncoordinated delay and apex delay charging solutions for EVs to reduce losses in the distribution system. In the case of a peak-avoiding delaying charging approach, the charging demand for EVs is shifted to off-peak hours, and the charging of EVs is delayed by an arbitrarily long amount of time. Rostami et al. [73] study the reconfiguration of a distribution system to reduce network costs while considering various EV charging patterns. Kavousi et al. [74] presents another work along the same lines. Rahmani et al. [75] use a combination of network reconfiguration and incentive-based management of EV fleets to reduce a distribution system's total operating cost. In conclusion, the optimum network reconfiguration method can increase the usage of EVs in smart grids.

In conclusion, utility operators provide electric power for every connected electric load in resident, commercial, and industrial areas. The parameters of the distribution system would be impacted by where the new loads are placed. As a result, the placement of EVCSs under the utility operator method optimises the distribution system's active power loss and voltage deviation. The suggested framework for the optimum position for charging stations is shown in Fig. 2.1, which only takes the distribution system into consideration.

2.4 The optimal location for the CS considers the network's superimposed for distribution and transportation.

The optimum location for charging stations involves interacting with the transport and distribution networks and is a non-convex non-combinatorial problem. Options for charging station locations should consider distribution and transportation systems.

To maximise the revenues from the CS through EV charging, the charging station owner pays all installation-related expenditures. As a result, the owner of the CS looks for CS sites with the highest revenues and lowest outlays. In order to determine the best CS location, the CS owner strategy considers the investment [76–78], operation [79, 80], maintenance [81] and land costs [82, 83].

The location of CS influences how EV users charge their vehicles. In order to estimate the predicted charging demand and the anticipated EV user cost, EV user behaviour is also considered. By employing hourly electric grid load scenarios, ac power flow has also estimated the expected cost of additional grid loss brought on by EV charging [84, 85].

Fast Charging Stations (FCE) are a capital-intensive component of the transport system; thus, their location must allow for a comprehensive and effective travel service [86]. Additionally, while employing a suitable spatial and temporal resolution, the planning paradigm has considered individual EV drivers' mobility [87].

The locations of the charging stations were chosen from a city planner's point of view, without consideration for utility operators, CS owners, EV users, or potential growth in the EV population. Therefore, this research focuses on the utility operators, EV owners and EV users' approach to enhancing performance in the distribution network, investor profit and charging preference of an EV user.

The FCE, a common attribute, has been assigned using the planning approach presented in the abovementioned articles. Concurrently, adding EVs to the electrical grid could increase peak demand, voltage drop, and energy loss. DGs and SCs are incorporated into the distribution system to reduce losses, enhance the voltage profile and balance the reactive power demand. The suggested framework for the optimum position for charging stations is shown in Fig. 2.2, which the network's superimpostion for distribution

and transportation.

2.5 Optimisation methods to address the charging station placement problem

The optimal positioning of the charging station problem has a sophisticated and multivariate objective function.

2.5.1 Selection of the optimisation technique

The fascinating exemplar is meta-heuristics, which operate on a method of preliminary guessing that is enhanced throughout finding as the algorithm identifies the optimal answer for the given mathematical model. Meta-heuristics require little to no data about the locations and training data and processes on a method of preliminary guessing. Despite systems with equal and unequal constraints, these algorithms can produce a viable yet best solution. The optimal answer is slower and requires much training data with machine learning methods. It is also important to note that multi-objective optimisation strategies have been created that could also handle the optimisation of several goals and produce results that do not contradict each other [88].

2.5.2 Mechanisms for addressing constraints

Constraints are typically set on the fitness values of evolutionary algorithms. Once a restriction is broken, a significant penalty is introduced, instantly increasing the fitness function's weight and causing the algorithms to recognise it as a quasi-solution.

Another strategy is referred to as the "constraint adjustment" method, in which a constraint is rounded off or shifted to a nearby feasible area if a decision variable's position on the restriction area violates the constraint. It is up to the researchers to choose the optimal approaches for the needed optimisation challenge, even if each technique has pros and cons for different optimisation situations [89].

2.5.3 EV optimisation is considered necessary

The innovation for creating EVs is currently in its infancy. The current vehicular transportation system is most designed for traditional systems, and in order for EVs to fully maximise their utility, they still need to evolve and acclimatise to this system [90, 91].

Implementing meta-heuristic-based evolutionary algorithms that can keep providing adaptable and dependable solutions for complicated EV innovations, beginning from their production, configuration, operation, and placement, is the most significant domain of study in EV optimisation [92].

"Goldberg's view" (1989) accurately illustrates how effective meta-heuristics are for solving real-world situations [93]. According to the article, optimisation can be used as a reliable and effective technique to identify the optimum solutions for most challenges with minimal to no knowledge of the solution's previous performance.

The disadvantage of using meta-heuristic optimisation approaches is the lack of guarantee that the chosen optimising technique will produce the optimum possible answer to the given situation. Further tuning may be necessary to address the ambiguity in how well meta-heuristics function in confined and unrestrained scenarios. It is not always a sensible choice to use single-objective optimisation techniques for multiobjective optimisation through different issue formulation methods. The infamous "No free lunch theory" [94] asserts that not every optimisation technique can solve every optimisation issue.

This variance in productivity among the metaheuristics can be attributed to many factors. First, every metaheuristic is just a modified form of an arbitrary search strategy that scours the search space in quest of a more compelling answer. Every search situation is different; for instance, swarm intelligence iteratively searches the search area depending on the animal, bird, fish, and other foraging behaviours [95]. Another search method involves the formation of the answer over time using an evolutionary approach that adheres to a predetermined set of parameters, intending to improve the solutions' accuracy [96] continually. In addition, "human behaviour-based algorithms" [97, 98] have gained popularity because of their simplicity, convenience of use and capacity to solve challenges involving both single and multiobjective optimisation that are limited and unrestrained.

The second major drawback is the optimum trade between exploration (diversifying solutions focused on global searching) and exploitation (intensifying solutions focused on local search) [99]. The suggested algorithms may efficiently traverse the search area because they can produce solutions with a high diversification for each iteration; however, the solutions' accuracy is lacking. In the opposite situation, algorithms that prioritise further exploiting a particular section of the search panorama could be unable to explore the area beyond it, becoming trapped at local optimum solutions and yielding

solutions with no population diversity. This phenomenon, called "local trapping," is a significant cause of the infamous "untimely converging," in which the problem's fitness at a preliminary phase does not get better as iterations advance. To prevent these circumstances, tuning improvements and a more thorough examination of the search area are necessary. Unique variables to change and adapt the search strategy may also be incorporated into current approaches to encourage the equivalence between exploration and exploitation [100].

Since algorithms and metaheuristics are the main determinants of optimisation, they are also given more weight. The basic tuning requirements, i.e., the iteration count [101] and the size of the population [102], are to be suitably tuned, prioritising the number of function evaluations and computing durations to obtain the optimum metaheuristic possible.

Although the effectiveness of bio-inspired algorithms has grown in recent years, the idea that they are preferable to other evolutionary, physics-based strategies is still up for debate. Optimal performance is frequently regarded as a vital point.

The various optimisation techniques chosen for EV optimisation during the previous two decades are graded based on their implementation in multiple domains. Deb et al. [103] propose NSGA-II, a system that uses improved mutation and crossover process to produce the future offspring population and then chooses the appropriate upcoming generation to use a non-dominated Pareto technique and crowd distance assessment method. James et al. [104] analyse the swarm behaviour, which includes intellectual and interpersonal memory components and inertial weight to direct the particle to the optimum option. With EV load and renewable power generation, Zhao et al. [105] developed an economic dispatch model using PSO. Ant colony optimisation (ACO) [106] is inspired by how ants travel across networks to locate good routes to feed using a pheromone-driven communication system. Dervis et al. [107] built a colony of artificial bees with feeding supplies, hired forager honeybees, and jobless forager bees with a path counter to effectively investigate the search space. Rao et al. [108] model a human behavioural-based optimisation method for optimising actual problems relying on the exchange of knowledge in a class engagement between instructors and learners. Mirjalili et al. [109] represent the group's vital leadership supervision process used by the grey wolf classed as alpha, beta, delta, and omega while wolves seek their target in an optimisation technique. In order to get at the ultimate planning of FCE, Akanksha et al. [110] utilised the multiobjective GWO method to find a non-dominated solution and

fuzzy satisfaction-based judgements. Rao et al. [111] developed an easier-to-implement algorithm-specific-parameter-less optimisation for both single and multiobjective restricted and unrestrained optimisation based on the solutions moving towards the optimum solutions while rejecting the worst solutions. An optimisation technique called Rao was just newly created [112]. Due to its ease and convenience of usage in optimisation purposes, it is widely used by researchers.

In summary the field of optimisation using metaheuristics is an excellent fit for the optimisation of EVs because these problem formulations demand a lot of numerical computation, an accurate solution that handles many dimensions, and many limitations that control the viability of the solutions.

2.6 Summary

This chapter presents a thorough analysis of the literature about several issues of the development of charging stations for electric vehicles. The installation of EVCS load degrades the power grid's functioning characteristics, according to the consensus of all the research on the subject.

2.6.1 Limitation

According to earlier studies, the EVCS placements problems formulation and related methods of the solution have the following drawbacks:

1. Most researchers neglect the distribution system's substation power factor while the optimal placement of EVCS.
2. Most of the research review does not consider future EV population expansion.
3. Most researchers have positioned the charging station (particularly fast charging) by considering the cost function while neglecting the effect of the charging station.
4. The planning of the charging stations takes into account the viewpoints of an urban architect rather than that of the utility operator of the distribution system, EV users, or charging station owners.
5. Most academics have thought about one or two deployment strategies for charging stations in places where doing so is not advised due to practical issues. The owner of the charging station, the distribution network's operator and the EV consumers

are all equally interested in formulating the issue for the optimum placements of charging stations.

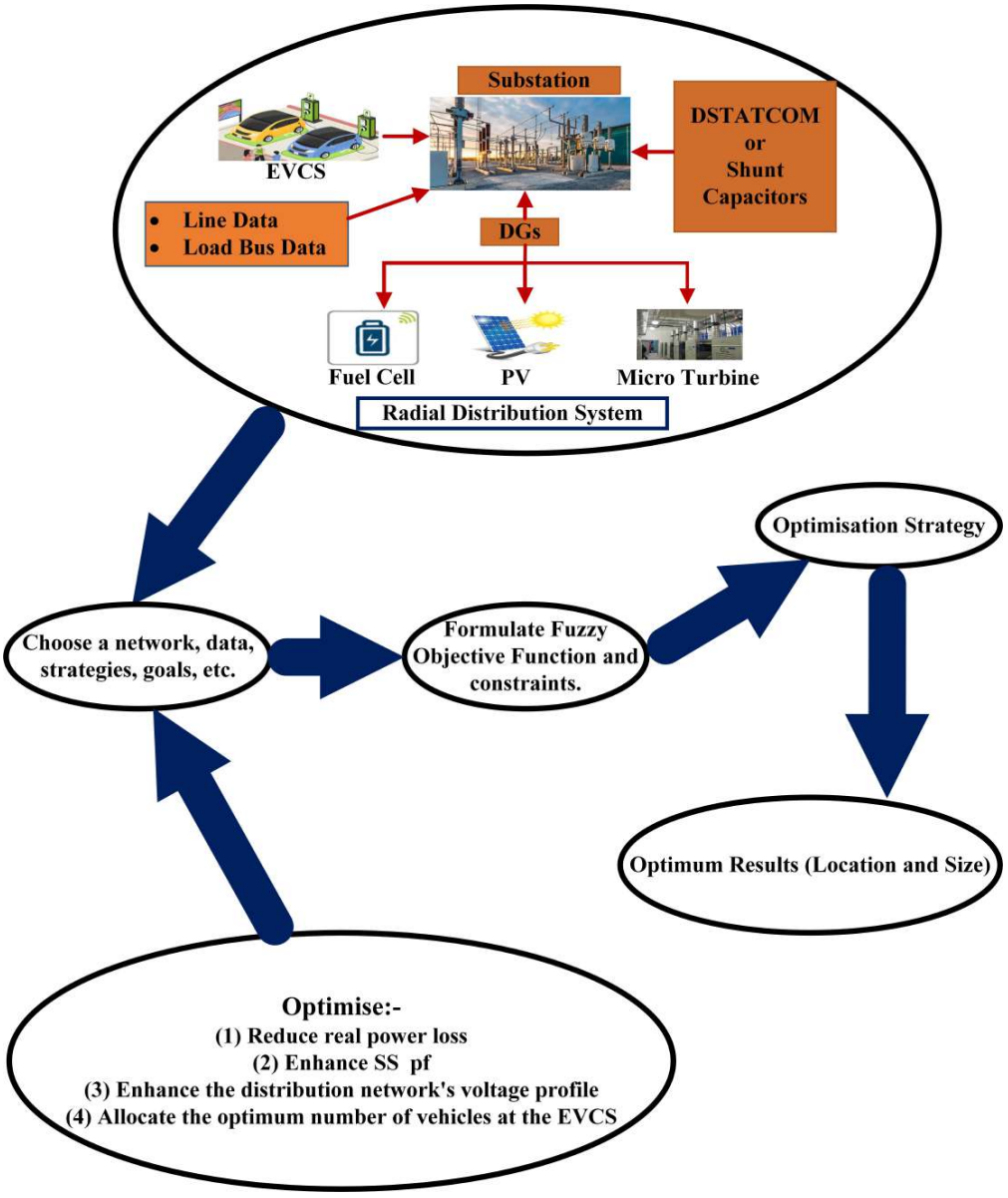

Figure 2.1: The charging station framework only considers the distribution system

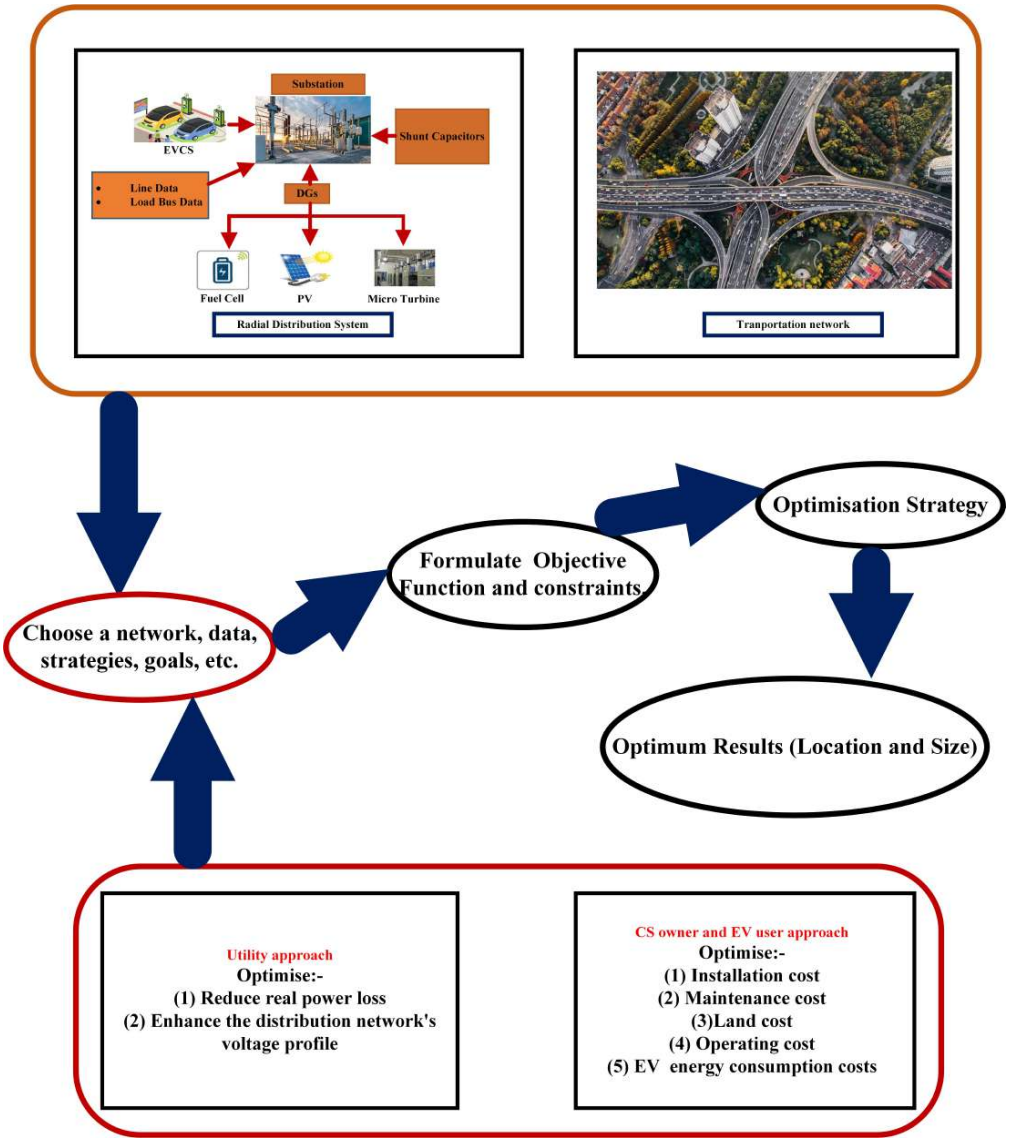

Figure 2.2: The charging station framework considering both distribution system and transportation network

Chapter 3
Two-Stage Optimal Placement of Electric Vehicle Charging Stations in a Distribution System

3.1 Introduction

Presently, EVs are preferred for road network transportation. Moreover, various government agencies and automobile industries are focusing on EVs due to their cheaper operating costs and because they have less of an impact on climatic change when compared to conventional engine vehicles. As EVs are rapidly increasing, EVCSs are being integrated into the distribution system (DST). Due to this, power demand is increasing, leading to an increase in the load level in the distribution line and a system voltage drop. Increased power losses and voltage instability cause power security problems in the distribution system. The world's perception of distributed renewable energy has changed significantly in recent decades due to its added economic, political, and ecological benefits. However, the improper placements of DGs make the operation of a sustainable distribution network more difficult and complex. DSTATCOMs are routinely installed by utility engineers to enhance the distribution system's voltage profile. In order to mitigate this problem, this paper includes simultaneous optimal sizing and citing of EVCSs, DGs and DSTATCOMs in the distribution system.

This chapter presents a fuzzy classified method for optimal sizings and two-stage placements of EVCSs, DGs and DSTATCOMs for 69-bus radial distribution systems using the RAO-3 algorithm. The prime objective of the proposed method is to (1) Reduce real power loss; (2) Enhance the substation (SS) power factor (pf); (3) Enhance the distribution network's voltage profile; and (4) Allocate the optimum number of vehicles at the charging stations.

The proposed fuzzified RAO-3 algorithm improves the substation pf in the distribution system. The fuzzy multi-objective function is utilized for the two stages of the EVCS, DG and DSTATCOM.

The rest of the chapter is structured as follows: Section 3.2 explains the fuzzy multi-objective problem formulation and its restrictions. Section 3.3 introduces the suggested

two-stage fuzzy multi-objective RAO-3 method. Section 3.4 presents the results and analyses, and Section 3.5 presents the summary.

3.2 Problem Formulation

This section presents fuzzy multi-objective functions for the optimal placements of DG, DSTATCOM and EVCS in various cases to improve the DST performance. This section presents the multi-objective function that focuses on reducing real power loss, enhancing the voltage profile of DST, enhancing the substation's power factor and the optimum number of electric vehicles at the EVCS.

The fuzzy domain membership function is presented for each objective. The membership function indicates the level of goal satisfaction. In the crisp domain, the membership function values are either zero or unity, whereas, in the fuzzy domain, they range from zero to unity. Consequently, the fuzzy set theory advances the classic style theory [113]. The membership function is a strictly monotonically declining continuous function with lower and upper bound values for the various goals described below. The trapezoidal memberships are used to obtain the desired multi-objective values, such as reduced power loss and improved voltage limitations [114]. The triangular function is used for additional objectives needed to mollify constraints, such as the SS power factor and DG penetration limit [114].

3.2.1 Fuzzification of Real Power Loss of the DST

The real power losses of the distribution system is shown below:

$$RPL = \sum_{j=1}^{nb-1} Pl_j \tag{3.1}$$

$$Pl_j = \frac{r_j \times \left\{ P_{j+1}^2 + Q_{j+1}^2 \right\}}{\left| v_{j+1} \right|^2} \tag{3.2}$$

Pl_j is the assumed test distribution network's branch real power loss, where P_{j+1} is the active power load and Q_{j+1} is the reactive power load injected at the load $(j+1)$ node. In the distribution network, resistance at the j^{th} node is r_j and the voltage at the $(j+1)^{th}$ node is v_{j+1}. The real power loss index $(RPLX)$ can be calculated as:

$$RPLX = \frac{RPL_{DGSC}}{RPL_{Base}} \tag{3.3}$$

RPL_{DGSC} is the active power loss with DG and DSTATCOM. The active power loss in the base situation is represented by RPL_{Base}. The fuzzified real power loss index ($\in^{RPLX}$) [69] is shown in Figure 3.1. $RPLX^{max}$ is considered unity. Based on utility necessity, $RPLX^{min}$ was selected, such that the active power loss was reduced to the desired value. The mathematical expression for the fuzzy set $\in^{RPLX}$ is explained in Equation (3.4).

$$\in^{RPLX} = \begin{cases} 1 & \text{for } RPLX \leq RPLX^{min} \\ \frac{RPLX^{max} - RPLX}{RPLX^{max} - RPLX^{min}} & \text{for } RPLX^{max} \leq RPLX \leq RPLX^{min} \\ 0 & \text{for } RPLX > RPLX^{max} \end{cases} \tag{3.4}$$

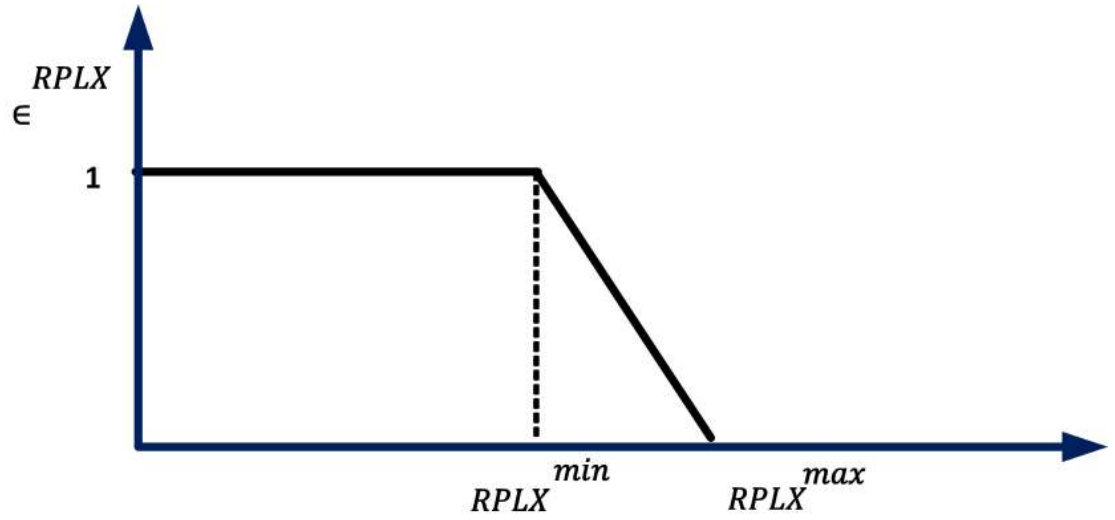

Figure 3.1: Reduction of real power loss.

3.2.2 Fuzzification of Voltage Nodes of the Distribution Network

The fuzzy membership function of voltage ($\in^{v_j}$) [69] of each node j in the distribution network is explained in Figure 3.2; mathematically, it can be explained in Equation (3.5): $v_{l1} = 0.94$, $v_{min} = 0.95$, $v_{max} = 1.05$ and $v_{l2} = 1.06$ are assumed. In this work, the fuzzy voltage performance ($\in^{v}$) is the minimum value of fuzzy membership of the voltage of each node of the distribution network considered. It can be defined as $\in^{v} = (1 - \min(\in^{v_j}))$.

$$\in^{v_j} = \begin{cases} 0 & \text{for } v_j \leq v_{l1} \\ \frac{v_j - v_{l1}}{v_{min} - v_{l1}} & \text{for } v_{l1} < v_j < v_{min} \\ 1 & \text{for } v_{min} \leq v_j \leq v_{max} \\ \frac{v_j - v_{max}}{v_{l2} - v_{max}} & \text{for } v_{max} < v_j < v_{l2} \\ 0 & \text{for } v_j > v_{l2} \end{cases} \tag{3.5}$$

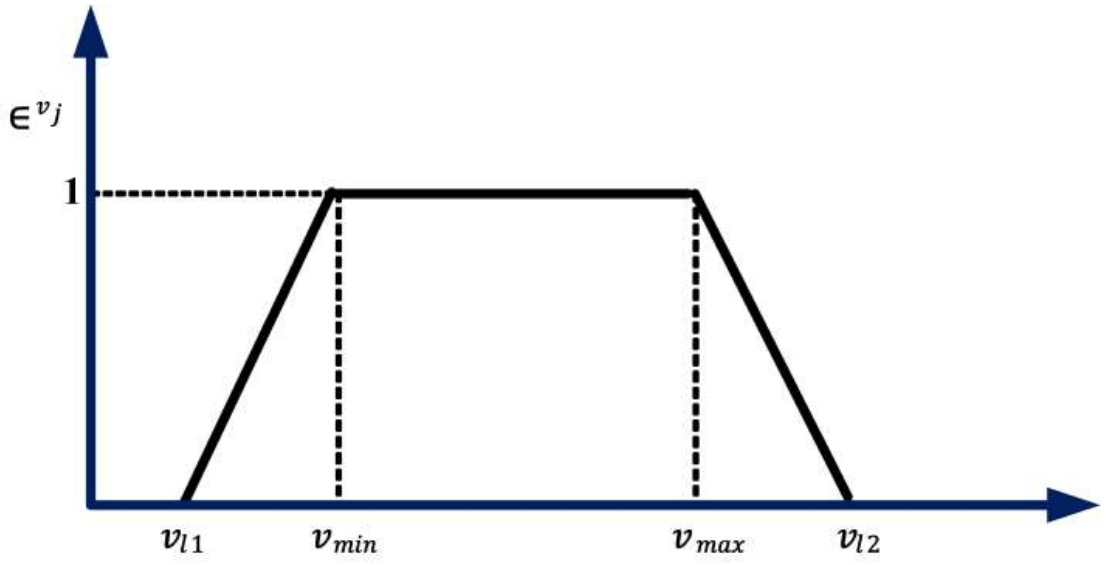

Figure 3.2: Bus voltage.

subsectionFuzzification of SS Power Factor The DG must operate at a lagged pf of 0.95 to increase the SS power factor (pf). It is possible to determine the SS power factor:

$$pf = \cos\left(\frac{S_{kW}^{SN}}{S_{kVA}^{SN}}\right) \tag{3.6}$$

$$S_{kW}^{SS} = \sum_{j=1}^{nb} P_j^{load} + Pl - \sum_{k=1}^{ndg} P_k^{DG} \tag{3.7}$$

$$S_{kVAr}^{SS} = \sum_{j=1}^{nb} Q_j^{load} + Ql - \sum_{m=1}^{nsc} Q_m^{SC} - \sum_{k=1}^{ndg} P_k^{DG} \times \emptyset_{dg} \tag{3.8}$$

$$S_{kVA}^{SS} = \sqrt{{S_{kW}^{SS}}^2 + {S_{kVAr}^{SS}}^2} \tag{3.9}$$

P^{DG} is the capacity of DG. ndg stands for the number of DGs installed in the DST. The

active power load connected to the j^{th} bus is P_j^{load}, and the total number of buses in the DST is *nb*. When DG, DSTATCOM, or EV charging stations are deployed, The distribution network's active power loss is termed Pl. The reactive power load linked to the j^{th} bus is Q_j^{load}, the DSTATCOM rating is Q_m^{SC}, and the total number of DSTATCOMs in the DST is *nsc*. When DG or DSTATCOM are implemented, the distribution network's reactive power loss is *Ql*.

The triangular fuzzy membership function [69] for the SS power factor $(\in^{pf})$ is shown in Figure 3.3 and the mathematical expression is shown in Equation (3.10).

$$\in^{pf} = \begin{cases} 0 & \text{for } pf \leq pf_{min} \\ \frac{pf - pf_{min}}{pf_s - pf_{min}} & \text{for } pf_{min} \leq pf \leq pf_s \\ \frac{pf_{max} - pf}{pf_{max} - pf_s} & \text{for } pf_s \leq pf \leq pf_{max} \\ 0 & \text{for } pf \leq pf_{max} \end{cases} \tag{3.10}$$

In the preceding equations, pf_{min} =0.85, pf_s =0.95, and pf_{max} = 1.0 are used. The desired power factor level is denoted as pf_s.

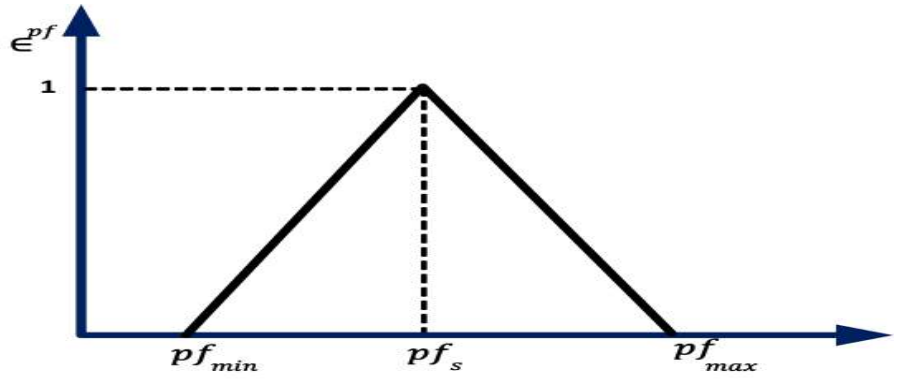

Figure 3.3: SS power factor.

3.2.3 Fuzzification of DG Penetration

Penetration of the DG index in the distribution network can be defined as the ratio of the number of DGs connected to the total real power load in the DST.

$$DGPI = \frac{\sum_{k=1}^{ndg} P^{dg}}{\sum_{j=1}^{nb} P^{load}} \tag{3.11}$$

Figure 3.4 shows the triangular fuzzification of the DG penetration ($\in^{DGPI}$) [69] limit; the mathematical expression is shown in the following Equation (3.12). $DGPI_{min} = 0.4$, $DGPI_s = 0.5$, $DGPI_{max} = 0.6$, respectively. $DGPI_s$ are the desired penetration levels in the distribution network. In this work, penetration is considered at 50%.

$$\in^{DGPI} = \begin{cases} 0 & \text{for } DGPI \leq DGPI_{min} \\ \frac{DGPI - DGPI_{min}}{DGPI_s - DGPI_{min}} & \text{for } DGPI_{min} \leq DGPI \leq DGPI_s \\ \frac{DGPI_{max} - DGPI}{DGPI_{max} - DGPI_s} & \text{for } DGPI_s \leq DGPI \leq DGPI_{max} \\ 0 & \text{for } DGPI \leq DGPI_{max} \end{cases} \tag{3.12}$$

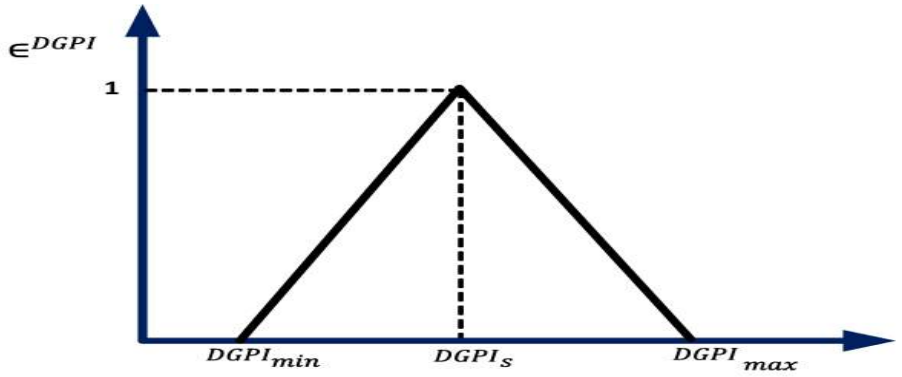

Figure 3.4: DG penetration.

3.2.4 Fuzzification of the EV Power Loss Index

With the EV index, the real power loss can be calculated as follows:

$$EVPI = \frac{EVPI^{EVLD}}{EVPI^{LD}} \tag{3.13}$$

$EVPI^{EVLD}$ is the active power loss with EV and other load losses. $EVPI^{LD}$ is the load loss. Here, the load can be DG, DSTATCOM, or any commercial load. The membership fuzzification of the EV power loss index ($\in^{EVPI}$) [69] is shown in Figure 3.5; the

mathematical expression is shown in Equation (3.14).

$$\in^{EVPI} = \begin{cases} 0 & \text{for } EVPI \leq EVPI_{min} \\ \frac{EVPI - EVPI_{min}}{EVPI_s - EVPI_{min}} & \text{for } EVPI_{min} \leq EVPI \leq EVPI_s \\ \frac{EVPI_{max} - EVPI}{EVPI_{max} - EVPI_s} & \text{for } EVPI_s \leq EVPI \leq EVPI_{max} \\ 0 & \text{for } EVPI \leq EVPI_{max} \end{cases} \tag{3.14}$$

$EVPI_{min} = 1$, $EVPI_s = 1.5$, $EVPI_{max} = 2$ respectively. $EVPI$ is always greater than 1 because power loss increases with the addition of the EV load in the distribution network.

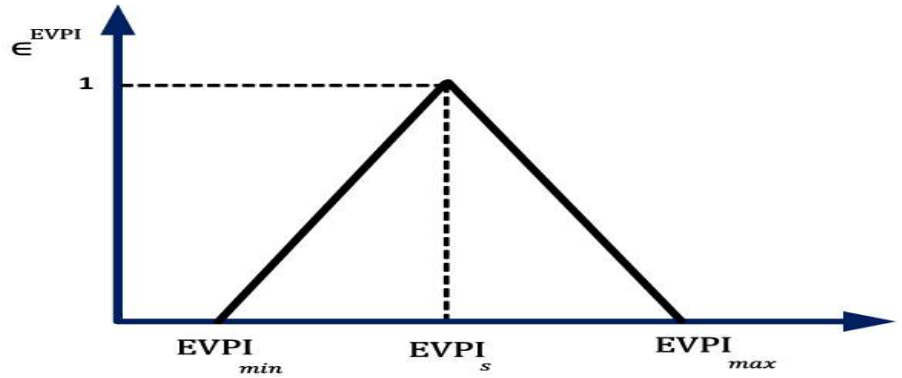

Figure 3.5: EV real power index.

3.2.5 Multi-Objective Fuzzy Function for Optimal Sizing and Location of EVCS, DG, and DSTATCOM

1. In the case-1 DG and DSTATCOM are placed optimally in the DST, then the following equation depicts multi-objective fuzzy functions for the DG and DSTATCOM optimum sites and sizings:

$$F_{zdc} = \frac{1}{\in^{RPLX} + \in^{pf} + \in^{v} + \in^{DGPI}} \tag{3.15}$$

2. The following equation depicts the fuzzy objective functions of the case-2 for the optimum location and sizing of EVCS:

$$F_{ze} = \frac{1}{(\in^{EVPI})} \tag{3.16}$$

The multi-objective fuzzy functions, explained in Equations (3.15)–(3.16), are minimized by using the RAO-3 algorithm subjected to different constraints. In this work, penetration of DG in the distribution network is considered to be 50 % of the total active power load; the reactive power injection is 50 % of the total reactive power.

$$0 < P_k^{DG} \leq P_{max}^{DG} \; where \; k = 1,\ 2,\ 3 \tag{3.17}$$

$$0 < Q_m^{sc} \leq Q_{max}^{sc} \; where \; k = 1,\ 2,\ 3 \tag{3.18}$$

P_k^{DG} and Q_m^{sc} are the DG power and DSTATCOM reactive power injection at the nodes in the distribution network at optimal locations.

3.3 Summary of RAO-3

The optimization algorithm Rao was recently created [112]. Rao-1, Rao-2 and Rao-3 are the three proposed Rao algorithms. This study chose it as a population-based approach because it is straightforward to employ in optimized applications. It also has fewer control factors because there is no metaphorical explanation. Once the halt condition is reached, only the swarm size needs to be changed. Compared to other algorithms, the RAO algorithm performs better statistically because it can ensure exploration performance while yielding superior exploitation, keeping an excellent balance between exploration and exploitation.

The three RAO algorithms follow similar processes. However, as seen in the following steps and shown in Figure 3.6, only the movement equation is different.

1. Initialize the system data and load profile.
2. Initialize the population (algorithm parameter), iteration and set the maximum iteration.
3. Randomly initialize the sizings and locations of EVCS, DG and DSTATCOM.
4. The objective function's indicated fitness function is put to the test.
5. Identify the best and worst solutions proposed by the population.
6. The revised solution is updated for all populations under the selected RAO algorithm as follows:

- RAO-1:

$$z'_{m,p,i} = z_{m,p,i} + rand_{1,m.i} \times (z_{m,b,i} - z_{m,w,i}) \tag{3.19}$$

- RAO-2:

$$\begin{aligned} z'_{m,p,i} = z_{m,p,i} + rand_{1,m.i} \times (z_{m,b,i} - z_{m,w,i}) \\ + rand_{2,m.i} \times (\mid z_{m,p,i} \; or \; z_{m,d,i} \mid - \mid z_{m,d,i} \; or \; z_{m,p,i} \mid) \end{aligned} \tag{3.20}$$

- RAO-3:

$$\begin{aligned} z'_{m,p,i} = z_{m,p,i} + rand_{1,m.i} \times (z_{m,b,i} - \mid z_{m,w,i} \mid) \\ + rand_{2,m.i} \times (\mid z_{m,p,i} \; or \; z_{m,d,i} \mid - (z_{m,d,i} \; or \; z_{m,p,i})) \end{aligned} \tag{3.21}$$

$z_{m,p,i}$ is the m^{th} variable's value for the p^{th} candidate in the i^{th} iteration. The best solution is denoted by $z_{m,b,i}$, whereas the worst solution is denoted by $z_{m,w,i}$. The Rao algorithm can guarantee exploration performance while producing superior exploitation, resulting in an excellent balance between exploitation and exploration, representing the method's higher statistical performance when compared to other algorithms.

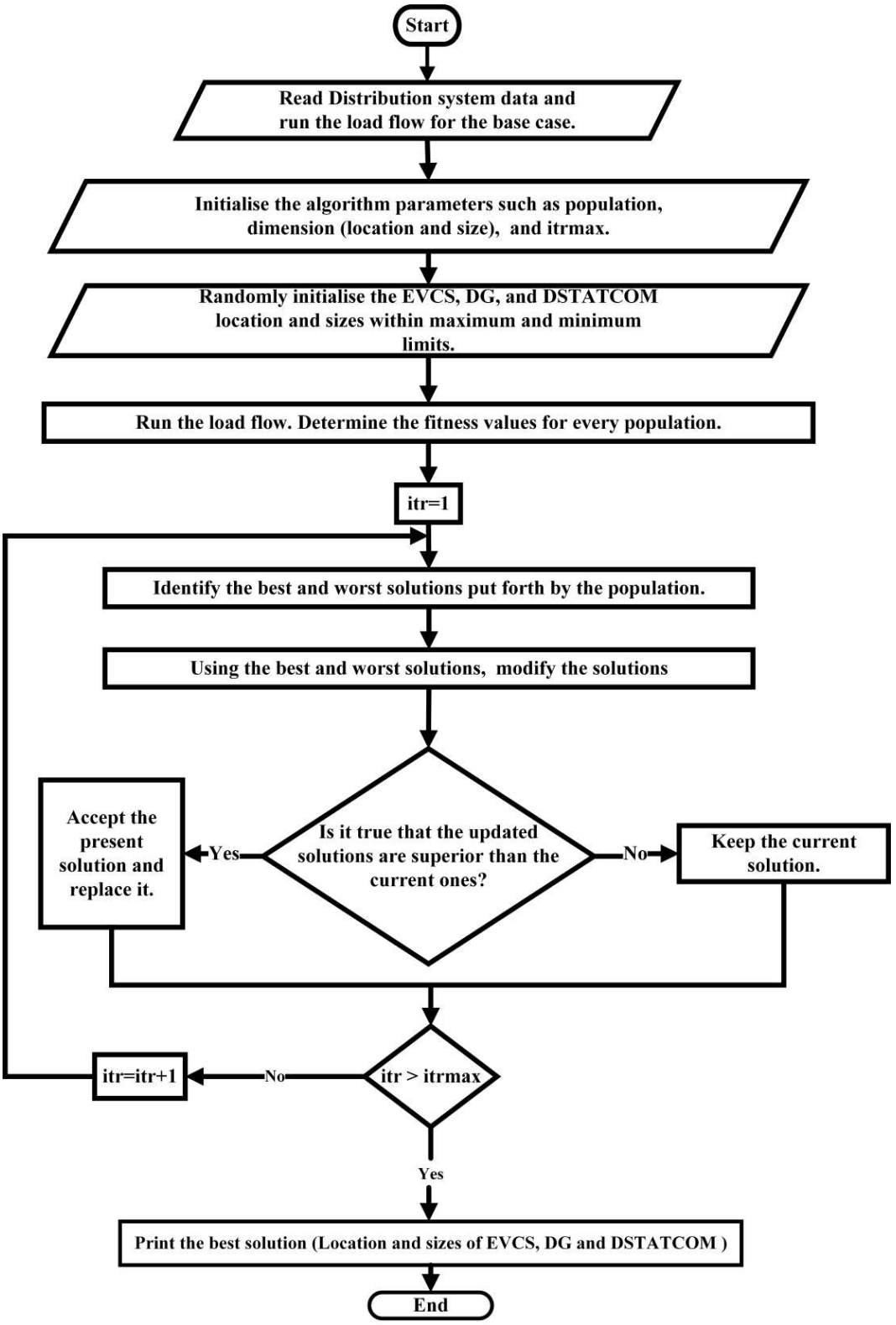

Figure 3.6: RAO-3 algorithm implementation flow chart.

3.4 Results and Discussion

For this study, a 69 bus radial distribution system is used. 100 MVA and 12.66 kV are the system's base values. For load flow studies, the backwards-forward sweep approach is preferred. The simulation is run with MATLAB 2017a software on a computer with an Intel Core i5 8th Gen processor and 8GB RAM. The total active power load is 3082.19 kW, the reactive power load is 2796.77 kVAr, total real losses are 225 kW and the lowest voltage is 0.9092 calculated from the load flow following data in the base case. The algorithm made the following assumptions: itrmax = 100 and population = 100.

This work addresses the appropriate placement and sizing of DGs and SCs units in the distribution network, containing three bus nodes of DGs units and three bus nodes of SCs units. Furthermore, five bus nodes are considered for optimal EVCS planning. In each charging station maximum of 50 EV can be charged. Nissan Altra Lithium-ion batteries are considered to have a rating of 6.5kW [69].

3.4.1 Cases

Two different scenarios were considered in the given DST for optimal sizings and locations of EVCS, DSTATCOM and DG.

- Stage 1: In this first stage, DSTATCOM and DG are integrated with the distribution network;
- Stage 2: In the second stage, EV charging stations are connected.

3.4.1.1 Stage 1

In the first stage, optimum citing and sizing of DG and DSTATCOM are done, with the help of a fuzzy multi-objective function, as shown in Equation (3.14). This fuzzy multi-objective used in Equation (3.14) is considered to maintain the substation power factor desired value, improve the voltage profile, and reduce the distribution system's active power losses. Optimum allocations of DG and DSTATCOM are done with the RAO-3 algorithm's help, as shown in Tables 3.1 and 3.2. From this work, it can be seen that in the proposed method, each bus voltage moves closer to unity and the distribution system's performance is enhanced. The fuzzy RAO-3 method is compared with a two-stage methodology [69], fuzzy TLBO, fuzzy GWO and fuzzy PSO. The performance of

the distributed system, voltage profile, and convergence of fitness is better with RAO-3, as depicted in Table 3.3 and Figures 3.7 and 3.8.

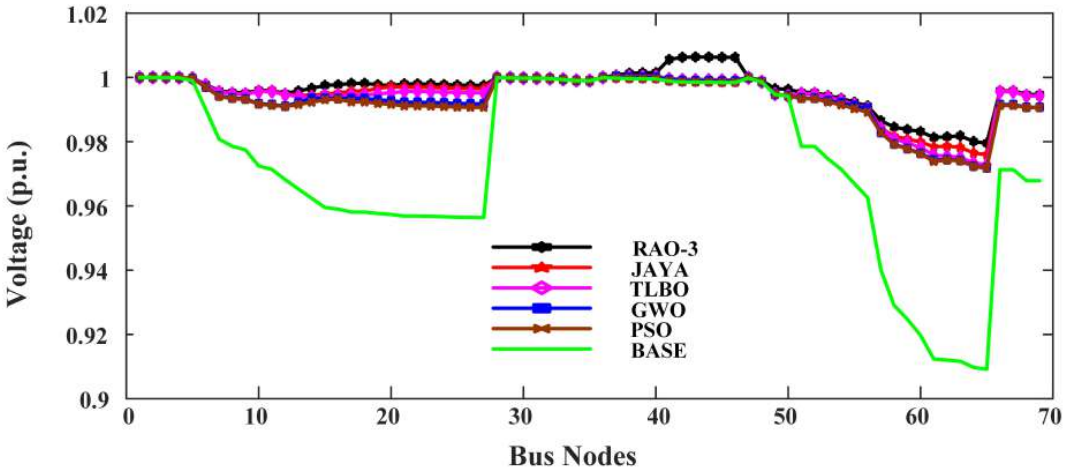

Figure 3.7: Voltage Curve.

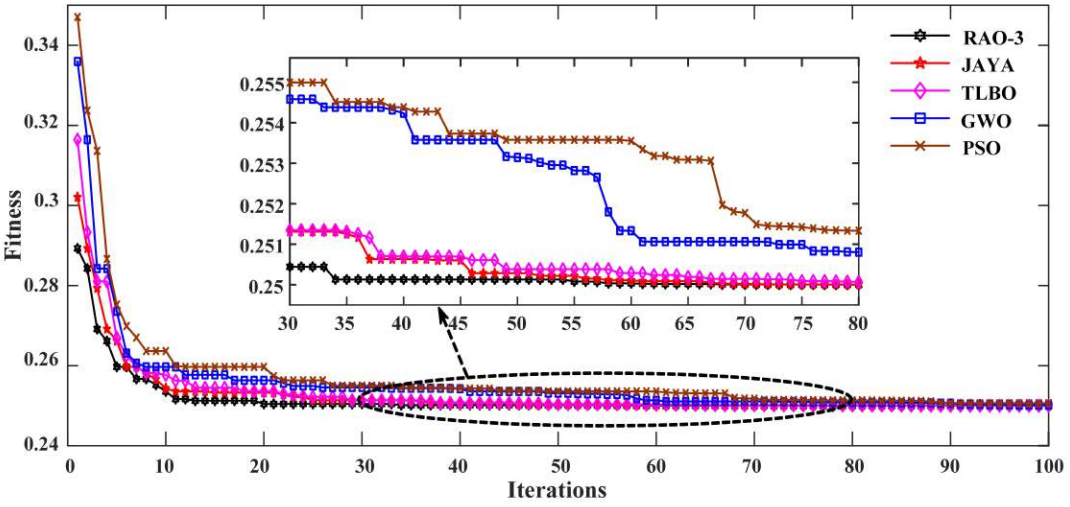

Figure 3.8: Fitness Curve of DG and DSTATCOM.

3.4.1.2 Stage 2

The EVCS is installed after the integration of the DG and DSTATCOM in the DST, which is the second stage. In this work, five optimum locations are preferred for locating the charging station. In each charging station, a maximum of 50 EVs are assumed. A fuzzy multi-objective was used for achieving this optimal location, as shown in Equation (3.15). The optimum number of EVs and optimum locations of EVCSs are shown in

Table 3.4. The single-line diagram of the 69-bus radial distribution system with EVCS, DG and DSTATCOM of two-stage is shown in Figure 3.9.

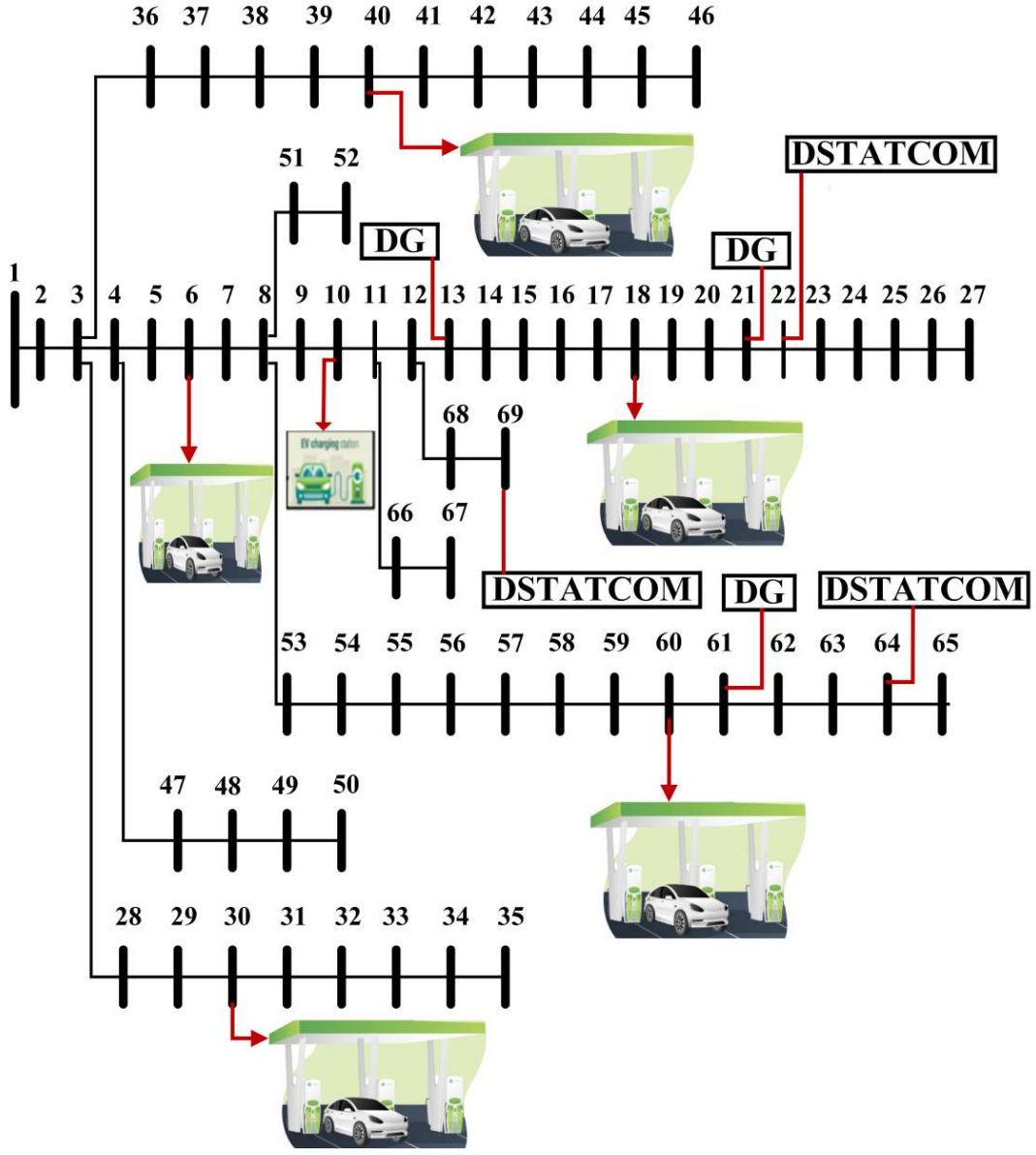

Figure 3.9: The single-line diagram of the 69-bus radial distribution system of two-stage methodology.

3.5 Summary

In stage-2, the active power loss is reduced to 84.675%, 15.92%compared to the base case and two-stage methodology [69]. The minimum voltage of the bus is improved to 0.97653 p.u. two-stage compared to the base case minimum voltage of 0.902. The

optimum no -of vehicles in two-stage is increased to 4.21%, compared to the two-stage methodology [69]. The final distribution of the active power loss and minimum voltage with DG, DSTATCOM and EV are shown in Table 3.5.

Table 3.1: DG optimum location and sizing

Fuzzy PSO		**Fuzzy GWO**		**Fuzzy TLBO**		**Fuzzy JAYA**		**Fuzzy RAO-3**	
DG Node location	DG Sizing (kW)	DG Node location	DG Sizing (kW)	DG Node location	DG Sizing (kW)	DG Node location	DG Sizing (kW)	DG Node location	DG Sizing (kW)
13	481.9379	61	887.9736	61	900.0000	61	900.0000	13	561.1438
61	737.8022	13	335.7383	23	499.5148	11	626.7025	21	643.5554
20	680.9627	23	677.1779	10	501.1851	24	373.9975	61	696.0012

Table 3.2: DSTATCOM optimum location and sizing

Fuzzy PSO		**Fuzzy GWO**		**Fuzzy TLBO**		**Fuzzy JAYA**		**Fuzzy RAO-3**	
Node location	Sizing (kVAr)	Node location	Sizing (kVAr)	Node location	Sizing (kVAr)	Node location	Sizing (kVAr)	Node location	Sizing (kVAr)
64	573.4461	21	484.6605	65	654.9968	23	432.3735	22	483.9325
12	383.6421	64	549.4658	24	510.2932	69	422.2525	69	432.9390
21	495.0255	69	417.6416	12	284.7286	62	596.9364	64	538.5364

Table 3.3: Performance comparison of 69 bus system

Stage-1	**Base case**	**Two-stage [69]**	**Fuzzy PSO**	**Fuzzy GWO**	**Fuzzy TLBO**	**Fuzzy JAYA**	**Fuzzy RAO-3**
SS Active Power (kW)	4027.19	1920.93	1921.6	1920.9	1920.8	1920.7	1920.4
SS Reactive Power (kVar)	2796.77	631.22	633.2409	631.2786	631.1990	631.0172	630.2859
SS Power factor (lag)	0.8214	0.95	0.95	0.95	0.95	0.95	0.95
DG Penetration (kW)	-	1900.11	1900.7	1900.7	1900.7	1900.7	1900.7
RPL (kW)	224.56	27.34	28.922	27.12	26.9835	26.7348	22.9920
Minimum Voltage (p.u.)	0.902	0.9461	0.9717	0.9718	0.9728	0.9795	0.9811

Table 3.4: Optimum number of EV and optimum location of EVCS

Fuzzy PSO		**Fuzzy GWO**		**Fuzzy TLBO**		**Fuzzy JAYA**		**Fuzzy RAO-3**	
Optimum node for EVCS	Optimum no of EV	Optimum node for EVCS	Optimum no of EV	Optimum node for EVCS	Optimum no of EV	Optimum node for EVCS	Optimum no of EV	Optimum node for EVCS	Optimum no of EV
60	35	6	40	30	41	18	37	30	36
42	37	40	35	18	43	39	37	60	33
20	35	10	36	7	33	42	49	6	44
6	41	45	40	40	33	33	36	40	40
30	37	19	34	61	36	24	36	18	45
Total no of EV	185	Total no of EV	185	Total no of EV	186	Total no of EV	195	Total no of EV	198

Table 3.5: Performance of 69 bus radial distribution system after installation of EVCS

Two-stage	**Base case**	**Two-Stage methodology [69]**	**Fuzzy PSO**	**Fuzzy GWO**	**Fuzzy TLBO**	**Fuzzy JAYA**	**Fuzzy RAO-3**
Real Power loss (kW)	224.56	41.01	43.383	40.6822	40.4744	40.1027	34.4876
Voltage minimum (p.u.)	0.902	0.9659	0.9671	0.9678	0.9689	0.9698	0.97653

Chapter 4

Simultaneous Optimal Placement of Electric Vehicle Charging Stations in a Distribution System

4.1 Introduction

The strategy proposed in the previous chapter reduces the overall power losses and improves the voltage profile. However after the inclusion of EVCS the substation power factor is not considered and future expansion of EVs in the distribution system is also unpredictable. This chapter, presents a fuzzy classified method for simultaneous optimal sizing and placement of EVCS, DG and DSTATCOM for 69 bus radial distribution systems using the RAO-3 algorithm. The characteristic curves of Li-ion batteries are utilised for load flow analysis to develop models for EV battery charging loads. The prime objective of the proposed method is to 1) reduce real power loss, 2) enhance Substation (SS) power factor (pf), 3) enhance the distribution network's voltage profile, and 4) allocate the optimum number of vehicles at the charging stations. Moreover, the existing system's performance for increased EV and distribution system loads is presented.

The rest of the chapter is structured as follows: Section 4.2 explains the fuzzy multi-objective problem formulation and its restrictions. In Section 4.3, from the battery charging characteristics, the charging load models for EV batteries were developed for the load flow analysis. Section 4.4 introduces the suggested fuzzy multi-objective RAO-3 method. Section 4.5 presents the results and analyses and Section 4.6 presents the summary.

4.2 Problem Formulation

This section presents fuzzy multi-objective functions for the simulatenous optimal placements of DG, DSTATCOM and EVCS to improve the DST performance. This section presents the multi-objective function that focuses on reducing real power loss, enhancing the voltage profile of DST, enhancing the substation's power factor, and the optimum number of electric vehicles at the EVCS. The fuzzy domain membership function is

presented for each objective. The membership function indicates the level of goal satisfaction. In the crisp domain, the membership function values are either zero or unity, whereas, in the fuzzy domain, they range from zero to unity.Consequently, the fuzzy set theory advances the classic style theory [113]. The membership function is a strictly monotonically declining continuous function with lower and upper bound values for the various goals described below. The trapezoidal memberships are used to obtain the desired multi-objective values, such as reduced power loss and improved voltage limitations [114]. The triangular function is used for additional objectives needed to mollify constraints, such as the SS power factor and DG penetration limit [114].

4.2.1 Fuzzification of Real Power Loss of the DST

The real power losses of the distribution system is shown below:

$$RPL = \sum_{j=1}^{nb-1} Pl_j \tag{4.1}$$

$$Pl_j = \frac{r_j \times \left\{ P_{j+1}^2 + Q_{j+1}^2 \right\}}{\left| v_{j+1} \right|^2} \tag{4.2}$$

Pl_j is the assumed test distribution network's branch real power loss, where P_{j+1} is the active power load and Q_{j+1} is the reactive power load injected at the load $(j+1)$ node. In the distribution network, resistance at the j^{th} node is r_j and the voltage at the $(j+1)^{th}$ node is v_{j+1}. The real power loss index $(RPLX)$ can be calculated as:

$$RPLX = \frac{RPL_{DGSC}}{RPL_{Base}} \tag{4.3}$$

RPL_{DGSC} is the active power loss with DG and DSTATCOM. The active power loss in the base situation is represented by RPL_{Base}. The fuzzified real power loss index ($\in {}^{RPLX}$) [69] is shown in Figure 4.1. $RPLX^{max}$ is considered unity. Based on utility necessity, $RPLX^{min}$ was selected, such that the active power loss was reduced to the desired value. The mathematical expression for the fuzzy set $\in {}^{RPLX}$ is explained in Equation (4.4).

$$\in^{RPLX} = \begin{cases} 1 & \text{for } RPLX \leq RPLX^{min} \\ \frac{RPLX^{max} - RPLX}{RPLX^{max} - RPLX^{min}} & \text{for } RPLX^{max} \leq RPLX \leq RPLX^{min} \\ 0 & \text{for } RPLX > RPLX^{max} \end{cases} \tag{4.4}$$

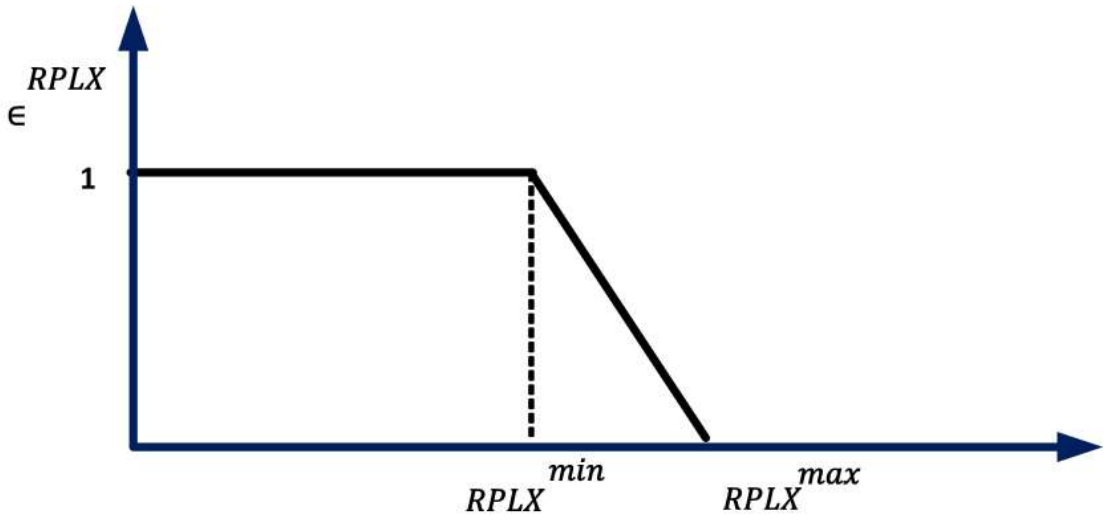

Figure 4.1: Reduction of real power loss.

4.2.2 Fuzzification of Voltage Nodes of the Distribution Network

The fuzzy membership function of voltage $(\in^{v_j})$ [69] of each node j in the distribution network is explained in Figure 4.2; mathematically, it can be explained in Equation (4.5): $v_{l1} = 0.94$, $v_{min} = 0.95$, $v_{max} = 1.05$ and $v_{l2} = 1.06$ are assumed. In this work, the fuzzy voltage performance $(\in^{v})$ is the minimum value of fuzzy membership of the voltage of each node of the distribution network considered. It can be defined as $\in^{v} = (1 - \min(\in^{v_j}))$.

$$\in^{v_j} = \begin{cases} 0 & \text{for } v_j \leq v_{l1} \\ \frac{v_j - v_{l1}}{v_{min} - v_{l1}} & \text{for } v_{l1} < v_j < v_{min} \\ 1 & \text{for } v_{min} \leq v_j \leq v_{max} \\ \frac{v_j - v_{max}}{v_{l2} - v_{max}} & \text{for } v_{max} < v_j < v_{l2} \\ 0 & \text{for } v_j > v_{l2} \end{cases} \tag{4.5}$$

subsectionFuzzification of SS Power Factor The DG must operate at a lagged pf of 0.95

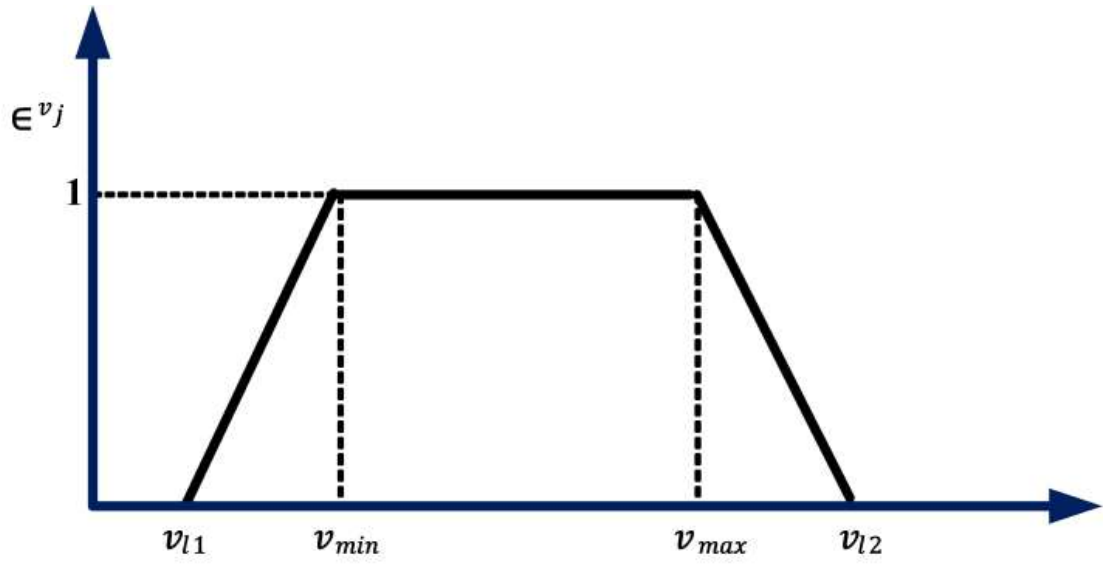

Figure 4.2: Bus voltage.

to increase the SS power factor (pf). It is possible to determine the SS power factor:

$$pf = \cos\left(\frac{S_{kW}^{SN}}{S_{kVA}^{SN}}\right) \tag{4.6}$$

$$S_{kW}^{SS} = \sum_{j=1}^{nb} P_j^{load} + Pl - \sum_{k=1}^{ndg} P_k^{DG} \tag{4.7}$$

$$S_{kVAr}^{SS} = \sum_{j=1}^{nb} Q_j^{load} + Ql - \sum_{m=1}^{nsc} Q_m^{SC} - \sum_{k=1}^{ndg} P_k^{DG} \times \emptyset_{dg} \tag{4.8}$$

$$S_{kVA}^{SS} = \sqrt{{S_{kW}^{SS}}^2 + {S_{kVAr}^{SS}}^2} \tag{4.9}$$

P^{DG} is the capacity of DG. ndg stands for the number of DGs installed in the DST. The active power load connected to the j^{th} bus is P_j^{load}, and the total number of buses in the DST is nb. When DG, DSTATCOM, or EV charging stations are deployed, The distribution network's active power loss is termed Pl. The reactive power load linked to the j^{th} bus is Q_j^{load}, the DSTATCOM rating is Q_m^{SC}, and the total number of DSTATCOMs in the DST is nsc. When DG or DSTATCOM are implemented, the distribution network's reactive power loss is Ql. The triangular fuzzy membership function [69] for the SS power factor $(\in^{pf})$ is shown in Figure 4.3 and the mathematical expression is shown in

Equation (4.10).

$$\in^{pf} = \begin{cases} 0 & \text{for } pf \leq pf_{min} \\ \frac{pf - pf_{min}}{pf_s - pf_{min}} & \text{for } pf_{min} \leq pf \leq pf_s \\ \frac{pf_{max} - pf}{pf_{max} - pf_s} & \text{for } pf_s \leq pf \leq pf_{max} \\ 0 & \text{for } pf \leq pf_{max} \end{cases} \tag{4.10}$$

In the preceding equations, pf_{min} =0.85, pf_s =0.95, and pf_{max} = 1.0 are used. The desired power factor level is denoted as pf_s.

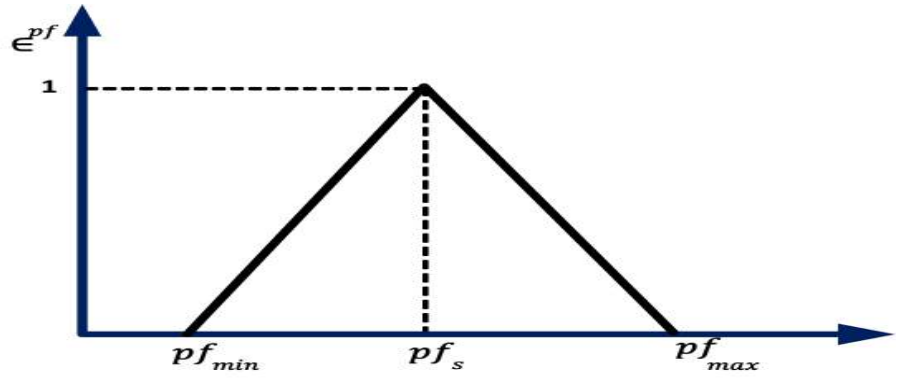

Figure 4.3: SS power factor.

4.2.3 Fuzzification of DG Penetration

Penetration of the DG index in the distribution network can be defined as the ratio of the number of DGs connected to the total real power load in the DST.

$$DGPI = \frac{\sum_{k=1}^{ndg} P^{dg}}{\sum_{j=1}^{nb} P^{load}} \tag{4.11}$$

Figure 4.4 shows the triangular fuzzification of the DG penetration ($\in^{DGPI}$) [69] limit; the mathematical expression is shown in the following Equation (4.12). $DGPI_{min} = 0.4$, $DGPI_s = 0.5$, $DGPI_{max} = 0.6$, respectively. $DGPI_s$ are the desired penetration

levels in the distribution network. In this work, penetration is considered at 50%.

$$\in^{DGPI} = \begin{cases} 0 & \text{for } DGPI \leq DGPI_{min} \\ \frac{DGPI - DGPI_{min}}{DGPI_s - DGPI_{min}} & \text{for } DGPI_{min} \leq DGPI \leq DGPI_s \\ \frac{DGPI_{max} - DGPI}{DGPI_{max} - DGPI_s} & \text{for } DGPI_s \leq DGPI \leq DGPI_{max} \\ 0 & \text{for } DGPI \leq DGPI_{max} \end{cases} \tag{4.12}$$

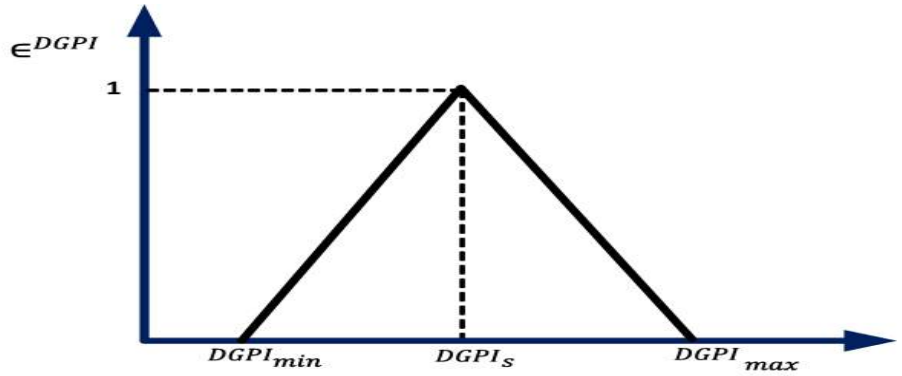

Figure 4.4: DG penetration.

4.2.4 Fuzzification of the EV Power Loss Index

With the EV index, the real power loss can be calculated as follows:

$$EVPI = \frac{EVPI^{EVLD}}{EVPI^{LD}} \tag{4.13}$$

$EVPI^{EVLD}$ is the active power loss with EV and other load losses. $EVPI^{LD}$ is the load loss. Here, the load can be DG, DSTATCOM, or any commercial load. The membership fuzzification of the EV power loss index ($\in^{EVPI}$) [69] is shown in Figure 4.5; the mathematical expression is shown in Equation (4.14).

$$\in^{EVPI} = \begin{cases} 0 & \text{for } EVPI \leq EVPI_{min} \\ \frac{EVPI - EVPI_{min}}{EVPI_s - EVPI_{min}} & \text{for } EVPI_{min} \leq EVPI \leq EVPI_s \\ \frac{EVPI_{max} - EVPI}{EVPI_{max} - EVPI_s} & \text{for } EVPI_s \leq EVPI \leq EVPI_{max} \\ 0 & \text{for } EVPI \leq EVPI_{max} \end{cases} \tag{4.14}$$

$EVPI_{min} = 1$, $EVPI_s = 1.5$, $EVPI_{max} = 2$ respectively. $EVPI$ is always greater than 1 because power loss increases with the addition of the EV load in the distribution network.

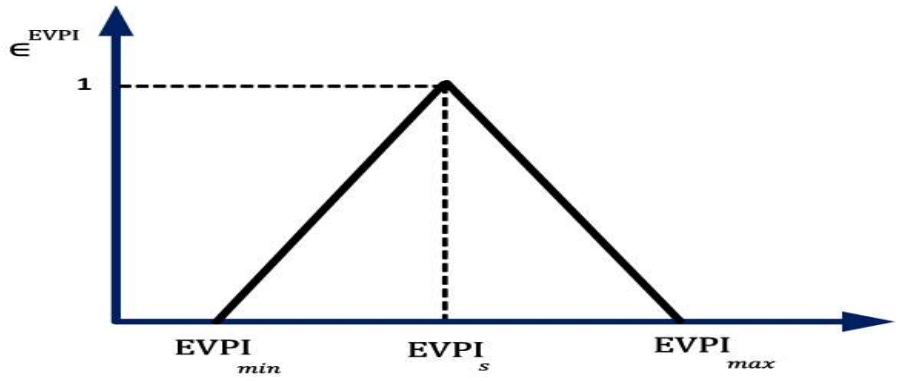

Figure 4.5: EV real power index.

4.2.5 Multi-Objective Fuzzy Function for Optimal Sizing and Location of EVCS, DG, and DSTATCOM

Multi-objective fuzzy functions for simultaneous optimum allocation of EVCS, DSTATCOM, and DG are shown in the following equation:

$$F_{zs} = \frac{1}{\in^{RPLX} + \in^{pf} + \in^{v} + \in^{DGPI} + \in^{EVPI}} \tag{4.15}$$

The multi-objective fuzzy functions, explained in Equation (4.15), are minimized by using the RAO-3 algorithm subjected to different constraints. In this work, penetration of DG in the distribution network is considered to be 50 % of the total active power load; the reactive power injection is 50 % of the total reactive power.

$$0 < P_k^{DG} \leq P_{max}^{DG} \; where \; k = 1,\ 2,\ 3 \tag{4.16}$$

$$0 < Q_m^{sc} \leq Q_{max}^{sc} \; where \; k = 1,\ 2,\ 3 \tag{4.17}$$

P_k^{DG} and Q_m^{sc} are the DG power and DSTATCOM reactive power injection at the nodes in the distribution network at optimal locations.

4.3 Modeling Battery Charging Load for EV

In this work, it is anticipated that EVs will be recharged from completely depleted states. Figure 4.6 can be used to produce the equation for the load flow analysis using the mod-

els for the battery charging loads [115]. The charging of a battery is shown in Equation (4.18) for both transient and steady state conditions. As a result, the exponential equations below can be used to estimate the battery power charging parameters.

$$P_{bEV}(t) = \begin{cases} P_{bEV}^{max}(1 - e^{\left(\frac{-\gamma \times t}{t_b}\right)}) & 0 \leq t \leq t_b \\ P_{bEV}^{max}\left(\frac{t_{max}-t}{t_{max}-t_b}\right) & t_b \leq t \leq t_{max} \\ 0 & t > t_{max} \end{cases} \tag{4.18}$$

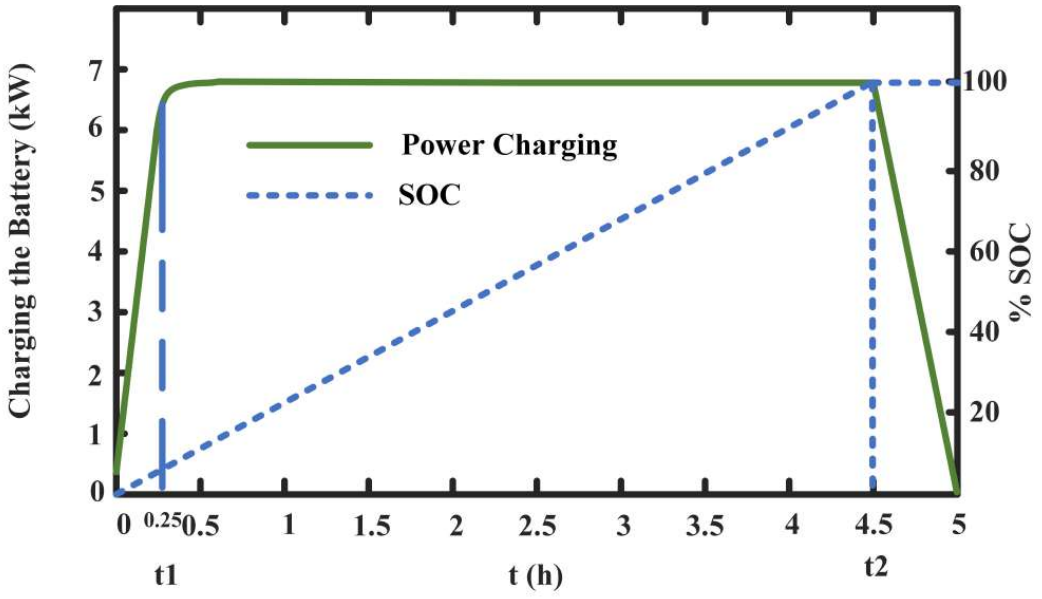

Figure 4.6: Li-ion battery charging characteristics.

$P_{bEV}(t)$ represents the instantaneous EV battery charging load. The maximum battery charging load for the substation is P_{bEV}^{max}.

$$\delta P_{bEV}^{max} = P_{bEV}^{max}\left(1 - e^{\left(\frac{-\gamma \times t_a}{t_b}\right)}\right) \tag{4.19}$$

$$\gamma = -\left(\frac{t_a}{t_b}\right) ln(1-\delta) \tag{4.20}$$

$t_a = 0.25\ h, t_b = 4.5\ h$, and $t_{max} = 5\ h$ are in the preceding Equations (4.18) and (4.20), respectively, taken from Figure 4.6. γ and δ are EV battery characteristic constants. Equation (4.20) (derived from Equation (4.19) can be used to find the value of γ. The EV battery's characteristic constants are alpha and beta. The fraction of maximum charging

load, expressed as 0.95, accounts for 95% of P_{bEV}^{max} at time t_a. Equation (4.21) can be utilized to establish the power charging equation when the batteries are charged from a zero-charge scenario P_{bEV}^{0}.

$$P_{bEV}(t) = P_{bEV}^{max}\left(1 - e^{\left(\frac{-\gamma \times t}{t_{cg}}\right)}\right) + P_{bEV}^{0}\left(e^{\left(\frac{-\gamma \times t}{t_{cg}}\right)}\right) \; 0 < t < t_{cg} \tag{4.21}$$

The t_cg is the time it takes to charge a battery from its starting charge position fully. The following equation can be used to describe the state of the power-charging battery.

$$SOC(t+1) = SOC(t) + P_{bEV}(t) \times \Delta(t) \tag{4.22}$$

Once reaching 100 % SOC, the batteries should be unplugged from the power supply to minimize battery damage caused by overcharging.

4.4 Summary of RAO-3

The optimization algorithm Rao was recently created [112]. Rao-1, Rao-2 and Rao-3 are the three proposed Rao algorithms. This study chose it as a population-based approach because it is straightforward to employ in optimized applications. It also has fewer control factors because there is no metaphorical explanation. Once the halt condition is reached, only the swarm size needs to be changed. Compared to other algorithms, the RAO algorithm performs better statistically because it can ensure exploration performance while yielding superior exploitation, keeping an excellent balance between exploration and exploitation.

The three RAO algorithms follow similar processes. However, as seen in the following steps and shown in Figure 4.7, only the movement equation is different.

1. Initialize the system data and load profile.
2. Initialize the population (algorithm parameter), iteration and set the maximum iteration.
3. Randomly initialize the sizings and locations of EVCS, DG and DSTATCOM.
4. The objective function's indicated fitness function is put to the test.
5. Identify the best and worst solutions proposed by the population.

6. The revised solution is updated for all populations under the selected RAO algorithm as follows:

   - RAO-1:

$$z'_{m,p,i} = z_{m,p,i} + rand_{1,m.i} \times (z_{m,b,i} - z_{m,w,i}) \tag{4.23}$$

   - RAO-2:

$$\begin{aligned} z'_{m,p,i} &= z_{m,p,i} + rand_{1,m.i} \times (z_{m,b,i} - z_{m,w,i}) \\ &+ rand_{2,m.i} \times (|\, z_{m,p,i} \; or \; z_{m,d,i} \,| \; - \; |\, z_{m,d,i} \; or \; z_{m,p,i} \,|) \end{aligned} \tag{4.24}$$

   - RAO-3:

$$\begin{aligned} z'_{m,p,i} &= z_{m,p,i} + rand_{1,m.i} \times (z_{m,b,i} - |\, z_{m,w,i} \,|) \\ &+ rand_{2,m.i} \times (|\, z_{m,p,i} \; or \; z_{m,d,i} \,| \; - (z_{m,d,i} \; or \; z_{m,p,i})) \end{aligned} \tag{4.25}$$

$z_{m,p,i}$ is the m^{th} variable's value for the p^{th} candidate in the i^{th} iteration. The best solution is denoted by $z_{m,b,i}$, whereas the worst solution is denoted by $z_{m,w,i}$. The Rao algorithm can guarantee exploration performance while producing superior exploitation, resulting in an excellent balance between exploitation and exploration, representing the method's higher statistical performance when compared to other algorithms.

4.5 Results and Discussion

A 69-bus radial distribution system is considered for the present analysis. The system's base values are 100 MVA and 12.66 kV. The backward–forward sweep method has been used for load flow studies. The proposed problem's simulation was carried out via MATLAB 2017a software installed on a computer with a processor Intel core i5 8th Gen, 8 GB RAM. Initially, i.e., at the base case from the load flow, the following data were obtained: the total real power load was 3082.19 kW, the reactive power load was 2796.77 kVAr, the minimum voltage was 0.9092 p.u., and the overall real power loss was 225 kW. The algorithm made the following assumptions: itrmax = 100 and population = 100.

The optimal positions and sizings of DG and DSTATCOM units were addressed in this work in the distribution system, which included three bus nodes of DG units and three bus nodes of DSTATCOM units. Moreover, for optimal planning of the EV charging station, five bus nodes were assumed, which is approximately 13% of the assumed distribution system bus nodes. In each charging station, a maximum of 50 EVs can be

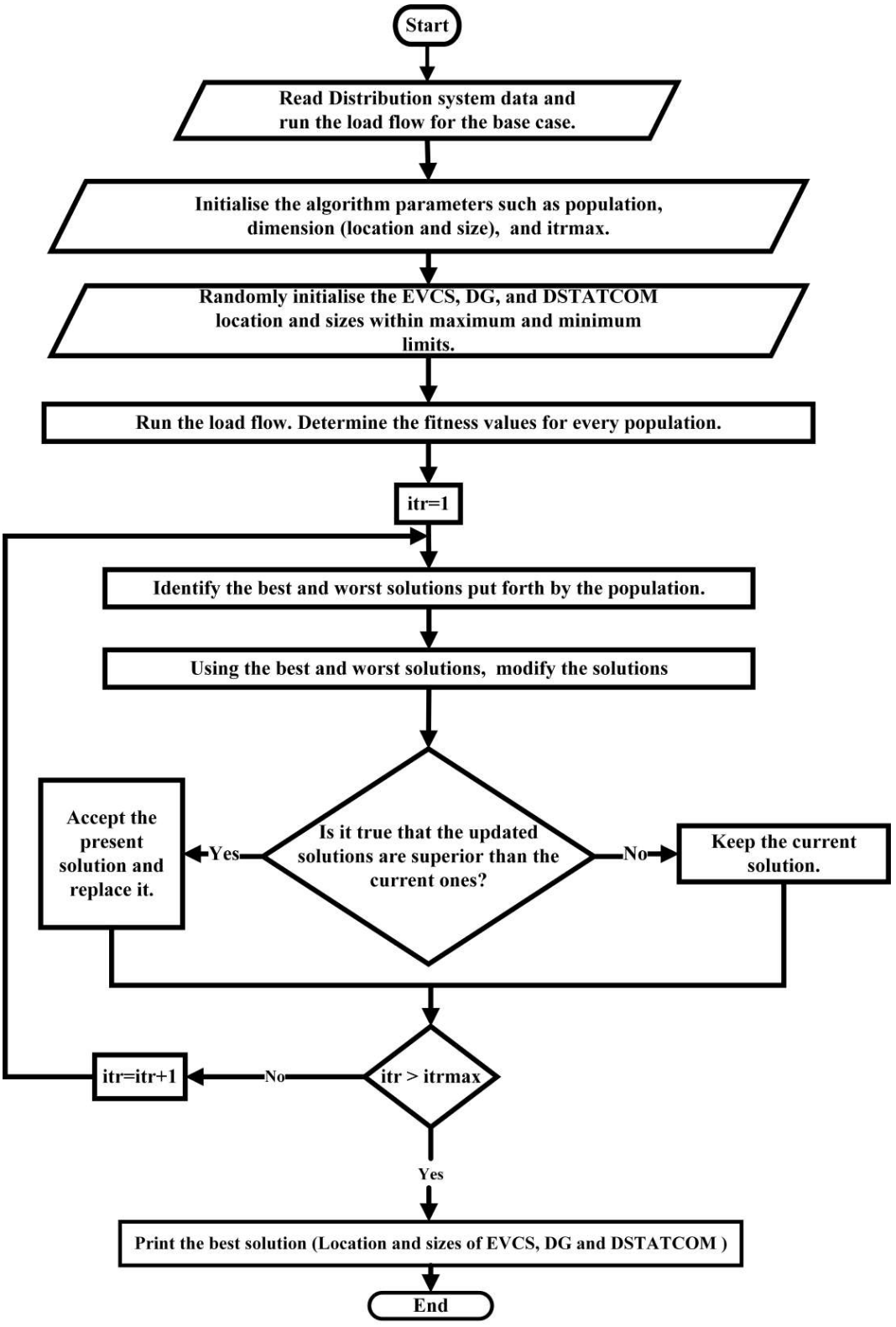

Figure 4.7: RAO-3 algorithm implementation flow chart.

charged. The characteristic charging curve is shown in Figure 4.6. Figure 4.6 shows that the Li-ion battery's maximum constant charge charging load is 6.5 kW.

In this work, DG, DSTATCOM, and EVCS were simultaneously (and optimally) placed via fuzzy multi-objective functions, as explained in Equation (4.15). In this scenario, the overall real power loss of the DST is reduced to 21.6085 kW, the voltage profile is enhanced, i.e., the minimum voltage of the DST is 0.988507 p.u. The optimum number of electric vehicles is increased, i.e., 209.

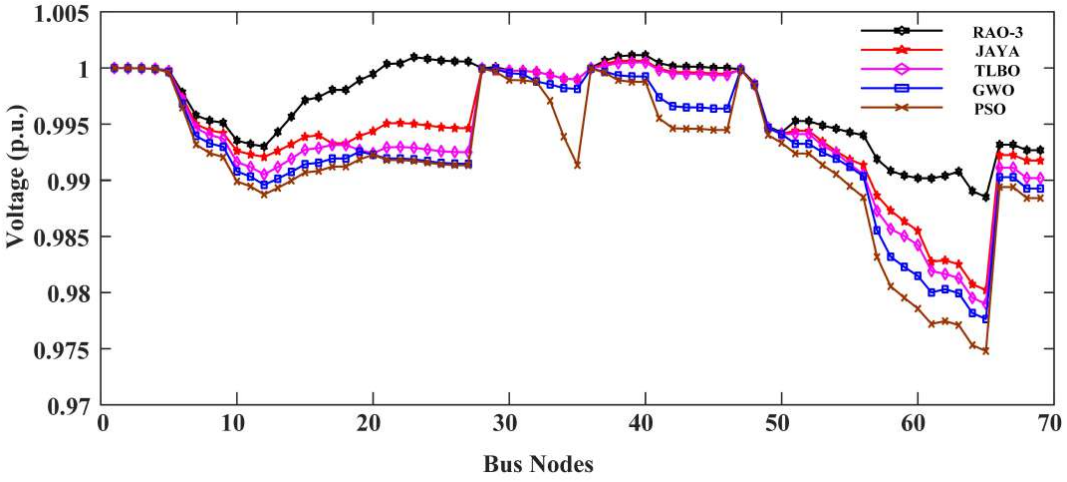

Figure 4.8: Voltage curve.

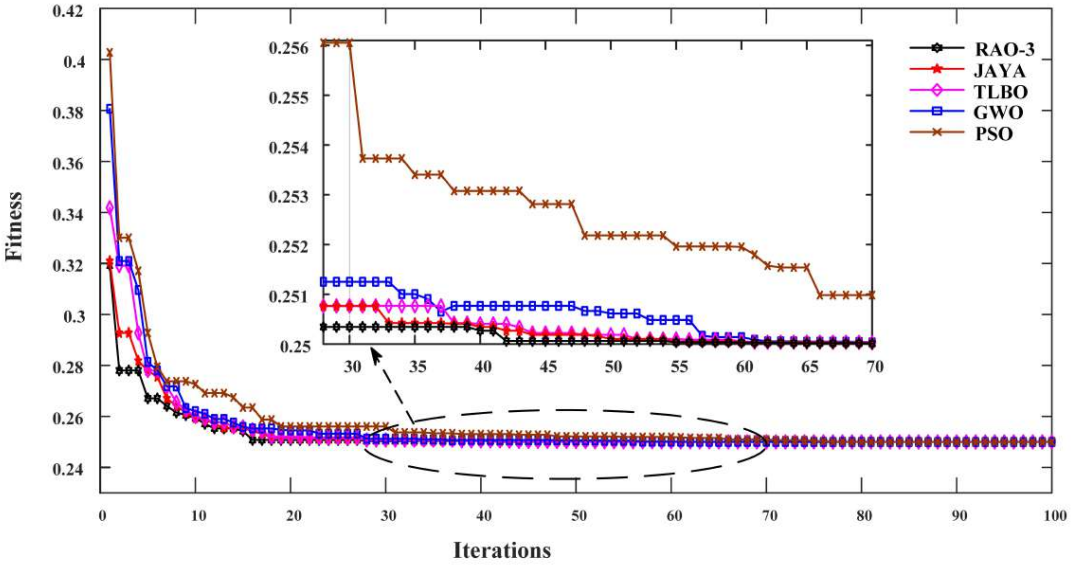

Figure 4.9: Fitness curve.

The optimum locations and sizings of DG and DSTATCOM were conducted, as shown in Tables 4.1 and 4.2. The optimal number of EVs and optimal locations of EVCSs were placed in the distribution system, as shown in Table 4.3. The performance of the distribution system can be analyzed in Table 4.4. The voltage profile curve and fitness function curves are shown in Figures 4.8 and 4.9. The single-line diagram of the 69-bus radial distribution system with EVCS, DG and DSTATCOM of simultaneous methodology is shown in Figure 4.10.

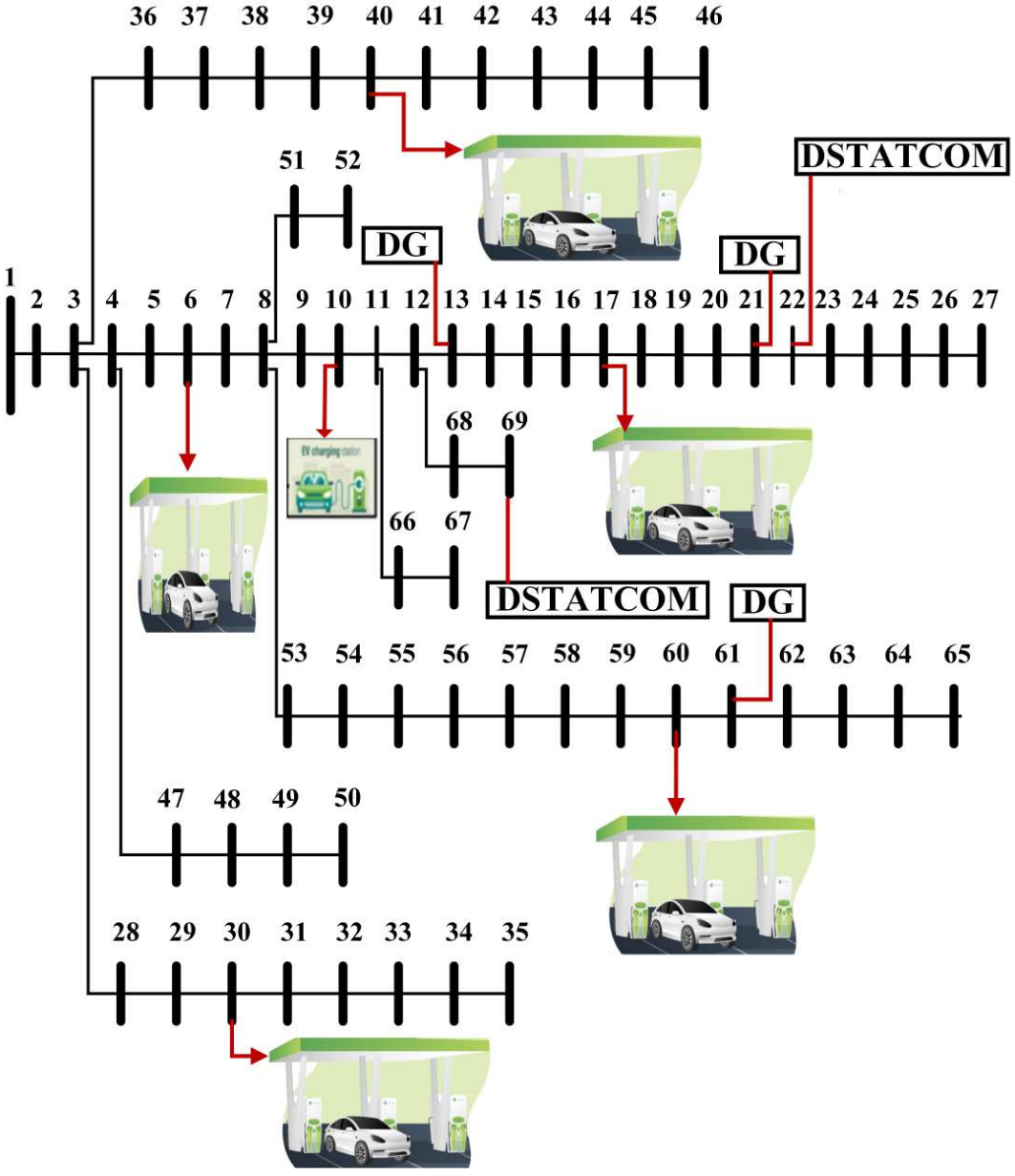

Figure 4.10: The single-line diagram of the 69-bus radial distribution system of Simultaneous methodology.

4.5.1 Analysis of the Enhancement of Distribution Load Growth

In this section, with the initial EV charging load with a simultaneous approach, the effect of enhancement of the distribution load is analyzed for the 69-bus radial DST in Figure 4.11. Active power loss decreases immensely with the integration of DSTATCOM and DGs in comparison to the base case. From Table 4.5, the real power loss reduces with the proposed methodology.

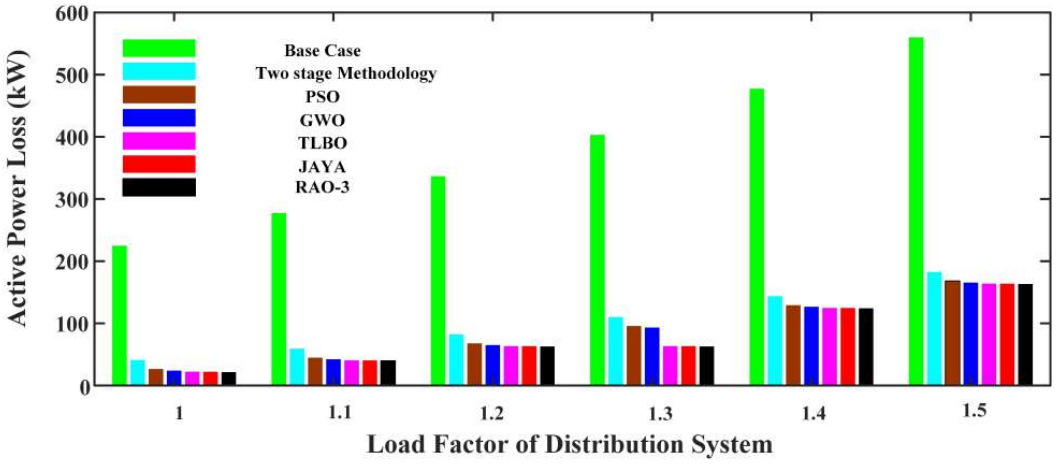

Figure 4.11: The impact of the rising DST system load on the performance of the 69-bus radial distribution system.

4.5.2 Analysis of Enhancement of EV Load

In this section, the effect of the enhancement of an EV load is analyzed with a simultaneous approach with different load factors of the distribution system. The proposed method of scenario 2 has the best performance compared to other scenarios. The EV load is increased up to 50 % of the initial load. Due to the enhancement of the EV load at various load conditions in distribution systems shown in Table 4.6, the power loss rises with rises in the EV load; however, with the fuzzy RAO-3 simultaneously proposed approach, the power loss is compared less with the base case.

The impact of the active power and reactive power consumed from SS with the enhancement of the EV load is depicted in Tables 4.7 and 4.8. Active power and reactive power consumed from SS can meet the rise in the EV load; with a simultaneously proposed approach, both active and reactive power consumed is less than the base case.

When the EV load increases, the impact on the minimum bus node voltage is analyzed

in Table 4.9. From Table 4.9, the minimum voltage reduces with a gradual enhancement of the EV load, and with a fuzzy RAO-3 simultaneous approach, a minimum bus node voltage remains within the standard limits.

4.5.3 Analysis of Transient Responses

Figure 4.12 depicts the impacts of EVs on EVCS node voltages. Batteries charge from a fully depleted to a completely charged state for 69-bus radial distribution systems under peak load conditions. It is also worth noting that, even with EV charging demand, the voltage quality may be maintained at a deservedly high level due to the availability of the complete DG capacity and DSTATCOM installations.

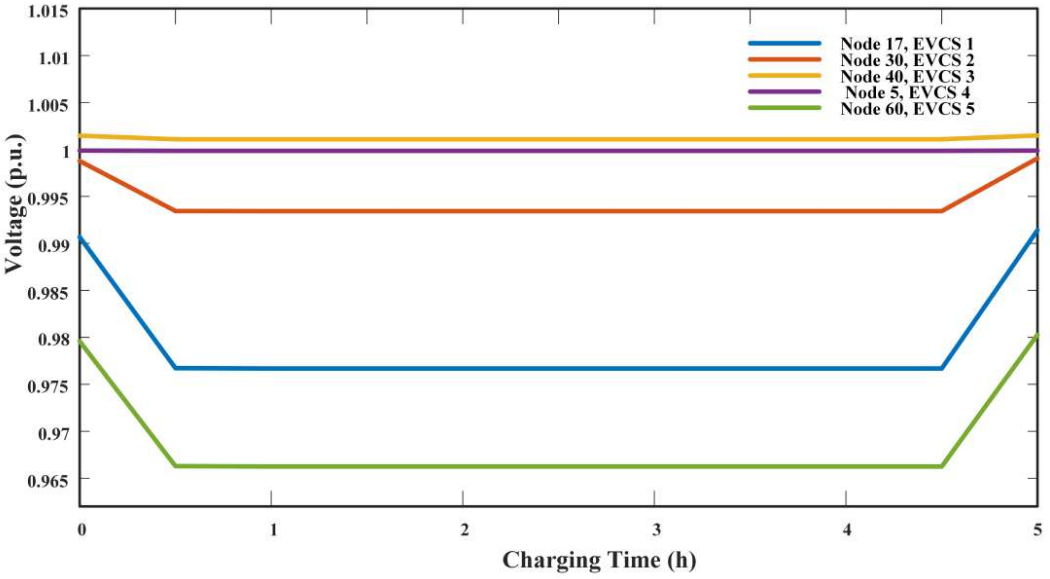

Figure 4.12: EVCS voltage transients.

4.6 Summary

In summary, the suggested approach enhances the test distribution system's performance, such as in simultaneous methodology the active power loss was reduced to 90.377%, 47.30%, and 37.341% compared to the base case, two-stage methodology [69], and two-stage methodology (chapter-1). The minimum voltage of the bus was enhanced to 0.988507 p.u. and 0.97653 p.u. in simultaneous methodology and two-stage methodology (chapter-1) compared to the base case minimum voltage of 0.902 p.u. The optimum number of vehicles in simultaneous methodology increased to 10% and 5.56%

compared to the two-stage methodology [69] in two-stage (chapter-1). Table 4.10 displays the comparison findings for all scenarios. Li-ion characteristic curves were used to develop P and Q load models for EV battery charging. Simulation results show that SS can support an EV load up to its active power supply's maximum level after the impact of the EV load growth under various loading situations. With the help of DG and DSTATCOM, the voltage profile can be kept at a reasonable level despite an increase in the EV load. The node voltages at the EVCS are impacted by the transient battery charging load, and at steady state charging, the node voltage maintains fair values with the help of DG and DSTATCOM. We show that the proposed method outperforms the stage-wise placement of various components in terms of (1) reducing active power loss, (2) improving substation power factors, (3) enhancing distribution network voltage profiles and (4) allocating the optimum number of vehicles at the charging stations.

Table 4.1: DG optimum location and sizing

Fuzzy PSO		**Fuzzy GWO**		**Fuzzy TLBO**		**Fuzzy JAYA**		**Fuzzy RAO-3**	
DG Node location	DG Sizing (kW)	DG Node location	DG Sizing (kW)	DG Node location	DG Sizing (kW)	DG Node location	DG Sizing (kW)	DG Node location	DG Sizing (kW)
21	653.8921	21	484.88	61	721.5755	14	489.8753	13	468.1426
61	780.7009	61	875.5393	13	482.7538	23	574.7970	61	900.0000
16	466.1071	12	540.2767	22	696.3707	61	836.0277	21	532.5574

Table 4.2: DSTATCOM optimum location and sizing

Fuzzy PSO		**Fuzzy GWO**		**Fuzzy TLBO**		**Fuzzy JAYA**		**Fuzzy RAO-3**	
Node location	Sizing (kVAr)	Node location	Sizing (kVAr)	Node location	Sizing (kVAr)	Node location	Sizing (kVAr)	Node location	Sizing (kVAr)
69	361.1784	69	299.43	23	313.5098	68	462.5327	64	468.3387
21	488.7751	64	673.4	69	466.6435	64	673.4000	69	464.8292
64	506.5490	24	388.42	64	598.5872	22	239.8411	22	446.1719

Table 4.3: Optimum number of EV and optimum location of EVCS

Fuzzy PSO		**Fuzzy GWO**		**Fuzzy TLBO**		**Fuzzy JAYA**		**Fuzzy RAO-3**	
Optimum node for EVCS	Optimum no of EV	Optimum node for EVCS	Optimum no of EV	Optimum node for EVCS	Optimum no of EV	Optimum node for EVCS	Optimum no of EV	Optimum node for EVCS	Optimum no of EV
39	41	59	30	39	44	59	39	40	47
30	39	30	41	31	36	5	48	60	40
4	33	41	39	18	37	41	40	17	36
17	28	18	33	6	38	18	35	30	40
60	45	6	43	60	35	60	37	5	46
Total no. of EV	186	Total no. of EV	186	Total no. of EV	190	Total no. of EV	199	Total no. of EV	209

Table 4.4: Performance comparison of 69 bus system

Simultaneous Methodology	**Base case**	**Fuzzy PSO**	**Fuzzy GWO**	**Fuzzy TLBO**	**Fuzzy JAYA**	**Fuzzy RAO-3**
SS Real power (kW)	4027.19	2220.7	2203.8	2163.3	2156.8	2119.1
SS Reactive power (kVAr)	2796.77	729.6046	724.4771	711.0508	708.7443	706.7995
SS Power factor	0.8214	0.95 lag	0.95 lag	0.95 lag	0.95 lag	0.95 lag
DG Penetration (kW)	-	1900.7	1900.7	1900.6997	1900.7	1900.7
Active Power loss (kW)	224.56	26.5745	23.985	22.1920	22.1257	21.6085
Voltage minimum (p.u.)	0.902	0.974789	0.977643	0.978995	0.980217	0.988507

Table 4.5: The impact of increased Distribution load on the 69 bus

Load factor	**Base-case**	**Two stage Methodology [69]**	**Fuzzy PSO**	**Fuzzy GWO**	**Fuzzy TLBO**	**Fuzzy JAYA**	**Fuzzy RAO-3**
1	224.8949	41.01	26.5745	23.985	22.1920	22.1257	21.6085
1.1	277.3206	59.22	44.7845	42.195	40.402	40.3357	39.8185
1.2	336.5602	89.22	67.8	65.195	63.402	63.34	62.82
1.3	403.0962	110.27	95.8345	93.245	91.452	91.3857	90.8685
1.4	477.4605	143.65	129.1845	126.6	124.842	124.7357	124.22
1.5	560.2671	182.66	168.1945	165.605	163.812	163.75	163.2285

Table 4.6: Impact on Active power loss (kW) in 69 bus radial DST

Load Factor	**Base Case**	**Initial EV Load**	**With 25% Rise in EV Load**	**With 40% RISE in EV Load**	**With 50% Rise in EV Load**
0.4	32.51	11.4535	13.652	18.943	20.5833
0.5	51.61	12.8789	15.0161	20.2530	21.2379
0.6	75.53	16.3617	18.2900	22.8646	23.5342
0.7	104.53	18.5627	20.7933	23.6172	26.2366
0.8	138.90	20.2054	22.0611	24.1741	28.5975
0.9	178.95	20.7181	23.432	25.5596	29.7692
1	225	21.6085	25.7404	26.8496	32.1375

Table 4.7: Impact on Active power (kW) consumed from SS in 69 bus radial DST

Load Factor	**Base Case**	**Initial EV Load**	**With 25% Rise in EV Load**	**With 40% Rise in EV Load**	**With 50% Rise in EV Load**
0.4	1553.39	1832.4	1954.38	2167.342	2239.6
0.5	1952.70	1928.1	2053.6	2207.3	2272.7
0.6	2356.84	1956.6	2155.5	2249.3	2316.2
0.7	2766.07	2015.1	2197	2283.1	2356.8
0.8	3180.66	2072.4	2200.8	2303.5	2379.9
0.9	3600.92	2104.3	2218.3	2331.0	2397.362
1	4027.19	2119.1	2247.8	2352.6	2405.1

Table 4.8: Impact on Reactive power (kVAr) consumed from SS in 69 bus radial DST

Load Factor	**Base Case**	**Initial EV Load**	**With 25% Rise in EV Load**	**With 40% Rise in EV Load**	**With 50% Rise in EV Load**
0.4	1092.69	601.2	631.21	710.95	731.8654
0.5	1370.85	630.1	678.551	725.066	745.5750
0.6	1651.20	641.3	700.4033	738.028	758.9
0.7	1933.83	652.53	723.6628	759.084	767.6204
0.8	2218.88	678.56	731.396	763.02	779.3336
0.9	2506.48	693.68	738.963	770.873	788.2645
1	2796.77	706.79	743.377	775.829	793.3322

Table 4.9: Impact on minimum distribution bus node 69 bus radial DST

Load Factor	**Base Case**	**Initial EV Load**	**With 25% Rise in EV Load**	**With 40% Rise in EV Load**	**With 50% Rise in EV Load**
0.4	0.9656	0.9970	0.9943	0.9858	0.9883
0.5	0.9574	0.9899	0.9861	0.9841	0.9824
0.6	0.9476	0.9893	0.9848	0.9833	0.9812
0.7	0.9383	0.9891	0.9837	0.9824	0.9780
0.8	0.9288	0.9889	0.9831	0.9792	0.9777
0.9	0.9191	0.9887	0.9825	0.9778	0.9768
1	0.9092	0.9885	0.9820	0.9714	0.9667

Table 4.10: Comparison results

Cases	Real Power loss (kW)	Voltage minimum (p.u.)	Total number of EV
Simultaneous methodology	21.6085	0.988507	209
Two stage Methodology (Chapter-1)	34.4876	0.97653	198
Two stage Methodology [69]	41.01	0.9461	190
Base Case	224.56	0.9020	-

Chapter 5

Optimal Network Reconfiguration of Distribution System with Electric Vehicle Charging Stations, Distributed Generation, and Shunt Capacitors

5.1 Introduction

The strategy proposed in the previous chapter reduces the overall power losses and improves the voltage profile. DSTATCOM was used in the previous chapter in order to balance the reactive power in the distribution system. However, in practical the DSTATCOM is quiet expensive.

This chapter, suggests an RAO-3 based on the fuzzy classification technique for the optimum EVCS, DGs, and SCs sizing and positioning for 69 bus radial distribution systems with network reconfiguration. The proposed method has the following advantages (i) lower active power loss, (ii) enhanced voltage profiles, (iii) improved power factor at the substation and (iv) optimum distribution of EVs at charging stations. Characteristic curves of Li-ion battery charging are utilised for load flow analysis to build EV battery charging loads models. The proposed simultaneous fuzzy multi-objective study with a reconfigured network can handle the optimal number of EVs in EVCS and maintain the substation power factor at the required level, yielding an impressive distribution system performance.

The rest of the paper is organised in the following manner: Section 5.2 discusses the fuzzy multi-objective formulation of the problem and its constraints. Section 5.3 discusses the fuzzy multi-objective RAO technique. Section 5.4 includes the results and analyses, whereas Section 5.5 has the summary.

5.2 Problem Formulation

The fuzzy-based multi-objective functions necessary for optimal deployment of EVCS, DGs, and SCs in order to improve distribution system performance are established in this section.

5.2.1 Substation Power Factor Membership Function:

The DGs primarily run at 0.95 lagging pf; hence, the goal is to improve the Substation (SN) pf to 0.95 lagging. The following equation can be used to compute the substation power factor.

$$pf = \cos\left(\frac{S_{kW}^{SN}}{S_{kVA}^{SN}}\right) \tag{5.1}$$

$$S_{kW}^{SN} = \sum_{m=1}^{nbs} P_m^{load} + Pl - \sum_{n=1}^{ndg} P_n^{DG} \tag{5.2}$$

$$S_{kVAr}^{SN} = \sum_{m=1}^{nbs} Q_m^{load} + Ql - \sum_{o=1}^{nsc} Q_o^{SC} - \sum_{n=1}^{ndg} P_n^{DG} \times \emptyset_{dg} \tag{5.3}$$

$$S_{kVA}^{SN} = \sqrt{{S_{kW}^{SN}}^2 + {S_{kVAr}^{SN}}^2} \tag{5.4}$$

S_{kW}^{SN} and S_{kVA}^{SN} are the active and reactive power drawn from the substation. P_n^{DG} is the capacity of the nth DG. The total no-of DGs installations is ndg. $\emptyset_{dg}$ is the DGs units' power factor angle. The m^{th} node's active power and reactive power loads are P_m^{load} and Q_m^{load}. nbs is the total number of buses in the distribution network. Pl is the real power loss and Ql is the reactive power loss of the distribution system. The capacity rating of shunt reactive is Q_o^{SC}. The total number of SCs installations is nsc.The fuzzy membership function for the SN Power-Factor (pf) [69] is depicted in Fig. 1(a), and the mathematical expression is given in Equation. (5.5).

$$\delta^{\,pf} = \begin{cases} 0 & \text{for } pf \le pf_{min} \\ \frac{pf - pf_{min}}{pf_s - pf_{min}} & \text{for } pf_{min} \le pf \le pf_s \\ \frac{pf_{max} - pf}{pf_{max} - pf_s} & \text{for } pf_s \le pf \le pf_{max} \\ 0 & \text{for } pf \le pf_{max} \end{cases} \tag{5.5}$$

pf_{min} = 0.85, pf_s = 0.95, pf_{max} = 1 are assumed.

5.2.2 DGs penetration membership function:

The DGP is the proportion of installed DGs to total active power load.

$$DGP = \frac{\sum_{n=1}^{ndg} P_n^{DG}}{\sum_{m=1}^{nbs} P_m^{load}} \tag{5.6}$$

The fuzzy membership function for the DGs penetration [69] is shown in Fig.1(b) and mathematical expression is given in Equation. (5.7).

$$\delta^{DGP} = \begin{cases} 0 & \text{for } DGP \leq DGP_{min} \\ \frac{DGP - DGP_{min}}{DGP_s - DGP_{min}} & \text{for } DGP_{min} \leq DGP \leq DGI_s \\ \frac{DGP_{max} - DGP}{DGP_{max} - DGP_s} & \text{for } DGP_s \leq DGP \leq DGP_{max} \\ 0 & \text{for } DGP \leq DGP_{max} \end{cases} \tag{5.7}$$

$DGP_{min} = 0.4,\ DGP_s = 0.5,\ DGP_{max} = 0.6$

5.2.3 Active power loss membership function:

The following equation depicts the distribution network's active power loss (AL):

$$AL = \sum_{m=1}^{nbs-1} Pl_m \tag{5.8}$$

Pl_m represents the branch active power loss [116], where formulated from the following equation: -

$$Pl_m = \frac{r_m \times \left\{P_{m+1}^2 + Q_{m+1}^2\right\}}{\left|v_{m+1}\right|^2} \tag{5.9}$$

whereP_{m+1} is the active power load injected at the load $(m+1)$ node and Q_{m+1} is the reactive power load.

The following formula can be used to determine the active power loss index (ALX):

$$ALX = \frac{AL_{DGSC}}{AL_{Base}} \tag{5.10}$$

With DGs and SCs, AL_{DGSC} denotes active power loss. AL_{Base} denotes the real power loss in the base case. The fuzzy membership function for the real power loss [69] is depicted in Fig.1(c) and mathematical expression is given in equation Eq. (5.11). $ALX^{max} = 1$. $ALX^{min}$is chosen based on utility necessity so that active power loss is minimized to a desirable value.

$$\delta^{ALX} = \begin{cases} 1 & \text{for } ALX \leq ALX^{min} \\ \frac{ALX^{max} - ALX}{ALX^{max} - ALX^{min}} & \text{for } ALX^{max} \leq ALX \leq ALX^{min} \\ 0 & \text{for } ALX > ALX^{max} \end{cases} \tag{5.11}$$

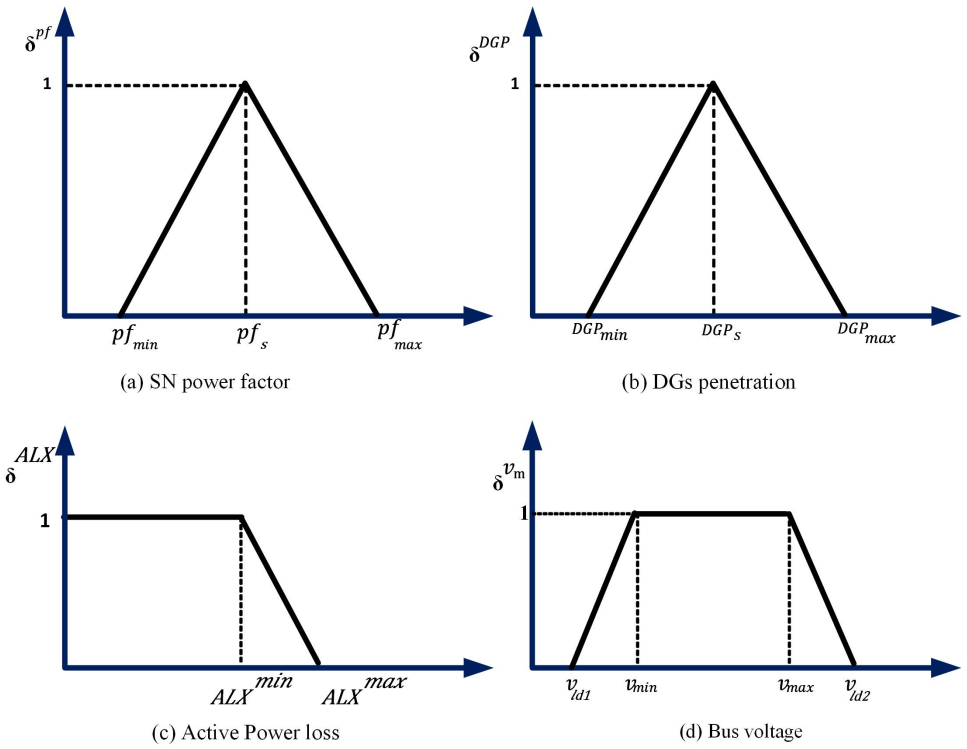

Figure 5.1: Fuzzy Membership function

5.2.4 Distribution system voltage membership function:

In Fig. 1(d), the fuzzy membership function of voltage [69] (δ^{v_m}) of each node m in the distribution system is explained, and it can be mathematically explained using Equation. (5.12). $v_{ld1} = 0.94, v_{min} = 0.95, v_{max} = 1.05, v_{ld2} = 1.06$ are assumed. The distribution system's fuzzy voltage limit is now defined as $\delta^{v} = (1 - \min(\delta^{v_m}))$

$$\delta^{v_m} = \begin{cases} 0 & \text{for } v_m \leq v_{ld1} \\ \frac{v_m - v_{ld1}}{v_{min} - v_{ld1}} & \text{for } v_{ld1} < v_m < v_{min} \\ 1 & \text{for } v_{min} \leq v_m \leq v_{max} \\ \frac{v_m - v_{max}}{v_{ld2} - v_{max}} & \text{for } v_{max} < v_j < v_{ld2} \\ 0 & \text{for } v_m > v_{ld2} \end{cases} \tag{5.12}$$

5.2.5 Distribution Network Reconfiguration methodology

To determine the efficacy of loss reduction, the researchers' proposed optimum network reconfiguration switching strategies must consider each feasible transition. The proposed network reconfiguration strategy [114] is described in detail in the following algorithm.

Step 1: Data from the system is read. Run the radial distribution networks load-flow application.

Step 2: Calculate the difference in voltage between the open tie switches, i.e., $\Delta v_{tie}(j)$, $j = 1,2,3 \ldots tie$.

Step 3: Determine which of the open tie switches has the greatest voltage difference.

Step 4: The tie switch "s" is closed, count how many loop branches (L_s) there are, including the tie branch.

Step 5: Open each branch in the loop one at a time to evaluate the value of each objective.

[for $j = 1$ *to* L_s, compute $\delta^{ALX}, \delta^{v_m}.D_s = \min(\delta^{ALX}, \delta^{v_m})$]

Step 6: Select the ideal solution for the "s" action of the tie switch i.e.,$O_s = \max(D_s)$)

Step 7: tie=tie-1

Step 8: Check to see if tie=0. If answer is yes, proceed to Step 11. If not, proceed to Step 10.

Step 9: Return to Step 2 after rearranging the code of the remaining tie switches.

Step 10: Results should be printed.

Step 11: Stop

5.2.6 Optimal allocations of EVs, DGs, and SCs using a multi-objective fuzzy function:

$$G_{zs} = \frac{1}{\delta^{ALX} + \delta^{pf} + \delta^{v} + \delta^{DGP}} \tag{5.13}$$

The propose method is to minimise fuzzy function described in Equation. (5.13), which is exposed to various constraints.

$$0 < P_n^{DG} \leq P_{max}^{DG} \; where \; n = 1,\ 2,\ 3 \tag{5.14}$$

$$0 < Q_o^{sc} \leq Q_{max}^{sc} \; where \; o = 1,\ 2,\ 3 \tag{5.15}$$

The DGs and SCs power injection at the optimal point in the distribution system are P_n^{DG} and Q_o^{sc}.

5.2.7 Battery charging load modelling for EVs:

Equations for load flow analysis using the battery charging load model [115] can be generated from Fig. (5.2). Equation. (5.16) depicts the charging of a battery for both steady-state and transient circumstances. The following exponential equations can be used to predict the power charging properties of batteries [69].

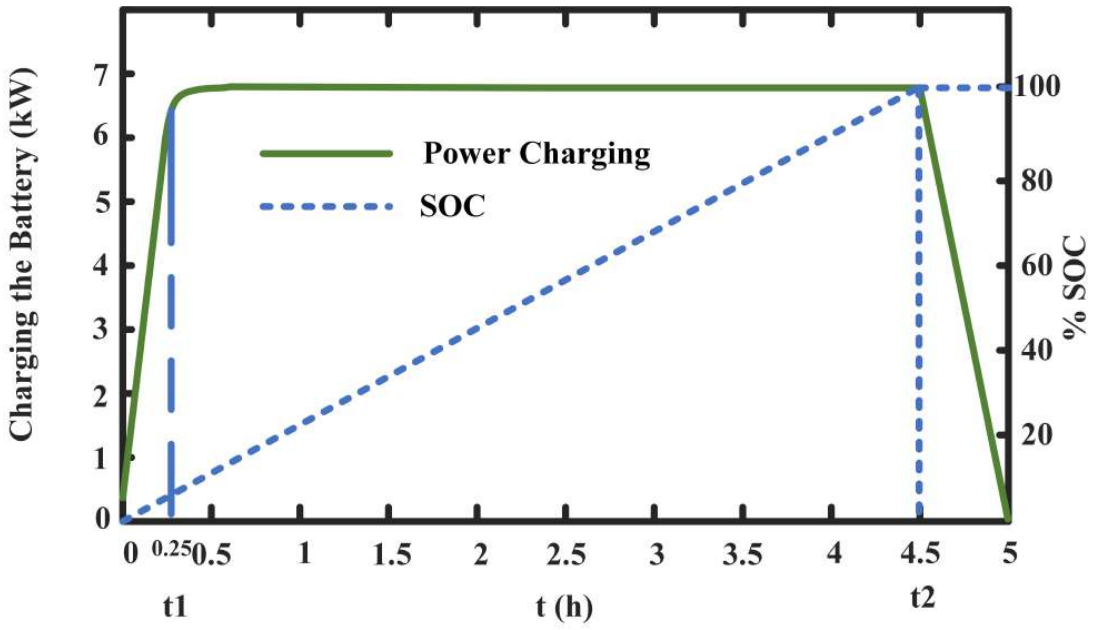

Figure 5.2: Li-ion Battery Charging Characteristics

$$P_{BEV}(t) = \begin{cases} P_{BEV}^{max}\left(1 - e^{\left(\frac{-\gamma \times t}{t_2}\right)}\right) & 0 \leq t \leq t_2 \\ P_{BEV}^{max}\left(\frac{t_m - t}{t_m - t_2}\right) & t_2 \leq t \leq t_m \\ 0 & t > t_m \end{cases} \tag{5.16}$$

The instantaneous electric vehicle battery charging load is $P_{BEV}(t)$. P_{BEV}^{max} is the substation's maximum battery charging load.

$$\delta P_{BEV}^{max} = P_{BEV}^{max}\left(1 - e^{\left(\frac{-\gamma \times t_1}{t_2}\right)}\right) \tag{5.17}$$

$$\gamma = -\left(\frac{t_2}{t_1}\right) ln(1-\delta) \tag{5.18}$$

$t_1 = 0.25\ h$, $t_2 = 4.5\ h$, and $t_m = 5\ h$ are in the preceding Equation. (5.16) and Equation. (5.17), respectively, taken from Fig. (5.2). The EV battery characteristic constants are γ and δ. δ is the proportion of maximum load for charging, with a value of 0.95 corresponding to 95% of P_{BEV}^{max} at time t_1. Equation. (5.18) (which may be derived from Equation. (5.17)) can be used to find the value of γ. The equation for power charging can be represented as Equation. (5.19). The batteries are charged from a zero-charge condition P_{BEV}^{0}.

$$P_{BEV}(t) = P_{BEV}^{max}\left(1 - e^{\left(\frac{-\gamma \times t}{t_c}\right)}\right) + P_{BEV}^{0}\left(e^{\left(\frac{-\gamma \times t}{t_c}\right)}\right) \quad 0 < t < t_c \tag{5.19}$$

The t_c represents the amount of time it takes to charge a battery from its starting charging position fully. The following equation can be used to represent the status of the power charging battery.

$$SOC(t+1) = SOC(t) + P_{BEV}(t) \times \Delta(t) \tag{5.20}$$

5.3 RAO-3 algorithm

The optimization algorithm Rao was just recently created [112]. Rao-1, Rao-2 and Rao-3 are the three proposed Rao algorithms. It was chosen as a population-based approach for this study because of its simplicity and ease of implementation in optimization applications. It has a few control parameters. The population size is the sole control parameter that must be changed once the stop criteria are met.The three RAO algorithms follow similar processes. However, as seen in the following steps and shown in Fig. (5.3), only the movement equation is different.

Step 1: Initialize the population (EVCS, DG and SC), their sizes, the number of EVs at random, and the maximum iteration.

Step 2: The fitness function mentioned in the objective function is evaluated.

Step 3: Determine the population's best and worst solutions.

Step 4: According to the chosen RAO algorithm,the new solution updated for all populations as follows:

a: RAO-1:

$$y'_{m,p,i} = y_{m,p,i} + rand_{1,m.i} \times (y_{m,b,i} - y_{m,w,i}) \tag{5.21}$$

b: RAO-2:

$$\begin{aligned} y'_{m,p,i} = y_{m,p,i} + rand_{1,m.i} \times (y_{m,b,i} - y_{m,w,i}) \\ + rand_{2,m.i} \times (|\, y_{m,p,i} \; or \; y_{m,d,i} \,| \; - \; |\, y_{m,d,i} \; or \; y_{m,p,i} \,|) \end{aligned} \tag{5.22}$$

c: RAO-3:

$$\begin{aligned} y'_{m,p,i} = y_{m,p,i} + rand_{1,m.i} \times (y_{m,b,i} - |\, y_{m,w,i} \,|) \\ + rand_{2,m.i} \times (|\, y_{m,p,i} \; or \; y_{m,d,i} \,| \; - \; (y_{m,d,i} \; or \; y_{m,p,i})) \end{aligned} \tag{5.23}$$

$y_{m,p,i}$ is the m^{th} variable's value for the p^{th} candidate in the i^{th} iteration. The best solution is denoted by $y_{m,b,i}$, whereas the worst solution is denoted by $y_{m,w,i}$. The Rao-3 algorithm can guarantee exploration performance while producing superior exploitation, resulting in an excellent balance between exploitation and explorations, representing the method's higher statistical performance when compared to other algorithms.

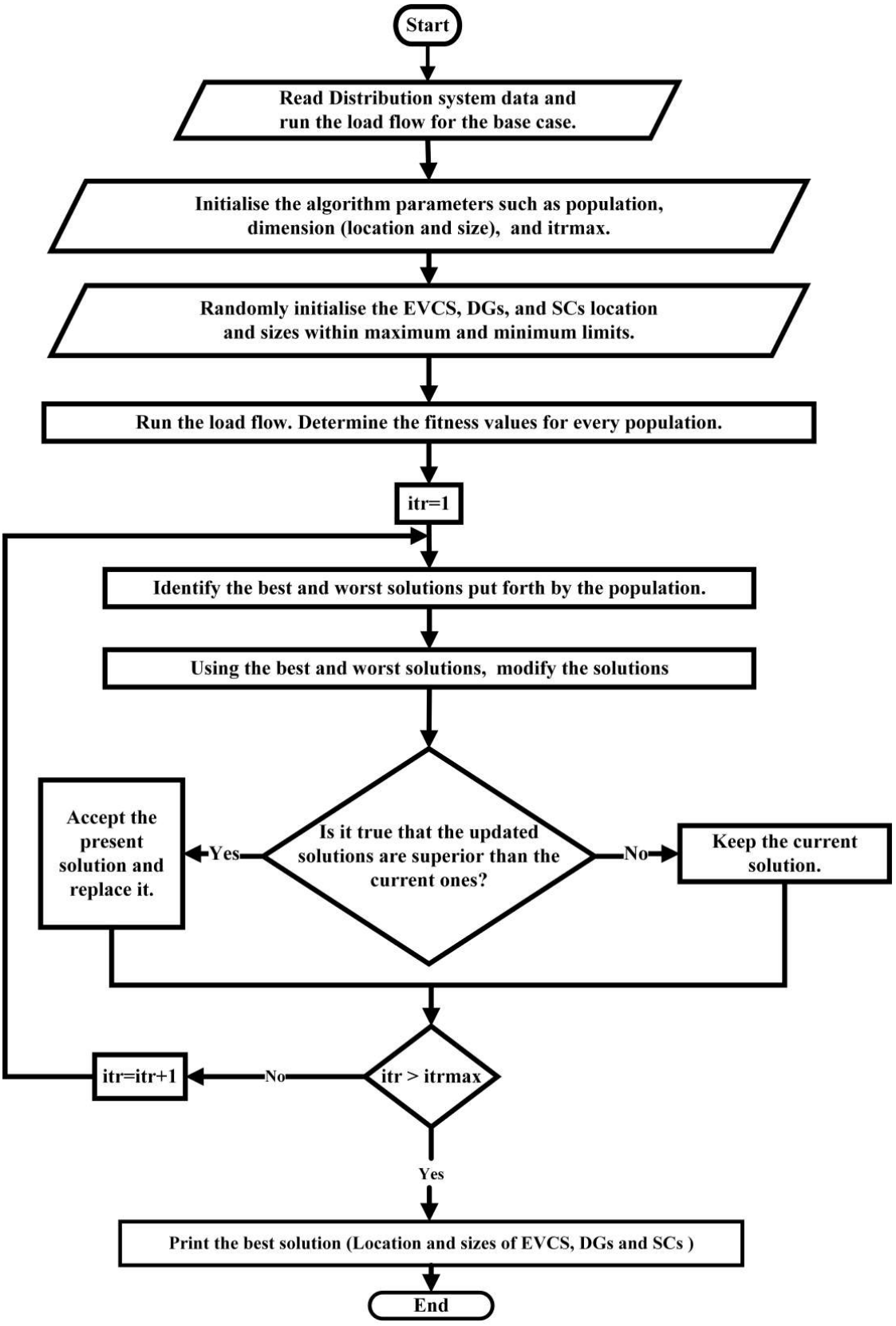

Figure 5.3: Rao-3 flow chart for the placment of EVCS, DGs, and SCs

5.4 Result and discussions

A 69 bus radial distribution system is considered for the present analysis. 100 MVA and 12.66 kV are the system's base values. Backwards-forward sweep method is used for load flow studies. Proposed problem, simulation is carried out in MATLAB 2017a software installed on a computer having processor intel core i5 8th Gen, 8GB RAM. Initially, i.e., at the base case from load flow following data are obtained total active power load is 3082.19 kW, the reactive power load is 2796.77 kVAr, total real losses are 225 kW, and the minimum voltage is 0.9092 p.u.

The optimal position and sizing of DG and SC units are addressed in this work in the distribution system, which includes three bus nodes of DG units and three bus nodes of SC units. Moreover, for optimal planning of the EV charging station, 5 bus nodes are assumed, which is approximately 13 % of the assumed distribution system bus nodes. In each charging station maximum of 50 EVs can be charged. The characteristic charging curve shown in Figure 5.2. From Figure 5.2, Li-ion battery's maximum constant charge charging load is 6.5 kW. Two scenarios are studied for EVCS, DGs, and SCs in a particular distribution network to be sized and placed optimally.

5.4.1 Scenario 1

With the help of the Rao-3 algorithm, DGs, SCs and EVCS are optimal sized and positioned fuzzy multi-objective functions defined in equation Equation. (5.13) in this paper. Table. (5.1) and Table. (5.2) shows the DGs and SCs optimal location and size. Table. (5.3) depicts the optimal number of EVs and EVCS are deployed. Table. (5.4) shows the distribution system's performance. Fig. (5.4) and Fig. (5.5) illustrate the fitness function and voltage profile curves, respectively. Fig. (5.6) shows a single line diagram of the 69-bus radial distribution system with EVCS, DGs and SCs from scenario 1.

The total power loss of the distribution network is decreased to 39.3467 kW, which is lower than the base case, and the voltage profile is improved, with the distribution system's minimum voltage being 0.9762 p.u. Compared to the two-stage process [69], the optimal number of cars is raised to 193.

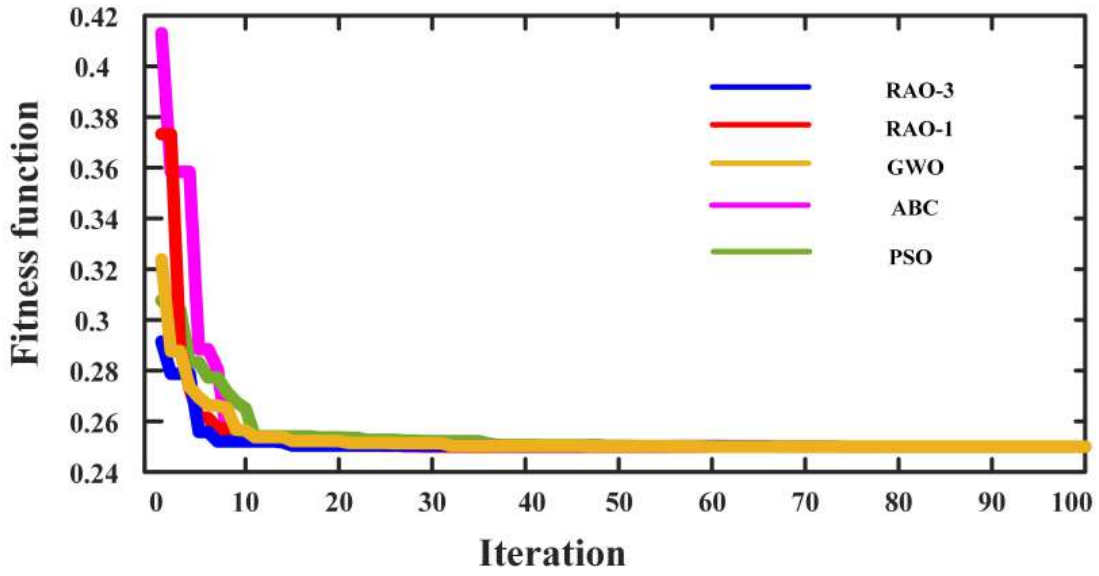

Figure 5.4: fitness curve

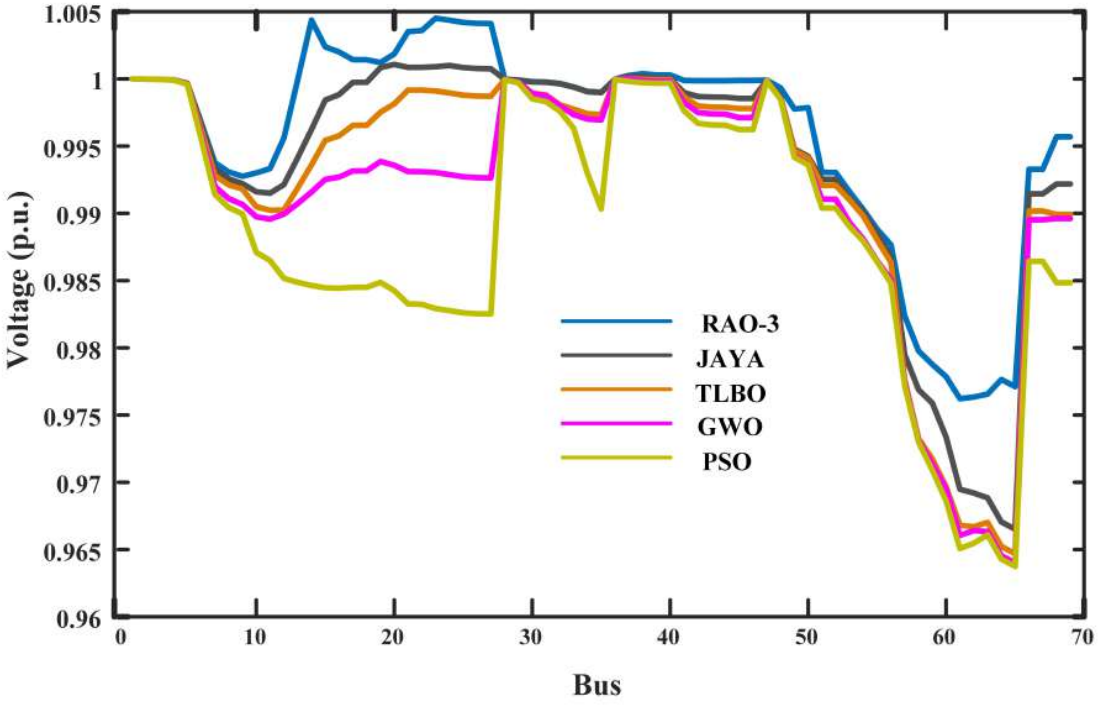

Figure 5.5: Voltage profile curve

5.4.2 Scenario 2

In this scenario, first network reconfiguration of 69 bus radial system is done.The system's real-power loss prior to reconfiguration is 224.95 kW, and the lowest system volt-

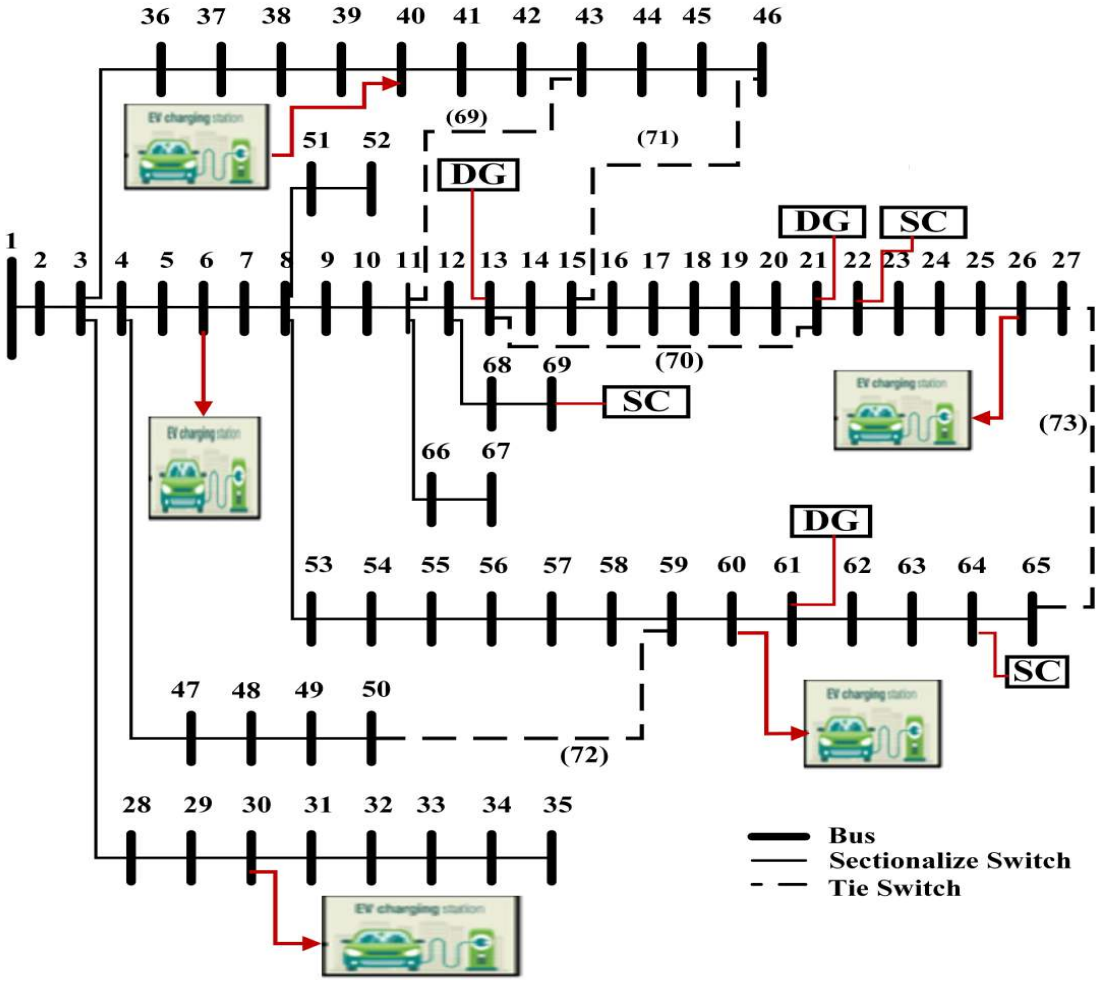

Figure 5.6: Single line Diagram of 69 bus with EVCS, DGs and SCs

age V_{min}=0.9092 p.u.

After network reconfiguration, the active power loss of 69 radial bus distribution network is reduced to 98.5512 kW, i.e., 56.1789 % power loss reduction, and minimum voltage is V_{min} =0.94947 p.u. which is shown in Fig. (5.7). Table. (5.5) represents the performances of distribution system after network reconfiguration. With this network reconfiguration, EVCS, DGs, and SCs are optimally placed with the help of fuzzy multi-objective functions explained in Equation. (5.13). Fig. (5.8)and Fig. (5.9) depict the fitness function and voltage profile curves, respectively. Fig. (5.10) shows a single line diagram of the after-network reconfiguration of the 69-radial bus with EVCS, DGs, and SCs from scenario 2. The optimal allocation of DGs and SCs are determined, as illustrated in Table. (5.6) and Table. (5.7). The optimal number of EVs and the optimal placement of EVCS are shown in Table. (5.8). Table. (5.9) examines the performance

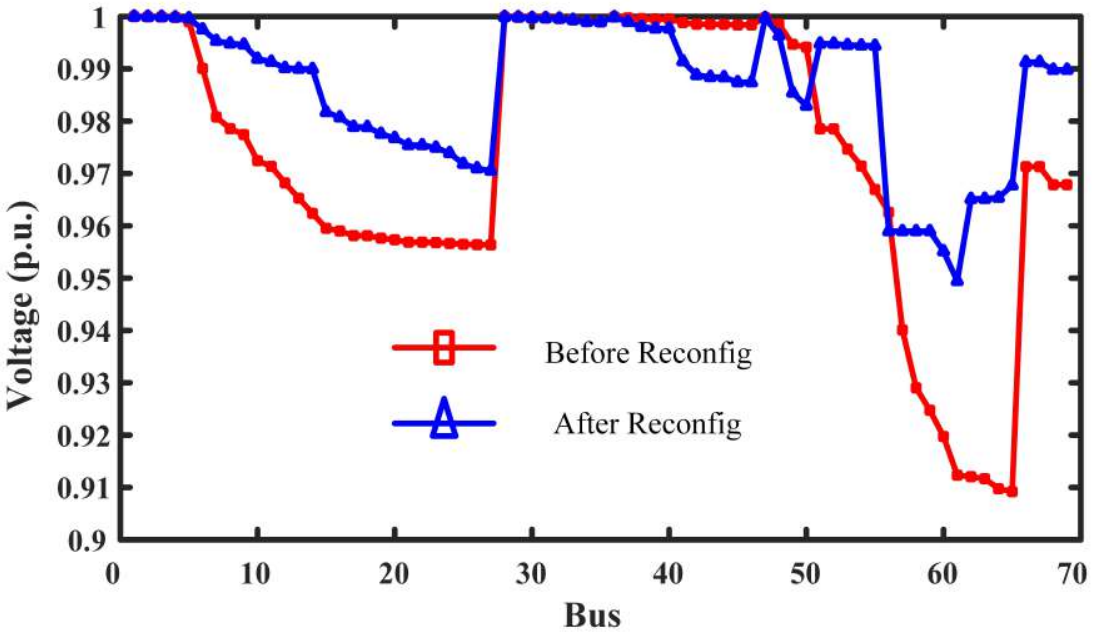

Figure 5.7: Voltage curve before and after reconfiguration

of the distribution system.

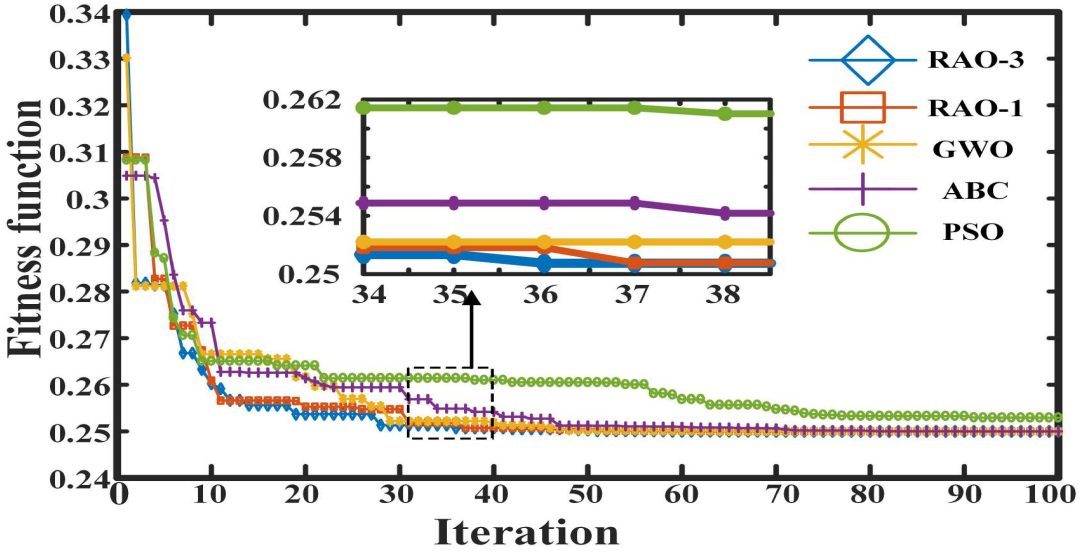

Figure 5.8: fitness curve

In this scenario, the distribution system's overall power loss is decreased to 18.0884 kW, which is lower than scenario 1 and the voltage profile is improved, with the distribution system's minimum voltage being 0.9905 p.u. The optimal number of EVs has been

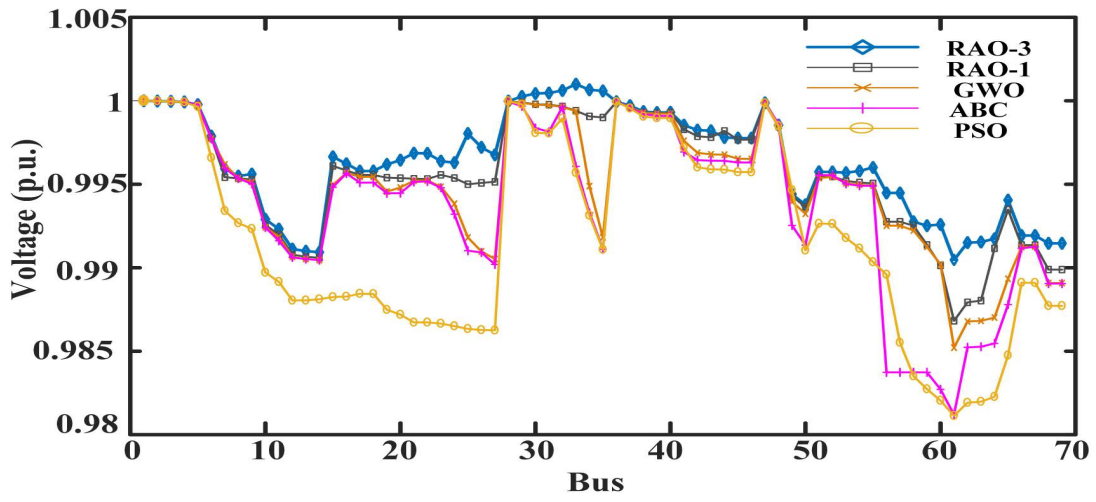

Figure 5.9: Voltage profile curve

increased to 213 vehicles.

Fig. (5.11) depicts the impact of EVs on EVCS node voltages. It is also worth noting that, even with EV charging demand, the voltage quality may be maintained at kept at deservedly high levels due to the availability of the complete DGs capacity and SCs installations.

5.5 Summary

In summary, the suggested approach scenario 2 (simultaneous placement of EVCS, DG, and SC with network reconfiguration utilising Rao-3) performs better than the other scenarios. Table. (5.10) compares the outcomes of all of the scenarios.

Compared to the base case, two-stage methodology [69] and scenario 1, the active power loss in scenario 2 is reduced to 91.9589 %, 55.89 % and 54.028 %. Compared to the base case minimum voltage of 0.9092, the bus's minimum voltage is enhanced to 0.9905 p.u. and 0.9762 p.u. in scenarios 2 and 1. Compared to the two-stage methodology [69] and scenario 1, the optimal number of EVs in scenario 2 increases to 12.1 % and 10.362 %.

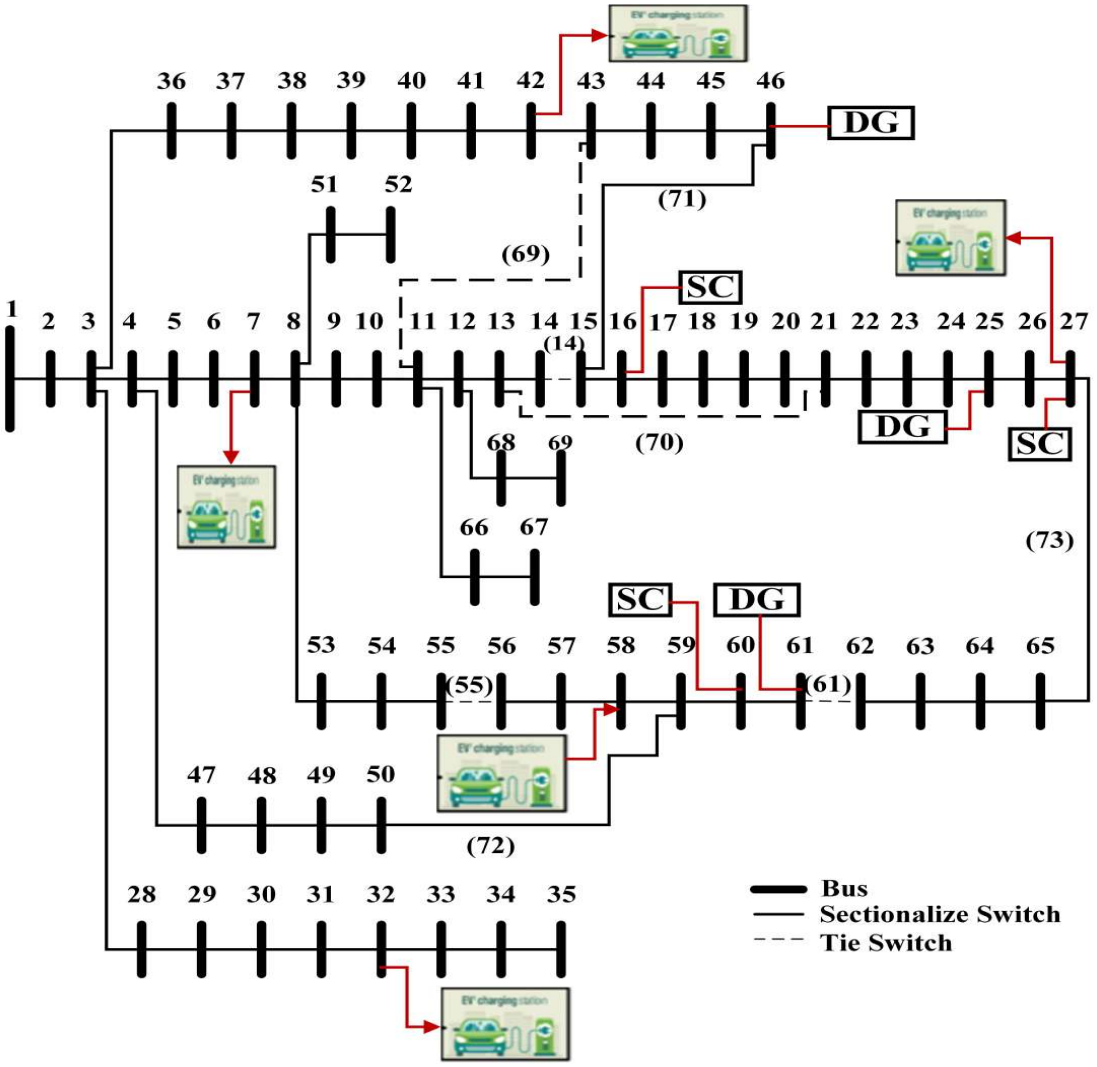

Figure 5.10: Single line Diagram of 69 bus with EVCS, DGs and SCs

Table 5.1: DG optimum location and sizing

Fuzzy PSO		**Fuzzy ABC**		**Fuzzy GWO**		**Fuzzy RAO-1**		**Fuzzy RAO-3**	
DGs Node location	DGs Sizing (kW)	DGs Node location	DGs Sizing (kW)	DGs Node location	DGs Sizing (kW)	DGs Node location	DGs Sizing (kW)	DGs Node location	DGs Sizing (kW)
63	900	19	529.4247	61	898.3838	61	806.9187	13	507.8488
23	900	61	871.2734	14	900	59	591.6334	21	539.3180
6	100.7	10	500.0016	24	102.3163	19	502.1479	61	853.5330

Table 5.2: SCs optimum location and sizing

Fuzzy PSO		**Fuzzy ABC**		**Fuzzy GWO**		**Fuzzy RAO-1**		**Fuzzy RAO-3**	
SCs Node location	SCs sizing (kVAr)	SCs Node location	SCs sizing (kVAr)	SCs Node location	SCs sizing (kVAr)	SCs Node location	SCs sizing (kVAr)	SCs Node location	SCs sizing (kVAr)
38	540.1420	32	457.3101	38	575.9351	50	511.6601	64	595.8269
58	582.9905	62	472.1094	62	519.4239	40	241.6474	69	372.0686
69	241.5578	28	455.2351	69	266.6933	12	635.2496	22	392.8228

Table 5.3: Optimum number of EV and optimum location of EVCS

Fuzzy PSO		**Fuzzy ABC**		**Fuzzy GWO**		**Fuzzy RAO-1**		**Fuzzy RAO-3**	
Optimum node for EVCS	Optimum no of EVs	Optimum node for EVCS	Optimum no of EVs	Optimum node for EVCS	Optimum no of EVs	Optimum node for EVCS	Optimum no of EVs	Optimum node for EVCS	Optimum no of EVs
31	24	48	34	10	31	53	38	6	38
19	38	9	41	40	35	56	37	18	45
48	32	45	33	36	36	3	33	30	35
43	31	47	36	45	36	37	50	60	30
32	42	18	33	35	43	39	30	40	45
Total no of EVs	167	Total no of EVs	177	Total no of EVs	181	Total no of EVs	188	Total no of EVs	193

Table 5.4: Performance comparison of 69 radial bus system

69 bus	**Base case**	**Fuzzy PSO**	**Fuzzy ABC**	**Fuzzy GWO**	**Fuzzy RAO-1**	**Fuzzy RAO-3**
SN Active power(kW)	4027.19	2240.2	2223.9	2218.7	2173.1	**2131.5**
SN Reactive power(kVAr)	2796.77	733.8005	730.9718	729.2853	709.6776	**702.5256**
SN pf (lag)	0.8214	0.95	0.95	0.95	0.95	**0.95**
DGs Penetration	-	1900.7	1900.7	1900.7	1900.7	**1900.7**
Real Power loss (kW)	224.56	45.1028	43.9486	43.7337	41.6879	**39.3467**
Voltage minimum (p.u.)	0.9092	0.965078	0.966049	0.966811	0.969482	**0.9762**

Table 5.5: Performances of distribution system after network reconfiguration

Entity	**Base case**	**PSO**	**ABC**	**GWO**	**RAO-1**	**RAO-3**
Tie Switches	69, 70, 71, 72, 73	17, 55, 61, 69, 71	9, 17, 56, 63, 71	14, 57, 61, 69, 70	14, 57, 61, 69, 70	**14, 55, 61, 69, 70**
Active Power loss (kW)	224.95	115.7826	112.8772	98.6046	98.6046	**98.5512 kW**
$V_{min}(p.u.)$	0.9092	0.94831	0.94831	0.94947	0.94947	**0.94947**

Table 5.6: DGs optimum location and sizing

Fuzzy PSO		**Fuzzy ABC**		**Fuzzy GWO**		**Fuzzy RAO-1**		**Fuzzy RAO-3**	
DGs Node location	DGs Sizing (kW)	DGs Node location	DGs Sizing (kW)	DGs Node location	DGs Sizing (kW)	DGs Node location	DGs Sizing (kW)	DGs Node location	DGs Sizing (kW)
61	812.6740	23	591.1429	21	535.7574	57	373.9585	61	885.1275
27	574.4756	61	850.1275	60	513.8592	61	797.9275	25	638.8911
45	513.2681	27	459.2271	61	851.0831	21	728.8167	46	377.6810

Table 5.7: SCs optimum location and sizing

Fuzzy PSO		**Fuzzy ABC**		**Fuzzy GWO**		**Fuzzy RAO-1**		**Fuzzy RAO-3**	
SCs Node location	SCs sizing (kVAr)	SCs Node location	SCs sizing (kVAr)	SCs Node location	SCs sizing (kVAr)	SCs Node location	SCs sizing (kVAr)	SCs Node location	SCs sizing (kVAr)
50	267.0198	48	493.5362	43	388.2457	61	441.8827	27	287.9169
61	351.9917	61	353.1125	58	363.0878	57	122.4775	60	514.4220
11	414.3575	51	206.4988	55	295.7983	28	449.6673	16	195.6782

Table 5.8: Optimum number of EV and optimum location of EVCS

Fuzzy PSO		**Fuzzy ABC**		**Fuzzy GWO**		**Fuzzy RAO-1**		**Fuzzy RAO-3**	
Optimum node for EVCS	Optimum no of EVs	Optimum node for EVCS	Optimum no of EVs	Optimum node for EVCS	Optimum no of EVs	Optimum node for EVCS	Optimum no of EVs	Optimum node for EVCS	Optimum no of EVs
19	36	28	36	31	38	39	39	**42**	**46**
42	35	44	39	38	39	38	41	**27**	**38**
36	44	30	36	28	34	37	44	**32**	**45**
38	40	47	39	37	44	28	39	**7**	**48**
48	35	25	40	35	35	36	43	**58**	**36**
Total no of EVs	190	Total no of EVs	190	Total no of EVs	190	Total no of EVs	206	Total no of EVs	**213**

Table 5.9: Performance comparison of 69 bus system

69 bus	**Base case**	**Fuzzy PSO**	**Fuzzy ABC**	**Fuzzy GWO**	**Fuzzy RAO-1**	**Fuzzy RAO-3**
SN Active power(kW)	4027.19	3303.3	3257.9	3155.33	3154.76	**3053.60**
SN Reactive power(kVAr)	2796.77	1085.71	1070.8	1037.106	1036.919	**1003.673**
SN pf (lag)	0.8214	0.95	0.95	0.95	0.95	**0.95**
Dg Penetration	-	1900.7	1900.7	1900.7	1900.7	**1900.7**
Real Power loss (kW)	224.56	20.06	19.64	19.09	18.2453	**18.0884**
Voltage minimum (p.u.)	0.9092	0.9811	0.9812	0.9852	0.9868	**0.9905**

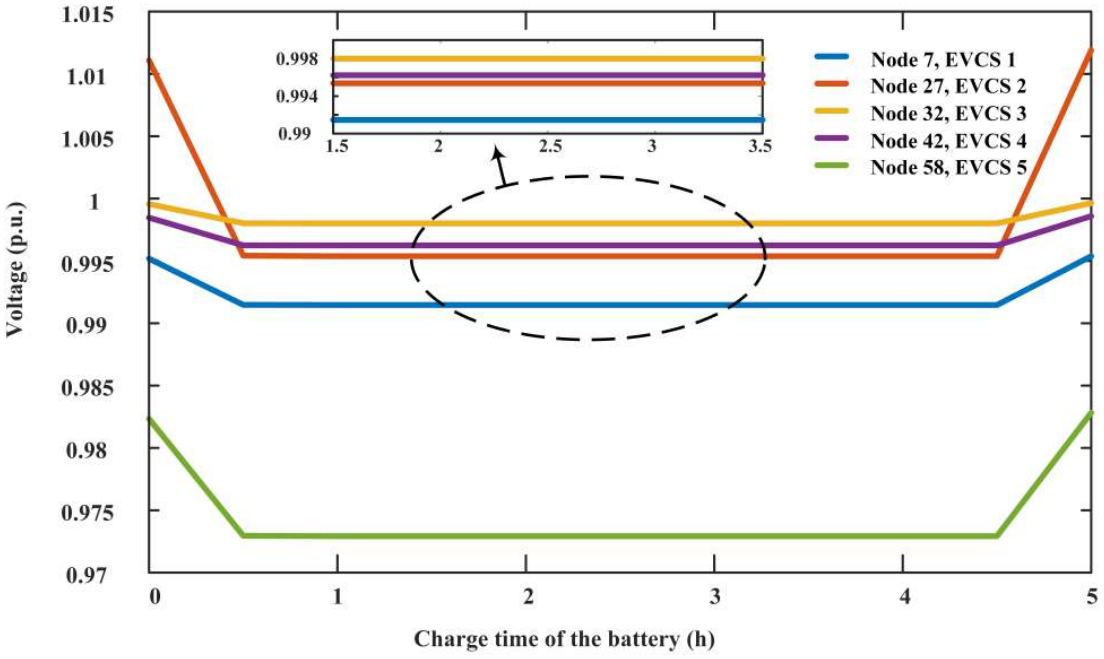

Figure 5.11: EVCS Voltage transients.

Table 5.10: Comparison results

Cases	Real Power loss (kW)	Voltage minimum (p.u.)	Total number of EV
scenario 2	**18.0884**	**0.9905**	**213**
scenario 1	39.3467	0.9762	193
Two stage Methodology [69]	41.01	0.9461	190
Base Case	224.56	0.9020	-

Chapter 6

Optimal Placement of Fast Charging Station for Integrated Electric-Transportation System using Multi-Objective Approach

6.1 Introduction

The usage of Electric Vehicles (EVs) for transportation is expected to continue growing, which opens up new possibilities for creating new smart grids. It offers a large-scale penetration of Fast Charging Stations (FCE) in a local utility network. A severe voltage fluctuation and increased active power loss might result from the inappropriate placement of the FCE as it penetrates the Distribution System (DST). This paper proposes a multi-objective optimisation for the simultaneous optimal allocation of FCEs, Distributed Generators (DGs) and Shunted Capacitors (SCs). The proposed Pareto dominance-based hybrid methodology incorporates the advantages of the Grey Wolf Optimiser and Particle Swarm Optimisation algorithm to minimise the objectives on 118 bus radial distribution systems. The proposed method outperforms some other existing algorithms in terms of minimising (a) active power loss costs of the distribution system, (b) voltage deviations, (c) FCE development costs, (d) EV energy consumption costs and (e) DG costs, as well as satisfying the number of FCEs and EVs in all zones based on transportation and the electrical network.

The remainder of this paper is structured as follows: Section 6.2 explains the formulation of the multi-objective issue and associated limitations. Section 6.3 presents the suggested hybrid GWO-PSO algorithm for the system under consideration. In Section 6.4, the results and analysis are covered. Section 6.5 discusses summary.

6.2 Problem Formulation

This section includes objective operations, such as DFC, EUC, CPDN, DVT and DGC being minimised.

In order to determine the optimal allocation of FCE, the proposed approach uses an arbitrary area, as depicted in Figure 6.1. Zones [117, 118] are created inside the research

area, such as zn_1, zn_2, zn_3, and zn_4, where the number of EVs is available in each zone. he assumption is that the number of EVs n each zone is located in the geographical centre. On a particular day, it was assumed that the FCE charges the Total Number of EVs ($NTEV$) in the considered area. $NTEV$ is calculated as:

$$NTEV = \sum_{z=1}^{zn} EV_{n,zn} \tag{6.1}$$

The number of committed EVs in the zone (zn) is represented by the value $EV_{n,zn}$.

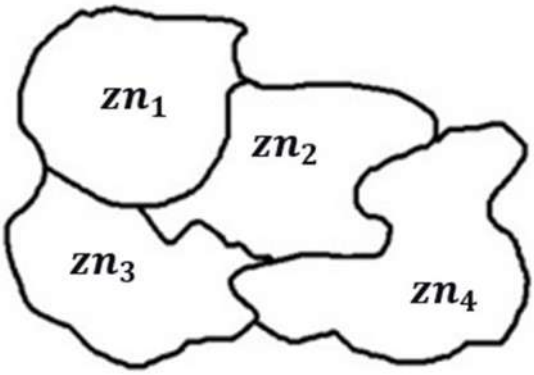

Figure 6.1: Illustrative zones with area.

6.2.1 Development Cost of FCEs (DFC)

DFC includes the cost of the charging station equipment and land cost. The equipment and land cost of charging station is a function of the number of charging connectors and capacity of charging stations [119].

$$DFC = C_{fixed} + 24 \times C_{land} \times NC(i) \times n_y + C_{cond} \times (NC(i) - 1) \times P_{cg} \tag{6.2}$$

FCE's fixed cost is denoted by C_{fixed} (USD). Since it deals with the equipment, the cost is almost similar among the different countries. C_{land} (in USD per meter) is the land rental cost yearly. The study time for the FCE consists of n_y years. The charger development cost is C_{cond}, $NC(i)$ is the number of connectors in charging stations in the ith FCE, and P_{cg} is the charging connector rated power (kW).

$$NC(i) = \sum_{z=1}^{zn} (max(PR_{EV}) \times EV_{n,zn} \times DFE(z,i)) \tag{6.3}$$

The probability that EVs will be charged in an hour (h) during a day is PR_{EV}. $DFE(z,i)$ is a decision binary variable, and if EVs in the zn are charged in the ith FCE, then $DFE(z,i) = 1$; otherwise, it is zero. The choice of EVs in the zn to the ith FCE is calculated by the minimal distance between the ith FCE to zn compared to the other FCE.

The capacity of the charging station's connectors differs between 50–250 kW. The rating of the ith FCE is calculated as:

$$P_{FCE} = NC(i) \times P_{cg} \tag{6.4}$$

6.2.2 Energy Consumption of EVs User Cost (EUC)

The EV user takes a particular route to reach the FCE. While driving, the EV consumes energy, and the cost related to energy consumption is represented by the EUC. In order to charge the batteries of EVs, which are situated at location zone zn to the nearest ith FCE, $EUC(zn,i)$ is calculated as [119]:

$$EUC(zn,i) = L(zn,i) \times CSE \times \sum_{hr=1}^{24} PR_{EV}(h) \times EV(zn) \times EP_h \tag{6.5}$$

The distance between the ith FCE and zone (zn) on a trajectory length is denoted as $L(zn,i)$. The electricity price in USD is represented by EP_h, and CSE is the specific energy consumption of EVs. EVs' CSE stands for their specific energy consumption.

6.2.3 Active Power loss of Distribution Network Cost (CPDN)

Since the EV demand is increasing, the load in the distribution network increases and distribution network power losses also increase. A non-linear relationship exists between the loading and the distribution network loss. The load varies from hour to hour on a particular day and during the year. A correct estimation of the distribution network power loss due to EV charging is required, i.e., the load variation must be considered. The Active power loss of the Distribution Network Cost($CPDN$) [119] of all seasons in a year is calculated as:

$$CPDN = \sum_{s=1}^{n_s} \sum_{hr=1}^{24} TPL(hr,s) \times N_{hr}(s) \times EP_h \tag{6.6}$$

The number of seasons is denoted as n_s, and TPL is the active power loss of the DST, including EV loads. The total number of hours throughout all seasons in a year is N_{hr}

6.2.4 Cost of DGs (DGC)

The cost of DGs includes the cost of investment C_{INV}, the cost of operation C_{OPR}, and the cost of maintenance C_{MAT} of DGs.

1. Cost of Investment: this includes various initial costs, such as money invested on unit construction, essential equipment, and installation for each generation unit. This cost can be expressed as:

$$C_{INV} = \sum_{d=1}^{ndg} (P_{dg,d} \times Cost_{INV}) \tag{6.7}$$

2. Cost of operation: the generation cost, fuel cost, and other similar costs are considered in the cost of operation C_{OPR}. It can be formulated as

$$C_{OPR} = \sum_{yr=1}^{n_{yr}} \sum_{d=1}^{n_{dg}} \left(P_{dg,d} \times TL_h \times CO_d \times \left(\frac{1+R_INF}{1+R_INT} \right)^{yr} \right) \tag{6.8}$$

3. Cost of Maintenance: This includes the cost required for restoring the unit equipment, renewal, and repairing.

$$C_{MAT} = \sum_{yr=1}^{n_{yr}} \sum_{d=1}^{n_{dg}} \left(P_{dg,d} \times TL_h \times CM_d \times \left(\frac{1+R_INF}{1+R_INT} \right)^{yr} \right) \tag{6.9}$$

Hours in a year are denoted by TL_h. The number of DGs considered for this study is n_{dg}, with n_{yr} being the total years for DG planning. Lastly, the DGC can be determined as:

$$DGC = C_{INV} + C_{OPR} + C_{MAT} \tag{6.10}$$

6.2.5 DVT

The improper placement of the FCE and DGs in the DST leads to voltage instability. This work calculates voltage deviations for 24 h of all seasons. Calculating the DVT of DST is as follows:

$$DVT = max\{1 - V(j)\} \qquad j = 1,2 \ldots nb \tag{6.11}$$

The voltage of the jth bus is $V(j)$, and the DST bus number is nb.

6.2.6 Multi-Objective Function

The optimum number of FCEs obtained using the proposed optimisation procedure is denoted by the symbol N_{FCE}. The primary purpose of the objective problem is to minimise the DFC, EUC, $CPDN$, DVT, and DGC by satisfying the constraints.

$$Min\left\{\sum_{k=1}^{N_{FCE}} DFC(k)+\sum_{l=1}^{NTEV} EUC(l)+CPDN+DGC+DVT\right\} \tag{6.12}$$

6.2.6.1 Constraints

To recharge the EVs from the research area, one FCE must be installed.

$$\sum_{k=1}^{NP_{FCE}} B(k)>0 \qquad k=1,2,3\ldots,\ NP_{FCE} \tag{6.13}$$

$B(k)$ is a binary decision variable; if the kth FCE is chosen, $B(k)=1$; otherwise, $B(k)=0$. NP_{FCE} is the number of feasible FCEs. At least one connector should be taken into account from the chosen FCE.

$$NC(k)\geq 0 \qquad k=1,2,3\ldots,\ NP_{FCE} \tag{6.14}$$

One optimal FCE is chosen by EVs from each zn depending on the displacement between zn to the kth FCE.

$$\sum_{z=1}^{zn} DFC(z,k)\times B(k)=1 \tag{6.15}$$

6.3 Overview of Hybrid GWO-PSO Algorithm

In the real world, the power system has multiple objective functions that should be optimised simultaneously. The objective function suggested in this work is optimised using a hybrid GWO-PSO technique [120]. The best features of GWO and PSO are combined to solve the problems. PSO [104] is a population-based metaheuristic optimisation algorithm. The greatest advantages of PSO is that it is simple to perform and has fewer controlling parameters.

$$Z_{p+1}^{itr} = Z_{p}^{itr}+v_{p+1}^{itr} \tag{6.16}$$

$$v_{p+1}^{itr} = v_p^{itr} + c_1 \times ran1 \times \left(P_{best}^{itr} - Z_p^{itr}\right) + c_2 \times ran2 \times \left(G_{best}^{itr} - Z_p^{itr}\right) \tag{6.17}$$

Here, Z_p is the position vector, v_p is the velocity vector, itr is the iteration, $p$vis the particle in the population, w is the inertia of the weight parameter, P_{best}^{itr} is the best position in the pth particle and G_{best}^{itr} is the best position in the available population. In the PSO algorithm, the main disadvantage is that the updated position and velocity of a particle cannot jump into another space with a global optimum and has a low convergence rate in the iterative process. Grey Wolf Optimisation (GWO) [109] is an intelligent swarm technique. GWO follows the hierarchy of leadership. Grey wolves are well coordinated and always live in packs. They always follow the social hierarchy, and, based on this hierarchy, they can be classified into four types of wolves, i.e., Alpha (α), Beta (β), Delta (δ), and Omega (ω). This social hierarchy is based on their fitness value. α is the top leader and makes the decisions (hunting, staying in one place, sleeping, etc.), and other members follow the order. β is subordinate to α, where β helps give suggestions to α for decision making and always ensures that other members follow the order given by α. δ is subordinate to β but superior to ω. ω is the follower and occupies the minuscule level in the hierarchy.

6.3.1 Encircling the Victim

During hunting, they encircle the prey. Encircling mathematical behaviour is modelled as

$$\vec{L} = \left|\vec{S}.\vec{Z}_p - \vec{Z}(itr)\right| \tag{6.18}$$

$$\vec{Z}(itr) = \vec{Z}_p(itr) - \vec{R}.\vec{L}t \tag{6.19}$$

itr denotes the current iteration, Z_p depicts the location of the prey, and Z represents the positioning of the grey wolf. It is possible to determine the vector coefficients $\vec{S}$ and $\vec{R}$ as

$$\vec{R} = 2.\vec{r}.rad_1 - \vec{r} \tag{6.20}$$

$$\vec{S} = 2.rad_2 \tag{6.21}$$

[0, 1] are the boundaries of the random vectors rad_1, rad_2. Through iterations, the coefficient $\vec{r}$ linearly declines from 2 to 0.

6.3.2 Hunting Procedure

α provides direction for the hunting process. A deeper understanding of the prey (optimal solution) is held by α, β, and δ. As alpha, beta, and delta change positions, other wolves in the back update the positions. Attacking can be expressed mathematically as follows:

$$\vec{L_\alpha} = \left|\vec{S}.\vec{Z_\alpha} - \vec{Z}\right| \tag{6.22}$$

$$\vec{L_\beta} = \left|\vec{S}.\vec{Z_\beta} - \vec{Z}\right| \tag{6.23}$$

$$\vec{L_\delta} = \left|\vec{S}.\vec{Z_\delta} - \vec{Z}\right| \tag{6.24}$$

$$\vec{Z_1} = \vec{Z_\alpha} - \vec{R_1}.(\vec{L_\alpha}) \tag{6.25}$$

$$\vec{Z_2} = \vec{Z_\beta} - \vec{R_2}.(\vec{L_\beta}) \tag{6.26}$$

$$\vec{Z_3} = \vec{Z_\delta} - \vec{R_3}.(\vec{L_\delta}) \tag{6.27}$$

$$\vec{Z}\,(itr+1) = \frac{\vec{Z_1} + \vec{Z_2} + \vec{Z_3}}{3} \tag{6.28}$$

6.3.3 Exploring and Attacking a Victim

When wolves attack their prey, and $|R| < 1$, the R-value should fall between [$-$2r, 2r]. Exploitation is the act of attacking prey. Exploration is the process through which they separate to look for the target. If $|R| > 1$, wolves are compelled to look for prey.

6.3.4 Hybrid GWO-PSO

Singh et al. [120] used low-level co-evolution mix hybrids for hybridising GWO with the PSO method. This algorithm's design philosophy integrates the GWO algorithm's exploration capability with the PSO algorithm's exploitation capability to maximise both types' strengths. The exploration and exploitation of the grey wolves in the search area are controlled by the inertia constant (w) rather than conventional mathematical calculations. The suggested equations update the positions of the first three agents in the search space.

$$\vec{L_\alpha} = \left|\vec{S}.\vec{Z_\alpha} - w \times \vec{Z}\right| \tag{6.29}$$

$$\vec{L_\beta} = \left|\vec{S}.\vec{Z_\beta} - w \times \vec{Z}\right| \tag{6.30}$$

$$\vec{L_\delta} = \left|\vec{S}.\vec{Z_\delta} - w \times \vec{Z}\right| \tag{6.31}$$

By revising the velocity and locations' equations as below, the GWO and PSO variants are combined.
Figure 6.2 depicts the hybrid GWO-PSO algorithm's flowchart. The hybrid GWO-PSO process' basic steps are as follows:

1. Initialise the parameters of GWO and PSO $\vec{R}$, $\vec{S}$, $\vec{r}$ and w; where $w = 0.5 + \text{rand}()/2$ and set maximum iteration.
2. Calculate an agent's fitness using Equations (6.29)–(6.31).
3. Update the velocity and location of the current search's grey wolf for each search using Equations (6.33) and (6.34).
4. $\vec{R}$, $\vec{S}$ and $\vec{r}$ are updated, Fitness of all wolves are computed.
5. Positions of α, β and δ are updated
6. Until the terminating requirements are met, repeat this process.

$$s = (v_p^{itr} + c_1 \times ran1 \times \left(\vec{Z}_1 - Z_p^{itr}\right) + c_2 \times ran2 \times \left(\vec{Z}_2 - Z_p^{itr}\right) + c_3 \times ran2 \times \left(\vec{Z}_3 - Z_p^{itr}\right) \tag{6.32}$$

$$v_{p+1}^{itr} = w \times \left(v_p^{itr} + s\right) \tag{6.33}$$

$$Z_{p+1}^{itr} = Z_p^{itr} + v_{p+1}^{itr} \tag{6.34}$$

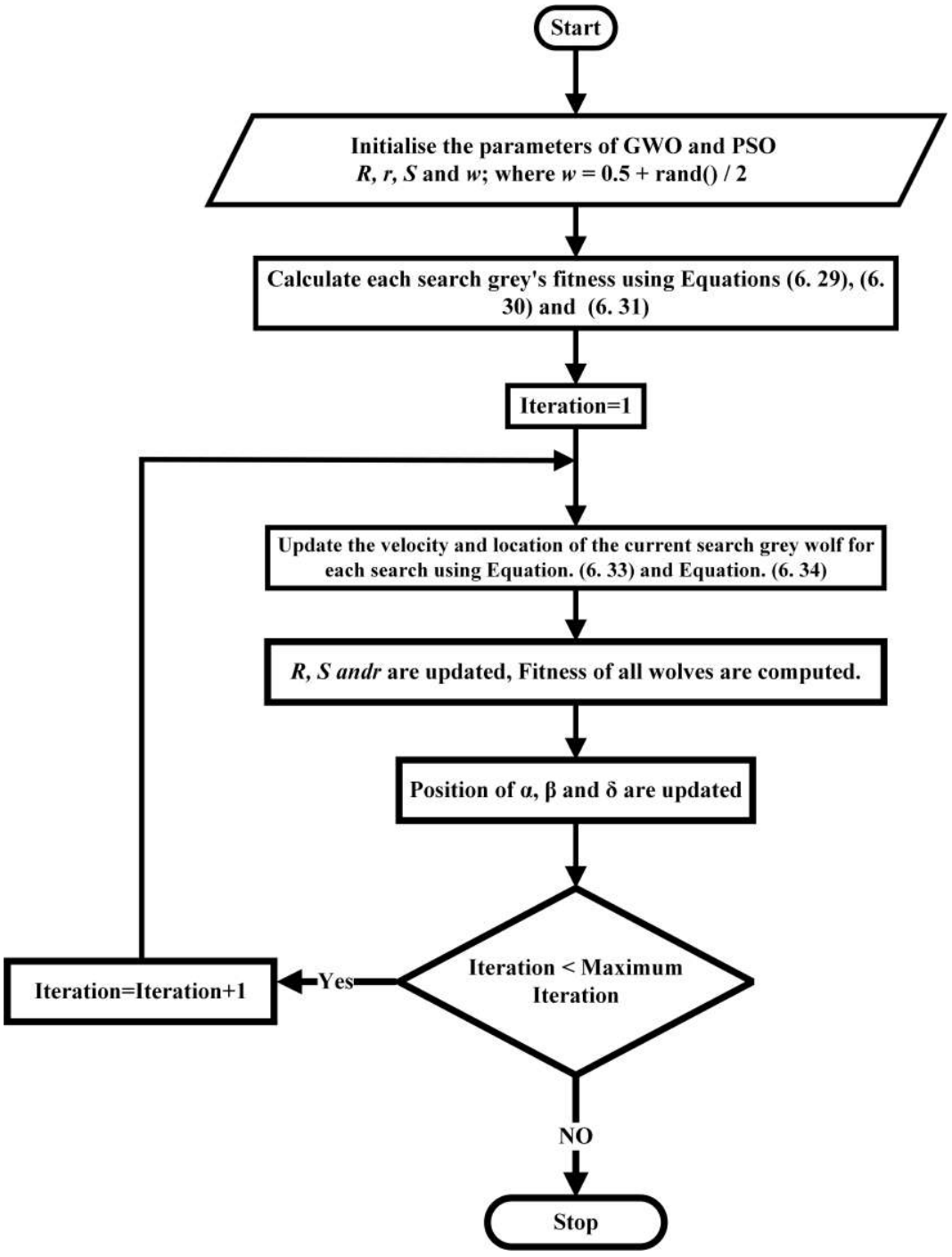

Figure 6.2: Hybrid GWO-PSO flowchart.

The multiple objective functions are constructed as a single goal function by selecting appropriate weights for each objective in all traditional approaches, such as the weighted objective approach. There are primarily two issues with determining the single objective's optimal value. The first is that while optimising a single objective function might

ensure the existence of a single optimal solution, in all practical uses, the judgement still wants access to other solutions. The second examines how each goal in a single objection function responds to its weights. Additionally, the classical approaches are ineffective when the objective function is much noisier and the factors in the search area are discontinuous.

Multiobjective Pareto front optimisation techniques are required to address multiobjective scenarios to get around the abovementioned issues. The hybrid methods are also quite effective at locating the best solution. In this work, hybrid GWO-PSO was utilised to meet the desired objectives.

Mirjalili et al. [121] proposed a set of non-dominated solutions, and one of these solutions must be chosen by the decision maker. Due to the subjectively inaccurate nature of the decision maker's assessment and the fact that it is straightforward to employ and has similarities to human thinking, the fuzzy satisfaction-based method [110] was employed in this case for ultimate decision-making.

6.4 Results and Discussion

In this chapter, four scenarios with various cases were explored using the suggested test system to determine the optimum distribution of FCE, DGs and SCs in a connected transportation network.

6.4.1 Proposed Methodology

This study used a 720 km^2 test area to apply the suggested strategy. The population of EVs in each research area zone is shown in Figure 6.3. There are 180 zones in the test area, each with a 4 km^2 $(2\ km \times 2\ km)$. As seen in Figure 6.4, a test area was connected to the 118 bus radial distribution system.

0	3	5	3	4	6	4	0	0	3	7	5	6	4	0
3	5	4	6	4	6	7	8	7	9	8	7	5	6	4
7	11	16	9	9	13	12	10	11	14	17	6	9	5	3
6	1	7	15	16	17	17	9	15	7	14	17	9	15	1
4	6	9	10	8	16	16	14	0	14	16	11	7	9	7
0	13	14	10	16	14	19	15	17	14	12	8	15	9	4
7	11	0	16	16	17	13	18	17	15	9	19	12	8	0
4	9	15	14	12	11	4	16	19	9	12	17	17	12	6
8	13	14	19	17	15	17	0	13	12	11	13	9	15	8
3	12	9	16	13	14	9	14	16	15	17	16	15	13	3
0	6	7	8	7	5	6	4	8	5	4	6	4	0	0
0	5	3	4	6	4	0	7	3	0	5	6	4	3	4

Figure 6.3: Zone EV population.

In this chapter, the total EV population was considered as 1632.

With the requirement that each FCE is roughly equally spaced apart, it has been assumed that 16 FCE might be put along the test area's major roadways. Figure 6.4 depicts 16 possible FCEs represented in the DST by the rhombus symbol. The simulation of the proposed problem was carried out in MATLAB 2017a software installed on a computer with a processor intel core i5 8th Gen and 8 GB RAM. A 118 distribution bus system was considered to carry out the analysis.

The distributed system's base values were as follows: 22.71 MW of real power, 11 kV, 100 MW and 1.7041 MVAr. The load curve [119] for different seasons is shown in Figure 6.5. For the optimum location and sizing of DGs and SCs in the distribution system, this paper considered five bus nodes of DGs units and three bus nodes of SCs units. From 5 a.m. to 9 p.m. every day, it is presumable that EVs are charged at the FCE. Figure 6.6 indicates the probability of daily EV charging. The DST and FCE parameters are represented in Table 6.1. Four different scenarios were analysed with the help of a hybrid GWO-PSO algorithm with a maximum of 500 iterations for appraising the proposed problem.

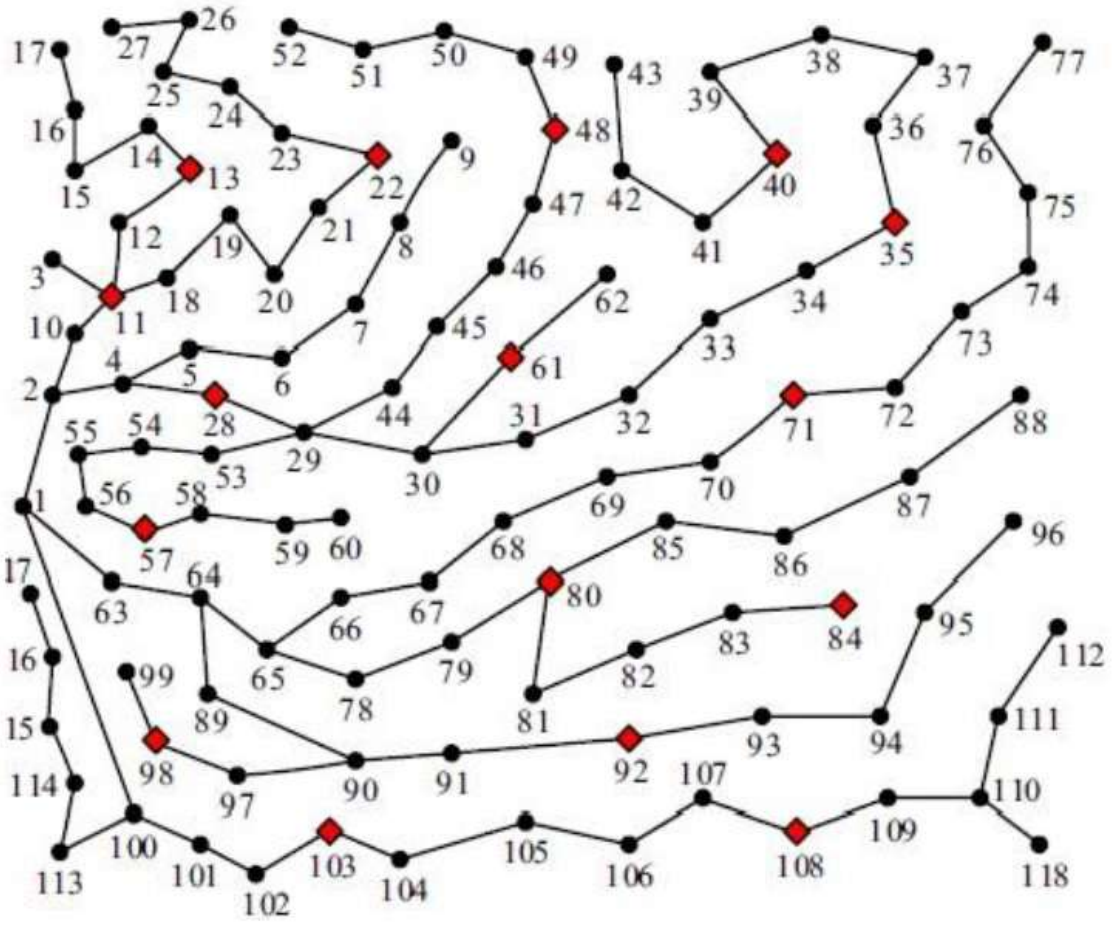

Figure 6.4: 118 bus distribution system in the proposed testing area.

Table 6.1: Study parameters.

Parameter	**Values**
NTEV	1632
n_y	5
NP_{FCE}	16
CSE	0.142 kWh/km
EP_h	USD 87.7/MWh
C_{land}	USD 240/M2 per year
C_{fixed}	USD 70,000
C_{cond}	USD 208.33/kW
P_{cg}	96 kW

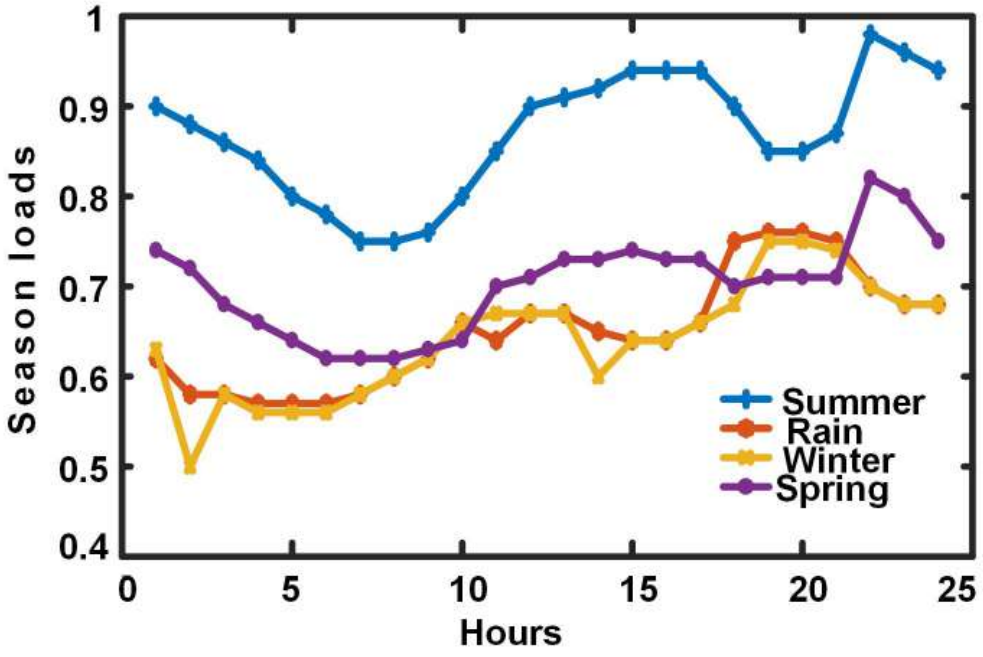

Figure 6.5: Load curve on an hourly basis for various seasons.

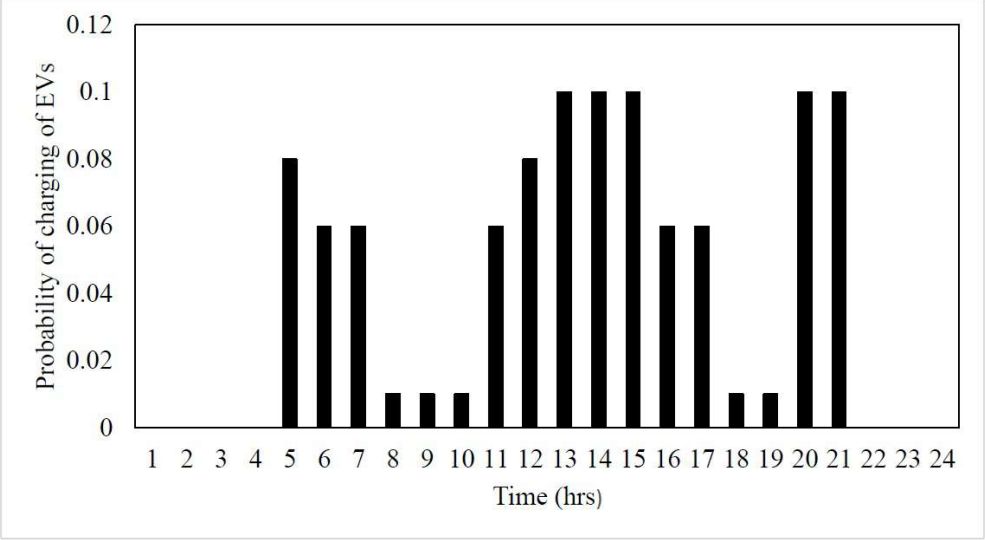

Figure 6.6: EVs' probability of being charged.

Due to its simple and independent structure from the problem, an optimisation method utilised in planning FCE, DGs and SCs can be applied to any test system. Additionally, the fuzzy satisfaction-based choice approach [110] allows decision makers to select the ultimate organising strategy under their preferences by selecting preferred values.

6.4.2 Scenario 1: Optimum Placement of FCE in DST Conjunction with Transportation Network

The optimal allocation of an FCE is achieved by minimising the EUC, CPDN ,and DVT of the DST. DGs are not considered; therefore, DGC in Equation (6.12) is zero. Since the total number of connectors in FCEs is almost constant, the DFC variation has an almost negligible effect on the objective function. Thus, the DFC is not considered to minimise the objective function in this scenario. In this scenario, three cases are taken:

(a) Case 1: Minimisation of EUC and CPDN.

(b) Case 2: Minimisation of DVT and CPDN.

(c) Case 3: Minimisation of DVT, CPDN, and EUC.

The optimal Pareto font for various cases in scenario 1 shows figures from Figure 6.7a–c. The best location and size of the FCE are obtained from the fuzzy satisfaction-based choice approach [110]. Table 6.2 displays the optimum FCE position and EV values, whereas Table 6.3 displays the optimal objective parameters.

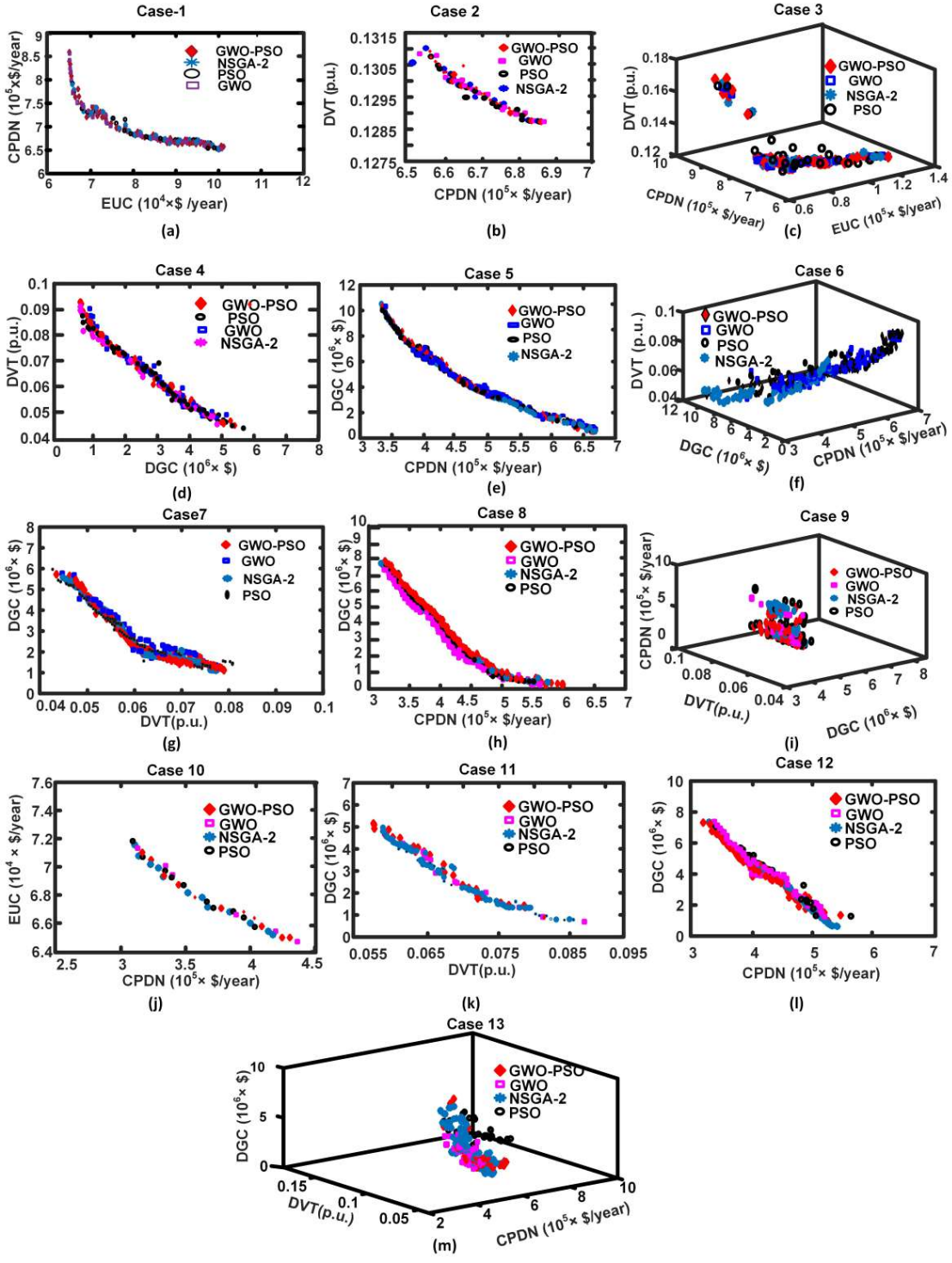

Figure 6.7: Optimal Pareto-front

6.4.3 Scenario 2: Optimal Positioning of DGs in DST with Previous Optimum FCE Load

DGs enhance the voltage profile and lower power losses in the DST. For the optimal DGs positioning, the optimal FCE load from case 3 is taken into account. This scenario takes into account three cases.

(a) Case 4: Minimisation of DGC and DVT.

(b) Case 5: Minimisation of CPDN and DGC.

(c) Case 6: Minimisation of DGC, DVT, and CPDN.

Figure 6.7d–f are displayed using the best pareto-front for various scenarios in scenario 2. The optimal location and size of DGs are obtained from the fuzzy satisfaction-based choice approach. For various cases in scenario 2, the optimum location and sizing of DGs are displayed in Table 6.4, and objective parameters are depicted in Table 6.5.

6.4.4 Scenario 3: Allocation of DGs and SCs in DST Optimally Using the Previous Optimal FCE Load

The optimal positioning of DGs and SCs is considered in the distributed system to enhance the voltage profile of the system. Three cases are used in this scenario for the optimal planning of DGs and SCs with the optimum load of the FCE from case 3.

(a) Case 7: Minimisation of DGC and DVT.

(b) Case 8: Minimisation of CPDN and DGC.

(c) Case 9: Minimisation of DGC, DVT, and CPDN.

The optimal pareto font for various cases in scenario 3 shows figures from Figure 6.7g–i. The optimal location and size of DGs and SCs are obtained from the fuzzy satisfaction-based choice approach. For various cases in scenario 3, the optimal sizing and location of DGs are shown in Table 6.6, Table 6.7 shows the optimal SCs position and sizing, and Table 6.8 shows the objective parameters.

6.4.5 Scenario 4: Simultaneous Optimum Location and Sizing of FCE, DGs, and SCs in DST

In this scenario, the optimum location and sizing of the FCE, DGs, and SC in a DST is achieved by coupling a transportation network to reduce the cost of CPDN, EUC, DGC and DVT. The following four cases are considered.

(a) Case 10: Minimisation of CPDN and EUC.

(b) Case 11: Minimisation of DGC and DVT.

(c) Case 12: Minimisation of CPDN and DGC.

(d) Case 13: Minimisation of DGC, DVT, and CPDN.

The optimal Pareto font for various cases is scenario 4, which shows figures from Figure 6.7j–m. The best location and size of FCE, DGs and SCs are obtained from the fuzzy satisfaction-based choice approach. For various cases in scenario 4, the optimal allocation of the FCE, number of EVs, DGs and SCs is shown in Tables 6.9–6.11. The objective is the parameters that are shown in Table 6.12.

6.5 Summary

This chapter proposes a multi-objective hybrid GWO-PSO algorithm for the simultaneous optimal planning of fast charging stations, distributed generators, and shunt capacitors in an integrated electric transportation system. Table 6.13 compares the outcomes of four scenarios. Hybrid GWO-PSO outperforms other algorithms in terms of performance. In case 13, the DVT decreased by 68.99%, 18.8% and 4.8% in comparison to case 3, case 6 and case 9. In case 13, the CPDN decreased by 53.21%, 22.41% and 7.68% in comparison to case 3, case 6 and case 9. The DGC is reduced to 5.1% and 1.7% in case 13 in comparison to cases 6 and 9. Similarly, the DFC and EUC were reduced to 22.56% and 19.8% in case 13 compared to all cases. Simultaneous optimal FCE, DGs and SCs in the coupled DST and road network give the best economical solution for the proposed method.

Table 6.2: The optimum FCE location and the optimum number of EVs

Cases	NSGA -2		PSO		GWO		GWO-PSO	
	FCE Location	Number of EVs	FCE Location	Number of EVs	FCE Location	Number of EVs	FCE Location	Number of EVs
Case-1	80	559	22	291	40	291	22	239
	103	83	35	413	11	170	11	170
	40	395	13	122	80	413	80	413
	13	112	80	397	13	137	13	122
	22	329	11	170	22	224	40	291
	11	154	40	239	35	397	35	397
Case-2	11	370	11	114	40	344	11	408
	22	253	28	170	61	173	28	114
	35	408	40	253	22	177	84	253
	28	114	22	285	11	150	35	370
	40	210	80	397	35	383	22	277
	84	277	35	413	80	405	28	114
Case-3	40	383	13	137	11	170	13	137
	61	177	11	170	28	114	11	170
	22	173	22	291	40	285	22	224
	11	150	80	397	22	253	80	413
	35	344	40	224	80	413	40	291
	80	405	35	413	35	397	35	397

Table 6.3: Objectives of scenario 1 that are optimal

Algorithms	Cases	DFC (M$)	EUC (M$/year)	CPDN (M$/year)	DVT (p.u.)
NSGA -2	1	4.2235	0.09233	0.6823	0.1325
	2	4.2225	0.09422	0.67730	0.1309
	3	4.2614	0.09078	0.68153	0.1308
PSO	1	4.2312	0.103231	0.69853	0.1345
	2	4.2309	0.105019	0.68730	0.1319
	3	4.3301	0.103618	0.69853	0.13173
GWO	1	4.2152	0.085878	0.68243	0.1308
	2	4.2140	0.086632	0.66840	0.1301
	3	4.224	0.084653	0.68129	0.1300
GWO-PSO	1	4.2053	0.084778	0. 67464	0.1301
	2	4.2052	0.08532	0.66730	0.1300
	3	4.15	0.083618	0.67129	0.1295

Table 6.4: Scenario 2: Optimal location and sizing of DGs

Cases	NSGA -2		PSO		GWO		GWO-PSO	
	DGs Location	DGs Size (MW)	DGs Location	DGs Size (MW)	DGs Location	DGsSize (MW)	DGs Location	DGs Size (MW)
Case-4	102	0.5020	75	0.5118	43	0.3764	49	0.2138
	75	0.7563	73	0.7723	77	0.9332	54	1.1365
	42	0.5002	48	0.9579	50	0.2400	72	0.1730
	62	0.5039	52	0.6249	53	0.7050	111	0.5406
	51	0.6407	108	0.5352	110	0.3217	76	0.9215
Case-5	73	1.3467	49	0.5641	47	0.7505	51	0.2895
	35	1.3012	113	0.8880	72	0.7327	84	0.9365
	80	1.1789	51	0.8688	75	0.5569	111	0.6758
	111	1.0722	83	0.6051	111	1.2189	74	1.0127
	51	0.6969	73	1.1742	50	0.8504	48	0.5020
Case-6	111	1.0385	110	1.2682	76	0.9847	54	1.5878
	74	1.4989	74	1.4116	111	0.8272	73	1.4037
	42	0.7511	82	0.5486	53	0.7631	83	1.0371
	54	0.9941	50	1.1380	70	0.7140	111	0.7847
	49	0.8780	53	0.7769	49	0.8662	96	1.1010

Table 6.5: Objectives of scenario 2 that are optimal

Algorithms	Cases	CPDN (M$/year)	DGC (M$)	DVT (p.u.)
NSGA -2	4	0.5278	3.5326	0.0677
	5	0.4398	6.8091	0.0565
	6	0.4081	6.2795	0.0462
PSO	4	0.476	4.1396	0.0592
	5	0.4404	4.9892	0.0566
	6	0.4042	7.1965	0.0457
GWO	4	0.5132	3.1348	0.0615
	5	0.4417	5.0003	0.0579
	6	0.4454	6.2583	0.0508
GWO-PSO	4	0.4931	3.6326	0.0564
	5	0.4750	4.1572	0.0684
	6	0.4051	5.0561	0.0503

Table 6.6: DGs' optimal location and sizing for scenario 3

Cases	NSGA -2		PSO		GWO		GWO-PSO	
	DGs Location	DGs Size (MW)	DGs Location	DGs Size (MW)	DGs Location	DGs Size (MW)	DGs Location	DGs Size (MW)
Case-7	75	0.4000	75	0.7629	17	0.1839	110	0.5540
	76	0.6827	71	0.1132	77	1.0291	47	0.3261
	26	0.1000	110	0.7330	103	0.1000	75	0.4110
	35	0.3800	72	1.3930	74	0.1000	77	0.4041
	54	0.2562	107	0.1000	46	0.1000	56	0.1276
Case-8	112	0.2264	72	0.8602	52	0.5007	75	0.5492
	51	0.3825	52	0.1674	86	0.4312	112	0.678
	110	0.4266	58	0.2686	52	0.2131	58	0.5035
	74	0.3401	25	0.1904	51	0.3846	62	0.5402
	15	0.1000	52	0.4417	71	0.3146	52	0.4235
Case-9	75	1.1995	118	0.6484	70	0.6849	73	0.2326
	47	1.6504	51	1.3910	110	0.8048	32	0.6461
	111	1.2904	70	1.6759	50	1.0038	77	1.6407
	8	0.3571	113	1.1950	75	0.8921	53	2.0730
	60	0.3935	76	0.5228	84	0.6258	108	1.0549

Table 6.7: Optimal location and sizing of SCs for scenario 3

Cases	NSGA -2		PSO		GWO		GWO-PSO	
	Location of SCs	Size of SCs (MVAr)	Location of SCs	Size of SCs (MVAr)	Location of SCs	Size of SCs (MVAr)	Location of SCs	Size of SCs (MVAr)
Case-7	48	0.6744	53	0.9704	38	0.1000	51	0.9504
	111	0.7627	61	0.1462	37	1.0000	35	0.3564
	21	0.7187	51	0.7401	48	0.3198	71	0.5740
Case-8	50	1.0000	51	0.5544	54	0.7152	111	0.9558
	70	1.0000	73	1.0000	11	0.8494	71	0.7703
	20	0.4638	109	0.9516	75	0.8960	35	0.7908
Case-9	50	0.6739	52	0.9023	51	0.9796	112	1.0000
	53	0.4210	57	0.8283	72	0.5760	75	0.8276
	77	0.4206	37	1.0000	95	0.8905	52	0.8558

Table 6.8: Scenario 3's Optimal objective parameters

Algorithms	Cases	CPDN (M$/year)	DGC (M$)	DVT (p.u.)
NSGA -2	7	0.49264	2.2132	0.0602
	8	0.5027	1.7956	0.0674
	9	0.37133	5.9512	0.0447
PSO	7	0.4853	3.7746	0.0503
	8	0.4555	2.3463	0.0600
	9	0.3974	6.8717	0.044275
GWO	7	0.55122	2.2180	0.0688
	8	0.4714	3.2785	0.0679
	9	0.3811	5.0512	0.05014
GWO-PSO	7	0.48759	1.8410	0.0560
	8	0.4295	2.2440	0.0621
	9	0.3402	4.8811	0.04287

Table 6.9: Optimal FCE location and EVs optimal numbers in scenario 4

Cases	NSGA -2		PSO		GWO		GWO-PSO	
	FCE Location	Numbers of EVs	FCE Location	Numbers of EVs	FCE Location	Numbers of EVs	FCE Location	Numbers of EVs
Case-10	28	159	103	192	103	192	57	268
	71	387	80	383	57	268	28	159
	80	364	71	368	80	310	80	310
	92	211	92	207	92	281	92	285
	98	220	98	220	71	319	71	319
	108	291	108	262	108	262	108	291
Case-11	22	199	57	187	40	301	22	222
	61	364	80	375	57	354	13	122
	103	123	84	419	22	183	40	216
	57	187	61	170	28	98	57	247
	80	395	40	308	61	309	84	439
	40	364	22	173	35	387	80	386
Case-12	22	366	103	242	40	467	40	486
	98	60	80	371	22	332	11	193
	28	114	35	553	11	104	48	195
	57	641	57	233	57	143	28	72
	103	25	48	49	80	488	80	444
	40	426	13	184	28	98	13	242
Case-13	13	147	103	192	13	242	80	445
	71	437	80	383	28	72	48	86
	92	229	71	368	11	193	98	105
	80	320	92	207	40	486	92	678
	40	280	98	220	80	539	57	131
	57	219	108	262	48	100	28	187

Table 6.10: Optimal positioning and sizing DGs for scenario 4

Cases	NSGA -2		PSO		GWO		GWO-PSO	
	DGs location	DGs Size (MW)	DGs location	DGs Size (MW)	DGs location	DGs Size (MW)	DGs location	DGs Size (MW)
Case-10	51	1.6040	77	0.6379	91	1.9655	108	1.3820
	111	2.2000	71	1.8732	73	1.8865	102	1.0985
	71	2.2000	22	1.2961	64	2.1657	80	2.2000
	98	2.2000	65	1.9889	113	1.8273	50	1.9288
	75	0.9668	9	1.1762	109	1.0029	74	1.2749
Case-11	101	0.1000	25	0.9424	70	0.2873	70	0.3393
	113	0.4778	7	0.1220	34	0.2730	35	0.1000
	33	1.0544	75	0.1566	30	0.4431	118	0.1000
	59	0.1294	15	1.0951	81	0.1339	11	0.3617
	42	0.1696	74	0.5410	49	0.5244	61	0.5362
Case-12	39	0.1018	23	0.1000	87	0.2801	61	0.3517
	21	0.1000	32	0.1832	45	0.6059	77	0.9536
	23	0.3469	22	0.3884	56	0.2757	18	0.1517
	40	0.1653	21	0.5953	18	0.2410	4	0.1000
	35	0.1000	112	0.8418	71	0.6929	47	0.1935
Case-13	27	0.1460	52	1.5916	76	0.6783	92	0.8716
	111	0.8800	113	1.2111	51	0.3924	97	1.2141
	71	1.4553	74	1.9814	48	0.1516	52	0.7196
	74	1.1841	84	1.2716	56	0.2267	76	0.9103
	53	0.8764	97	0.1425	52	0.3262	85	0.3911

Table 6.11: Optimal positioning and sizing of SCs for scenario 4

Cases	NSGA -2		PSO		GWO		GWO-PSO	
	SCs location	SCs Size (MVAr)	SCs location	SCs Size (MVAr)	SCs location	SCs Size (MVAr)	SCs location	SCs Size (MVAr)
Case-10	69	0.3683	5	0.6186	45	0.5395	16	0.8859
	35	0.7996	111	0.8791	81	0.7605	49	0.6926
	75	0.8182	68	0.4768	74	0.7618	28	0.6991
Case-11	7	0.3598	65	0.5128	61	0.5898	9	0.2953
	75	0.6733	100	0.4838	71	0.7295	41	0.4587
	77	1.0000	56	0.5476	66	0.1924	72	0.9477
Case-12	111	0.9884	73	0.2574	52	0.4971	47	0.4543
	4	0.8163	67	0.9924	111	1.0000	74	0.4977
	70	0.9816	6	0.9711	50	0.4938	58	0.2046
Case-13	75	0.6120	75	0.2094	34	0.2979	112	0.3724
	7	0.6329	23	0.9019	35	0.5958	74	0.6310
	78	0.5705	70	0.5205	31	0.2898	106	0.5835

Table 6.12: Scenario 4's optimal objective parameters

Algorithms	Cases	DFC (M$)	EUC (M$/year)	CPDN (M$/year)	DGC (M$)	DVT (p.u.)
NSGA -2	10	3.5	0.06689	0.26418	11.159	0.0402
	11	3.45	0.08294	0.59928	2.3499	0.0625
	12	3.432	0.11420	0.55862	9.9048	0.0790
	13	3.432	0.072511	0.39972	5.5265	0.0492
PSO	10	3.9352	0.067315	0.51552	8.4839	0.0792
	11	3.9352	0.069653	0.63463	3.4765	0.0713
	12	3.89	0.098993	0.59747	2.5659	0.0873
	13	3.89	0.089961	0.51552	8.4839	0.0792
GWO	10	3.3	0.065888	0.34226	10.766	0.0669
	11	3.3	0.089744	0.59830	2.0220	0.0732
	12	3.425	0.088993	0.47761	2.5499	0.0767
	13	3.425	0.076576	0.52962	4.8601	0.0707
GWO-PSO	10	3.4715	0.065773	0.40880	9.5935	0.0810
	11	3.48	0.070837	0.51632	1.7488	0.0720
	12	3.2135	0.079180	0.42562	2.1300	0.0693
	13	3.2135	0.067005	0.31404	4.7970	0.0408

Table 6.13: Four scenarios' comparison results

Scenarios	Cases	Algorithm	DFC (M$)	EUC (M$/year)	CPDN (M$/year)	DGC (M$)	DVT (p.u.)
4	13	NSGA-2	3.432	0.072511	0.39972	5.5265	0.0492
		PSO	3.89	0.089961	0.51552	8.4839	0.0792
		GWO	3.425	0.076576	0.52962	4.8601	0.0707
		GWO-PSO	**3.2135**	**0.067005**	**0.31404**	**4.7970**	**0.0408**
3	9	NSGA-2	4.42101	0.090780	0.37133	5.9512	0.0447
		PSO	4.3830	0.1036180	0.3974	6.8717	0.044275
		GWO	4.3520	0.0846530	0.381101	5.0512	0.05014
		GWO-PSO	**4.15**	**0.083618**	**0.3402**	**4.8811**	**0.04287**
2	6	NSGA-2	4.421	0.09078	0.4081	6.2795	0.0462
		PSO	4.383	0.103618	0.4042	7.1965	0.0457
		GWO	4.352	0.084653	0.4454	6.2583	0.0508
		GWO-PSO	**4.15**	**0.083618**	**0.4051**	**5.0561**	**0.0503**

Chapter 7
Conclusion

7.1 Summary and Important Finding

EVs are a potential future option for the road transportation system for the following generation. Issues from abrupt climate change, rising crude oil prices, and the depletion of fossil fuels constantly encourage consumers to pursue alternative energy sources for transportation systems. Due to the significant initial price of EV batteries, EVs remain high compared to conventional vehicles. Since it emits little carbon dioxide compared to an ICE vehicle, an EV is environmentally fair and fuel efficient. Even though batteries have undergone significant advancements in recent years, today's Li-ion battery has a lower energy density and a shorter lifespan.

The requirement for charging infrastructural expansion has grown as the EVs industry share increases. Different planning concerns for EV charging infrastructure are included in the current research. This research aims to develop viable EV charging infrastructure and to use effective and cutting-edge methods for the location of charging stations. Charging stations are a network component that provides electricity for recharging EV batteries. Proper site selection and charging station size are crucial to lessen the adverse effects on EVs.

A thorough analysis of the scientific literature on planning for charging infrastructure is provided . The primary research shortcomings in this field of study are noted. The primary goals of the investigation endeavor are chosen after determining the significant research gaps.

Therefore, two strategies for the appropriate placement of EVCSs have been evaluated in this work. In the first strategy, only the distribution network is considered. Utility companies must provide the electricity needed to operate all connected electrical loads in homes, residential, business, and industrial regions. The utility operator strategy is used to position CS in the optimum possible way, taking the distribution system solely into account. The utility operator's placing of EVCS considers factors, including reducing bus voltage and the distribution system's overall power loss.

In the second strategy, both distribution and superimposed transportation networks are

considered. This approach considers charging station owners, EV users, and utility operators' views to obtain distribution performance and economic benefits.

For 69-bus radial distribution systems utilising the RAO-3 algorithm, a fuzzy classified technique for optimum sizings and two-stage deployments of EVCSs, DGs and DSTATCOMs. Due to which it enhances the distribution system's performance.

A fuzzy classified method for simultaneous optimal sizing and placement of EVCS, DG and DSTATCOM for 69 bus radial distribution systems using the RAO-3 algorithm is proposed. Li-ion characteristic curves are employed to build P and Q load models for charging EV batteries. As a result of increasing EV load under different loading conditions, simulation findings indicate that the substation can handle EV load until the maximum level of its active power supply. Despite an increase in EV demand, the bus voltages can be maintained at a tolerable level with the aid of DGs and DSTATCOM. The transient battery charging load affects the node voltages at the EVCS, and at steady-state charging, the bus node voltages are maintained at adequate levels with the aid of DGs and DSTATCOMs.

The Rao-3 algorithm is used to accomplish the optimal location and size of EVCS, DGs, and SCs without and with network reconfiguration. It demonstrated that the suggested technique outscored the without network reconfiguration and two-stage placing of various components in aspects of

1. Active power loss was decreased.
2. Substation power factor was improved.
3. The bus voltages of the distribution system were enhanced.
4. Additionally, the best number of EVs was facilitated in the EVCS.

An interconnected electric transportation system uses the multi-objective hybrid GWO-PSO algorithms to predict the best locations for rapid charging stations, DGs and SCs. Different case studies were carried out using the suggested strategy for simultaneous deployment of FCE, DGs and SCs, as well as single stage-wise placement.

7.2 Future Scope

The following future study trends are recommended based on the discussions mentioned earlier:

1. The substation power factor can be further enhanced by using minimum quantity of DSTATCOM or SCs.

2. The voltage profile of the distribution system can be further improved with less number of DGs and SCs or DSTATCOM.

3. Modernizing the power infrastructure and advancing EV usage in V2G technologies have been made possible recently by the growth of the smart grid. However, the cost of smart metering, integrated solutions, and intelligent communications networks among an EV and a smart grid would surely increase for intelligent discharging and charging networks.

4. Future study, bigger test system with real case scenarios has to be incorporated.

5. Advanced optimisation techniques can be utilised, to achieve the required objective such as to further reducing power loss and enhancing voltage profile.

6. An excellent new research topic for the foreseeable future is the practical analysis of hybrid charging stations.

Bibliography

[1] W. Wang and Y. Cheng, "Optimal charging scheduling for electric vehicles considering the impact of renewable energy sources," in *2020 5th Asia Conference on Power and Electrical Engineering (ACPEE)*, pp. 1150–1154, IEEE, 2020.

[2] G. Napoli, A. Polimeni, S. Micari, L. Andaloro, and V. Antonucci, "Optimal allocation of electric vehicle charging stations in a highway network: Part 1. methodology and test application," *Journal of Energy Storage*, vol. 27, p. 101102, 2020.

[3] W. Jing, Y. Yan, I. Kim, and M. Sarvi, "Electric vehicles: A review of network modelling and future research needs," *Advances in Mechanical Engineering*, vol. 8, no. 1, p. 1687814015627981, 2016.

[4] N. Adnan, S. M. Nordin, M. A. bin Bahruddin, and M. Ali, "How trust can drive forward the user acceptance to the technology? in-vehicle technology for autonomous vehicle," *Transportation research part A: policy and practice*, vol. 118, pp. 819–836, 2018.

[5] A. Singh, "Electric vehicle market size, share, analysis, growth by 2027," *Allied Market, Research, April*, 2020.

[6] "These countries have the most electric cars; check list." `https://www.livemint.com/auto-news/`. Accessed: 12-08-2021 [Online].

[7] L. Cozzi, T. Gould, S. Bouckart, D. Crow, T. Kim, C. Mcglade, P. Olejarnik, B. Wanner, and D. Wetzel, "World energy outlook 2020," *vol*, vol. 2050, pp. 1–461, 2020.

[8] C. Cities, "Plug-in electric vehicle handbook for consumers," *US Department of Energy, United States*, 2011.

[9] K. Ramalingam and C. Indulkar, "Overview of plug-in electric vehicle technologies," in *Plug In Electric Vehicles in Smart Grids*, pp. 1–32, Springer, 2015.

[10] S. Mehta, "Electric plug-in vehicle/electric vehicle, status report," *Electr. Eng*, pp. 1–15, 2010.

[11] T.-D. Nguyen, S. Li, W. Li, and C. C. Mi, "Feasibility study on bipolar pads for efficient wireless power chargers," in *2014 IEEE Applied Power Electronics Conference and Exposition-APEC 2014*, pp. 1676–1682, IEEE, 2014.

[12] Y. Zheng, Z. Y. Dong, Y. Xu, K. Meng, J. H. Zhao, and J. Qiu, "Electric vehicle battery charging/swap stations in distribution systems: comparison study and optimal planning," *IEEE transactions on Power Systems*, vol. 29, no. 1, pp. 221–229, 2013.

[13] R. P. Brooker and N. Qin, "Identification of potential locations of electric vehicle supply equipment," *Journal of Power Sources*, vol. 299, pp. 76–84, 2015.

[14] K. Morrow, D. Karner, and J. E. Francfort, "Plug-in hybrid electric vehicle charging infrastructure review," 2008.

[15] P. Morrissey, P. Weldon, and M. O'Mahony, "Future standard and fast charging infrastructure planning: An analysis of electric vehicle charging behaviour," *Energy Policy*, vol. 89, pp. 257–270, 2016.

[16] C. Cities, "Plug-in electric vehicle handbook for public charging station hosts," *US Department of Energy Publication No. DOE/GO-102012-3275*, 2012.

[17] D. Mayfield and C. F. Ohio, "Siting electric vehicle charging stations," *Editor Carlotta Collette*, 2012.

[18] F. Mwasilu, J. J. Justo, E.-K. Kim, T. D. Do, and J.-W. Jung, "Electric vehicles and smart grid interaction: A review on vehicle to grid and renewable energy sources integration," *Renewable and sustainable energy reviews*, vol. 34, pp. 501–516, 2014.

[19] T. Bräunl, "Synthetic engine noise generation for improving electric vehicle safety," *International journal of vehicle safety*, vol. 6, no. 1, pp. 1–8, 2012.

[20] L. Raslavičius, B. Azzopardi, A. Keršys, M. Starevičius, Ž. Bazaras, and R. Makaras, "Electric vehicles challenges and opportunities: Lithuanian review," *Renewable and Sustainable Energy Reviews*, vol. 42, pp. 786–800, 2015.

[21] Y. P. Leong, S. I. Mustapa, and A. H. Hashim, "Climate change challenges on co 2 emission reduction for developing countries: A case for malaysia's agenda for action.," *International Journal of Climate Change: Impacts & Responses*, vol. 2, no. 4, 2011.

[22] J. C. Gómez and M. M. Morcos, "Impact of ev battery chargers on the power quality of distribution systems," *IEEE transactions on power delivery*, vol. 18, no. 3, pp. 975–981, 2003.

[23] P. Mitra and G. Venayagamoorthy, "Wide area control for improving stability of a power system with plug-in electric vehicles," *IET generation, transmission & distribution*, vol. 4, no. 10, pp. 1151–1163, 2010.

[24] Z. Wang and R. Paranjape, "An evaluation of electric vehicle penetration under demand response in a multi-agent based simulation," in *2014 IEEE electrical power and energy conference*, pp. 220–225, IEEE, 2014.

[25] R. Sioshansi, R. Fagiani, and V. Marano, "Cost and emissions impacts of plug-in hybrid vehicles on the ohio power system," *Energy Policy*, vol. 38, no. 11, pp. 6703–6712, 2010.

[26] J. A. Orr, A. E. Emanuel, and D. J. Pileggi, "Current harmonics, voltage distortion, and powers associated with electric vehicle battery chargers distributed on the residential power system," *IEEE Transactions on Industry Applications*, no. 4, pp. 727–734, 1984.

[27] P. Phonrattanasak and N. Leeprechanon, "Optimal placement of ev fast charging stations considering the impact on electrical distribution and traffic condition," in *2014 International Conference and Utility Exhibition on Green Energy for Sustainable Development (ICUE)*, pp. 1–6, IEEE, 2014.

[28] K. Qian, C. Zhou, and Y. Yuan, "Impacts of high penetration level of fully electric vehicles charging loads on the thermal ageing of power transformers," *International Journal of Electrical Power & Energy Systems*, vol. 65, pp. 102–112, 2015.

[29] W. Su, H. Eichi, W. Zeng, and M.-Y. Chow, "A survey on the electrification of transportation in a smart grid environment," *IEEE Transactions on Industrial Informatics*, vol. 8, no. 1, pp. 1–10, 2011.

[30] L. Drude, L. C. P. Junior, and R. Rüther, "Photovoltaics (pv) and electric vehicle-to-grid (v2g) strategies for peak demand reduction in urban regions in brazil in a smart grid environment," *Renewable Energy*, vol. 68, pp. 443–451, 2014.

[31] E. A. Nanaki and C. J. Koroneos, "Comparative economic and environmental analysis of conventional, hybrid and electric vehicles–the case study of greece," *Journal of cleaner production*, vol. 53, pp. 261–266, 2013.

[32] H. Ma, F. Balthasar, N. Tait, X. Riera-Palou, and A. Harrison, "A new comparison between the life cycle greenhouse gas emissions of battery electric vehicles and internal combustion vehicles," *Energy policy*, vol. 44, pp. 160–173, 2012.

[33] P. Taylor, "When an electric car dies, what will happen to the battery?," *Scientific American*, vol. 14, 2009.

[34] D. B. Richardson, "Electric vehicles and the electric grid: A review of modeling approaches, impacts, and renewable energy integration," *Renewable and Sustainable Energy Reviews*, vol. 19, pp. 247–254, 2013.

[35] K. Jorgensen, "Technologies for electric, hybrid and hydrogen vehicles: Electricity from renewable energy sources in transport," *Utilities Policy*, vol. 16, no. 2, pp. 72–79, 2008.

[36] A. Weis, P. Jaramillo, and J. Michalek, "Estimating the potential of controlled plug-in hybrid electric vehicle charging to reduce operational and capacity expansion costs for electric power systems with high wind penetration," *Applied Energy*, vol. 115, pp. 190–204, 2014.

[37] M. Z. Zeb, K. Imran, A. Khattak, A. K. Janjua, A. Pal, M. Nadeem, J. Zhang, and S. Khan, "Optimal placement of electric vehicle charging stations in the active distribution network," *IEEE Access*, vol. 8, pp. 68124–68134, 2020.

[38] D. Steen *et al.*, "Impacts of fast charging of electric buses on electrical distribution systems," *CIRED-Open Access Proceedings Journal*, vol. 2017, no. 1, pp. 2350–2353, 2017.

[39] A. Y. Lam, Y.-W. Leung, and X. Chu, "Electric vehicle charging station placement: Formulation, complexity, and solutions," *IEEE Transactions on Smart Grid*, vol. 5, no. 6, pp. 2846–2856, 2014.

[40] G. Saldaña, J. I. San Martin, I. Zamora, F. J. Asensio, and O. Oñederra, "Electric vehicle into the grid: Charging methodologies aimed at providing ancillary services considering battery degradation," *Energies*, vol. 12, no. 12, p. 2443, 2019.

[41] J. C. Mukherjee and A. Gupta, "A review of charge scheduling of electric vehicles in smart grid," *IEEE Systems Journal*, vol. 9, no. 4, pp. 1541–1553, 2014.

[42] L. Chen, C. Xu, H. Song, and K. Jermsittiparsert, "Optimal sizing and sitting of evcs in the distribution system using metaheuristics: A case study," *Energy Reports*, vol. 7, pp. 208–217, 2021.

[43] M. H. Moradi, M. Abedini, S. R. Tousi, and S. M. Hosseinian, "Optimal siting and sizing of renewable energy sources and charging stations simultaneously based on differential evolution algorithm," *International Journal of Electrical Power & Energy Systems*, vol. 73, pp. 1015–1024, 2015.

[44] J. C. Gómez and M. M. Morcos, "Impact of ev battery chargers on the power quality of distribution systems," *IEEE transactions on power delivery*, vol. 18, no. 3, pp. 975–981, 2003.

[45] S. W. Hadley, "Evaluating the impact of plug-in hybrid electric vehicles on regional electricity supplies," in *2007 iREP Symposium-Bulk Power System Dynamics and Control-VII. Revitalizing Operational Reliability*, pp. 1–12, IEEE, 2007.

[46] I. Sharma, C. Canizares, and K. Bhattacharya, "Smart charging of pevs penetrating into residential distribution systems," *IEEE Transactions on Smart Grid*, vol. 5, no. 3, pp. 1196–1209, 2014.

[47] P. Papadopoulos, S. Skarvelis-Kazakos, I. Grau, L. M. Cipcigan, and N. Jenkins, "Electric vehicles' impact on british distribution networks," *IET Electrical Systems in Transportation*, vol. 2, no. 3, pp. 91–102, 2012.

[48] A. Dubey and S. Santoso, "Electric vehicle charging on residential distribution systems: Impacts and mitigations," *IEEE Access*, vol. 3, pp. 1871–1893, 2015.

[49] P. Richardson, D. Flynn, and A. Keane, "Optimal charging of electric vehicles in low-voltage distribution systems," *IEEE Transactions on Power Systems*, vol. 27, no. 1, pp. 268–279, 2011.

[50] J. T. Salihi, "Energy requirements for electric cars and their impact on electric power generation and distribution systems," *IEEE Transactions on industry applications*, no. 5, pp. 516–532, 1973.

[51] L. Zhang, T. Brown, and G. S. Samuelsen, "Fuel reduction and electricity consumption impact of different charging scenarios for plug-in hybrid electric vehicles," *Journal of Power Sources*, vol. 196, no. 15, pp. 6559–6566, 2011.

[52] C. Chen and S. Duan, "Optimal integration of plug-in hybrid electric vehicles in microgrids," *IEEE Transactions on Industrial Informatics*, vol. 10, no. 3, pp. 1917–1926, 2014.

[53] L. Longo, "Optimal design of an ev fast charging station coupled with storage in stockholm," 2017.

[54] A. Kumar, N. K. Meena, A. R. Singh, Y. Deng, X. He, R. Bansal, and P. Kumar, "Strategic integration of battery energy storage systems with the provision of distributed ancillary services in active distribution systems," *Applied Energy*, vol. 253, p. 113503, 2019.

[55] F. Ahmad, M. S. Alam, S. M. Shariff, and M. Krishnamurthy, "A cost-efficient approach to ev charging station integrated community microgrid: A case study of indian power market," *IEEE Transactions on Transportation Electrification*, vol. 5, no. 1, pp. 200–214, 2019.

[56] F. Ahmad, M. S. Alam, S. M. Shariff, and M. Krishnamurthy, "A cost-efficient approach to ev charging station integrated community microgrid: A case study of indian power market," *IEEE Transactions on Transportation Electrification*, vol. 5, no. 1, pp. 200–214, 2019.

[57] R. Sirjani and A. R. Jordehi, "Optimal placement and sizing of distribution static compensator (d-statcom) in electric distribution networks: A review," *Renewable and Sustainable Energy Reviews*, vol. 77, pp. 688–694, 2017.

[58] S. Jazebi, S. H. Hosseinian, and B. Vahidi, "Dstatcom allocation in distribution networks considering reconfiguration using differential evolution algorithm," *Energy conversion and Management*, vol. 52, no. 7, pp. 2777–2783, 2011.

[59] S. A. Taher and S. A. Afsari, "Optimal location and sizing of dstatcom in distribution systems by immune algorithm," *International Journal of Electrical Power & Energy Systems*, vol. 60, pp. 34–44, 2014.

[60] S. Devi and M. Geethanjali, "Optimal location and sizing determination of distributed generation and dstatcom using particle swarm optimization algorithm," *International Journal of Electrical Power & Energy Systems*, vol. 62, pp. 562–570, 2014.

[61] S. R. Salkuti, "Optimal allocation of dg and d-statcom in a distribution system using evolutionary based bat algorithm," *International Journal of Advanced Computer Science and Applications*, vol. 12, no. 4, 2021.

[62] T. Yuvaraj, K. Ravi, and K. Devabalaji, "Dstatcom allocation in distribution networks considering load variations using bat algorithm," *Ain Shams Engineering Journal*, vol. 8, no. 3, pp. 391–403, 2017.

[63] A. Pratap, P. Tiwari, R. Maurya, and B. Singh, "Minimisation of electric vehicle charging stations impact on radial distribution networks by optimal allocation of dstatcom and dg using african vulture optimisation algorithm," *International Journal of Ambient Energy*, pp. 1–20, 2022.

[64] M. Mohammadi, "Particle swarm optimization algorithm for simultaneous optimal placement and sizing of shunt active power conditioner (apc) and shunt capacitor in harmonic distorted distribution system," *Journal of Central South University*, vol. 24, no. 9, pp. 2035–2048, 2017.

[65] S. M. Sajjadi, M.-R. Haghifam, and J. Salehi, "Simultaneous placement of distributed generation and capacitors in distribution networks considering voltage stability index," *International Journal of Electrical Power & Energy Systems*, vol. 46, pp. 366–375, 2013.

[66] M. H. Moradi, A. Zeinalzadeh, Y. Mohammadi, and M. Abedini, "An efficient hybrid method for solving the optimal sitting and sizing problem of dg and shunt capacitor banks simultaneously based on imperialist competitive algorithm and genetic algorithm," *International Journal of Electrical Power & Energy Systems*, vol. 54, pp. 101–111, 2014.

[67] N. Jain, S. Singh, and S. Srivastava, "Pso based placement of multiple wind dgs and capacitors utilizing probabilistic load flow model," *Swarm and Evolutionary Computation*, vol. 19, pp. 15–24, 2014.

[68] S. G. Naik, D. Khatod, and M. Sharma, "Optimal allocation of combined dg and capacitor for real power loss minimization in distribution networks," *International Journal of Electrical Power & Energy Systems*, vol. 53, pp. 967–973, 2013.

[69] S. R. Gampa, K. Jasthi, P. Goli, D. Das, and R. Bansal, "Grasshopper optimization algorithm based two stage fuzzy multiobjective approach for optimum sizing

and placement of distributed generations, shunt capacitors and electric vehicle charging stations," *Journal of Energy Storage*, vol. 27, p. 101117, 2020.

[70] S. Civanlar, J. Grainger, H. Yin, and S. Lee, "Distribution feeder reconfiguration for loss reduction," *IEEE Transactions on Power Delivery*, vol. 3, no. 3, pp. 1217–1223, 1988.

[71] S. Huang, Q. Wu, L. Cheng, and Z. Liu, "Optimal reconfiguration-based dynamic tariff for congestion management and line loss reduction in distribution networks," *IEEE Transactions on Smart Grid*, vol. 7, no. 3, pp. 1295–1303, 2015.

[72] H. Cui, F. Li, X. Fang, and R. Long, "Distribution network reconfiguration with aggregated electric vehicle charging strategy," in *2015 IEEE Power & Energy Society General Meeting*, pp. 1–5, IEEE, 2015.

[73] M.-A. Rostami, A. Kavousi-Fard, and T. Niknam, "Expected cost minimization of smart grids with plug-in hybrid electric vehicles using optimal distribution feeder reconfiguration," *IEEE Transactions on Industrial Informatics*, vol. 11, no. 2, pp. 388–397, 2015.

[74] A. Kavousi-Fard, S. Abbasi, A. Abbasi, and S. Tabatabaie, "Optimal probabilistic reconfiguration of smart distribution grids considering penetration of plug-in hybrid electric vehicles," *Journal of Intelligent & Fuzzy Systems*, vol. 29, no. 5, pp. 1847–1855, 2015.

[75] M. Rahmani-Andebili and M. Fotuhi-Firuzabad, "An adaptive approach for pevs charging management and reconfiguration of electrical distribution system penetrated by renewables," *IEEE Transactions on Industrial Informatics*, vol. 14, no. 5, pp. 2001–2010, 2017.

[76] G. Battapothula, C. Yammani, and S. Maheswarapu, "Multi-objective optimal planning of fcss and dgs in distribution system with future ev load enhancement," *IET Electrical Systems in Transportation*, vol. 9, no. 3, pp. 128–139, 2019.

[77] A. Awasthi, K. Venkitusamy, S. Padmanaban, R. Selvamuthukumaran, F. Blaabjerg, and A. K. Singh, "Optimal planning of electric vehicle charging station at the distribution system using hybrid optimization algorithm," *Energy*, vol. 133, pp. 70–78, 2017.

[78] H. Zhang, Z. Hu, Z. Xu, and Y. Song, "An integrated planning framework for different types of pev charging facilities in urban area," *IEEE Transactions on Smart Grid*, vol. 7, no. 5, pp. 2273–2284, 2015.

[79] S. Deb, K. Tammi, X.-Z. Gao, K. Kalita, and P. Mahanta, "A hybrid multi-objective chicken swarm optimization and teaching learning based algorithm for charging station placement problem," *IEEE Access*, vol. 8, pp. 92573–92590, 2020.

[80] B. Faridpak, H. F. Gharibeh, M. Farrokhifar, and D. Pozo, "Two-step lp approach for optimal placement and operation of ev charging stations," in *2019 IEEE PES Innovative Smart Grid Technologies Europe (ISGT-Europe)*, pp. 1–5, IEEE, 2019.

[81] M. Moradijoz, F. Moazzen, S. Allahmoradi, M. P. Moghaddam, and M. Haghifam, "A two stage model for optimum allocation of electric vehicle parking lots in smart grids," in *2018 Smart Grid Conference (SGC)*, pp. 1–5, IEEE, 2018.

[82] Z. Tian, W. Hou, X. Gu, F. Gu, and B. Yao, "The location optimization of electric vehicle charging stations considering charging behavior," *Simulation*, vol. 94, no. 7, pp. 625–636, 2018.

[83] H. Simorgh, H. Doagou-Mojarrad, H. Razmi, and G. B. Gharehpetian, "Cost-based optimal siting and sizing of electric vehicle charging stations considering demand response programmes," *IET Generation, Transmission & Distribution*, vol. 12, no. 8, pp. 1712–1720, 2018.

[84] W. Kong, Y. Luo, G. Feng, K. Li, and H. Peng, "Optimal location planning method of fast charging station for electric vehicles considering operators, drivers, vehicles, traffic flow and power grid," *Energy*, vol. 186, p. 115826, 2019.

[85] T. Yi, X.-b. Cheng, H. Zheng, and J.-p. Liu, "Research on location and capacity optimization method for electric vehicle charging stations considering user's comprehensive satisfaction," *Energies*, vol. 12, no. 10, p. 1915, 2019.

[86] A. Abdalrahman and W. Zhuang, "Pev charging infrastructure siting based on spatial–temporal traffic flow distribution," *IEEE Transactions on Smart Grid*, vol. 10, no. 6, pp. 6115–6125, 2019.

[87] Y. Xu, S. Çolak, E. C. Kara, S. J. Moura, and M. C. González, "Planning for electric vehicle needs by coupling charging profiles with urban mobility," *Nature Energy*, vol. 3, no. 6, pp. 484–493, 2018.

[88] S. Bandaru and K. Deb, "Metaheuristic techniques," in *Decision sciences*, pp. 709–766, CRC Press, 2016.

[89] M. Abdel-Basset, L. Abdel-Fatah, and A. K. Sangaiah, "Metaheuristic algorithms: A comprehensive review," *Computational intelligence for multimedia big data on the cloud with engineering applications*, pp. 185–231, 2018.

[90] A. Bötke, E. Erensoy, and C. Sevginer, "Modeling and validation processes of an electric vehicle with statistical energy analysis," in *Euronoise*, pp. 1417–1422, 2015.

[91] M. Nikowitz, "Advanced hybrid and electric vehicles," *System Optimization and Vehicle Integration, Springer*, 2016.

[92] T. J. Böhme and B. Frank, "Hybrid systems, optimal control and hybrid vehicles," *Cham, CH: Springer International*, pp. 401–428, 2017.

[93] G. A. Cowan, "Annual report to the us department of energy on doe grant defg05-88er25054," 1988.

[94] D. H. Wolpert and W. G. Macready, "No free lunch theorems for optimization," *IEEE transactions on evolutionary computation*, vol. 1, no. 1, pp. 67–82, 1997.

[95] M. Abdel-Basset, L. Abdel-Fatah, and A. K. Sangaiah, "Metaheuristic algorithms: A comprehensive review," *Computational intelligence for multimedia big data on the cloud with engineering applications*, pp. 185–231, 2018.

[96] A. Darwish, "Bio-inspired computing: Algorithms review, deep analysis, and the scope of applications," *Future Computing and Informatics Journal*, vol. 3, no. 2, pp. 231–246, 2018.

[97] J. Del Ser, E. Osaba, D. Molina, X.-S. Yang, S. Salcedo-Sanz, D. Camacho, S. Das, P. N. Suganthan, C. A. C. Coello, and F. Herrera, "Bio-inspired computation: Where we stand and what's next," *Swarm and Evolutionary Computation*, vol. 48, pp. 220–250, 2019.

[98] I. Boussaïd, J. Lepagnot, and P. Siarry, "A survey on optimization metaheuristics," *Information sciences*, vol. 237, pp. 82–117, 2013.

[99] E. K. Burke, M. Gendreau, M. Hyde, G. Kendall, G. Ochoa, E. Özcan, and R. Qu, "Hyper-heuristics: A survey of the state of the art," *Journal of the Operational Research Society*, vol. 64, no. 12, pp. 1695–1724, 2013.

[100] C. P. Igiri, Y. Singh, and R. C. Poonia, "A review study of modified swarm intelligence: particle swarm optimization, firefly, bat and gray wolf optimizer algorithms," *Recent Advances in Computer Science and Communications (Formerly: Recent Patents on Computer Science)*, vol. 13, no. 1, pp. 5–12, 2020.

[101] S. Yang, Z. Yang, Y. Fu, and H. Liu, "Reducing the number of function evaluations in derivative-free algorithm for bound constrained optimization," *Evolutionary Intelligence*, pp. 1–10, 2019.

[102] A. P. Engelbrecht, "Fitness function evaluations: A fair stopping condition?," in *2014 IEEE symposium on swarm intelligence*, pp. 1–8, IEEE, 2014.

[103] K. Deb, A. Pratap, S. Agarwal, and T. Meyarivan, "A fast and elitist multiobjective genetic algorithm: Nsga-ii," *IEEE transactions on evolutionary computation*, vol. 6, no. 2, pp. 182–197, 2002.

[104] J. Kennedy and R. Eberhart, "Particle swarm optimization," in *Proceedings of ICNN'95-international conference on neural networks*, vol. 4, pp. 1942–1948, IEEE, 1995.

[105] J. Zhao, F. Wen, Z. Y. Dong, Y. Xue, and K. P. Wong, "Optimal dispatch of electric vehicles and wind power using enhanced particle swarm optimization," *IEEE Transactions on industrial informatics*, vol. 8, no. 4, pp. 889–899, 2012.

[106] M. Dorigo and C. Blum, "Ant colony optimization theory: A survey," *Theoretical computer science*, vol. 344, no. 2-3, pp. 243–278, 2005.

[107] D. Karaboga and B. Basturk, "A powerful and efficient algorithm for numerical function optimization: artificial bee colony (abc) algorithm," *Journal of global optimization*, vol. 39, no. 3, pp. 459–471, 2007.

[108] R. V. Rao, V. J. Savsani, and D. Vakharia, "Teaching–learning-based optimization: a novel method for constrained mechanical design optimization problems," *Computer-aided design*, vol. 43, no. 3, pp. 303–315, 2011.

[109] S. Mirjalili, S. M. Mirjalili, and A. Lewis, "Grey wolf optimizer," *Advances in engineering software*, vol. 69, pp. 46–61, 2014.

[110] A. Shukla, K. Verma, and R. Kumar, "Multi-objective synergistic planning of ev fast-charging stations in the distribution system coupled with the transportation network," *IET Generation, Transmission & Distribution*, vol. 13, no. 15, pp. 3421–3432, 2019.

[111] R. Rao, "Jaya: A simple and new optimization algorithm for solving constrained and unconstrained optimization problems," *International Journal of Industrial Engineering Computations*, vol. 7, no. 1, pp. 19–34, 2016.

[112] R. Rao, "Rao algorithms: Three metaphor-less simple algorithms for solving optimization problems," *International Journal of Industrial Engineering Computations*, vol. 11, no. 1, pp. 107–130, 2020.

[113] L. A. Zadeh, G. J. Klir, and B. Yuan, *Fuzzy sets, fuzzy logic, and fuzzy systems: selected papers*, vol. 6. World Scientific, 1996.

[114] J. Savier and D. Das, "Impact of network reconfiguration on loss allocation of radial distribution systems," *IEEE Transactions on Power Delivery*, vol. 22, no. 4, pp. 2473–2480, 2007.

[115] K. Qian, C. Zhou, M. Allan, and Y. Yuan, "Modeling of load demand due to ev battery charging in distribution systems," *IEEE transactions on power systems*, vol. 26, no. 2, pp. 802–810, 2010.

[116] D. Das, H. Nagi, and D. Kothari, "Novel method for solving radial distribution networks," *IEE Proceedings-Generation, Transmission and Distribution*, vol. 141, no. 4, pp. 291–298, 1994.

[117] A. R. Di Fazio, M. Russo, and M. De Santis, "Zoning evaluation for voltage control in smart distribution networks," in *2018 IEEE International Conference on Environment and Electrical Engineering and 2018 IEEE Industrial and Commercial Power Systems Europe (EEEIC/I&CPS Europe)*, pp. 1–6, IEEE, 2018.

[118] Z. Jia and F. Qi, "Network clustering algorithm based on fast detection of central node," *Scientific Programming*, vol. 2022, 2022.

[119] P. Sadeghi-Barzani, A. Rajabi-Ghahnavieh, and H. Kazemi-Karegar, "Optimal fast charging station placing and sizing," *Applied Energy*, vol. 125, pp. 289–299, 2014.

[120] N. Singh and S. Singh, "Hybrid algorithm of particle swarm optimization and grey wolf optimizer for improving convergence performance," *Journal of Applied Mathematics*, vol. 2017, 2017.

[121] S. Mirjalili, S. Saremi, S. M. Mirjalili, and L. d. S. Coelho, "Multi-objective grey wolf optimizer: a novel algorithm for multi-criterion optimization," *Expert Systems with Applications*, vol. 47, pp. 106–119, 2016.

Author's Publications

International Journals (Published)

1. **Ajit Kumar Mohanty**, Suresh Babu Perli, and Salkuti Surender Reddy. "Optimal Allocation of Fast Charging Station for Integrated Electric-Transportation System Using Multi-Objective Approach."Sustainability **(MDPI)** 14 (2022): 14731. **(SCI)**. https://www.mdpi.com/2071-1050/14/22/14731.

2. **Ajit Kumar Mohanty**, Suresh Babu Perli, and Salkuti Surender Reddy. "Fuzzy-Based Simultaneous Optimal Placement of Electric Vehicle Charging Stations, Distributed Generators, and DSTATCOM in a Distribution System". Energies **(MDPI)** 15 (2022). **(SCI)**. https://www.mdpi.com/1996-1073/15/22/8702.

3. **Ajit Kumar Mohanty**, Suresh Babu Perli. "Fuzzy logic based multi-objective approach for optimal allocation of charging stations for electric vehicles", e-Prime-Advances in Electrical Engineering, Electronics and Energy **(Elsevier)** 2 (2022). **(Scopus)** https://doi.org/10.1016/j.prime.2022.100089.

International Conferences (Published)

4. **Ajit Kumar Mohanty**, Suresh Babu Perli, "Multi Objective Optimal Planning of Fast Charging station and Distributed Generators in a Distribution System," 2021 IEEE 2nd International Conference On Electrical Power and Energy Systems (ICEPES), Bhopal, India, DOI: 10.1109/ICEPES52894.2021.9699774

International Conferences (Published)

5. **Ajit Kumar Mohanty**, Suresh Babu Perli, "Optimal Placement of Electric Vehicle Charging Stations Using JAYA Algorithm" Recent Advances in Power Systems, 2021, Springer, pp: 259–266, Singapore.

International Journals (Accepted)

6. **Ajit Kumar Mohanty**, Suresh Babu Perli, " Fuzzy Based Optimal Network Reconfiguration of Distribution System with Electric Vehicle Charging Stations, Distributed Generation, and Shunt Capacitors", *Submitted in Journal Advances in Electrical and Electronic Engineering*, 2022. **(Scopus)**

Bio-data

Name	Ajit Kumar Mohanty
Father's Name	Dhirendra Kumar Mohanty
Date of Birth	03-08-1987
Nationality	Indian
Mobile No.	9441233804, 8247839885
Email id	ajitchinu@gmail.com
Permanent Address	Flat No. 303, SS Plaza, Udayagiri Vihar, Patrapada, Bhubaneswar, Odisha PIN: - 75101

Educational Qualifications

- Doctorate of Philosophy 2018- 2023
  National Institute of Technology Warangal, Telangana.
- Master in Engineering (Power System), 2011-2013
  National Institute of Technology, Tiruchirappalli
- Bachelor of Engineering (Electrical and Electronics Engineering). 2005-2009
  Sanketika Vidya Parishad of Engineering college, Visakhapatnam.

Academic Achievements: -

- Qualified Olychem-2002 and attended chemistry Olympiad.
- Served as technical advisor to team PESAC during masters.